

**CHROMATOGRAPHY BASED METHODS FOR
DETERMINATION OF TRACE ELEMENTS IN
NUCLEAR MATERIALS**

By

VIJAY M. TELMORE

Enrolment No.: CHEM01201304011

Bhabha Atomic Research Centre, Mumbai

*A thesis submitted to the
Board of Studies in Chemical Sciences
In partial fulfillment of requirements
for the Degree of*

DOCTOR OF PHILOSOPHY

of

HOMI BHABHA NATIONAL INSTITUTE



December, 2019

Homi Bhabha National Institute

Recommendations of the Viva Voce Committee

As members of the Viva Voce Committee, we certify that we have read the dissertation prepared by **Vijay M. Telmore** entitled "Chromatography Based Method For Determination of Trace Elements in Nuclear Materials" and recommend that it may be accepted as fulfilling the thesis requirement for the award of Degree of Doctor of Philosophy.


Chairman - **Dr. S. K. Mukerjee**

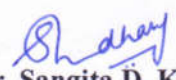
Date **17.09.2020**


Guide / Convener - **Dr. S. Kannan**

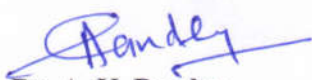
Date **17.9.2020**

Examiner - **Dr. Charu Arora**

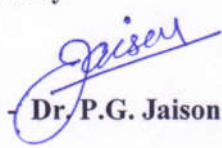
Date


Member 1- **Dr. Sangita D. Kumar**

Date **17.09.2020**


Member 2- **Dr. A. K. Pandey**

Date **17.9.2020**


The Technology Adviser - **Dr. P.G. Jaison**

Date **17/09/2020**

Final approval and acceptance of this thesis is contingent upon the candidate's submission of the final copies of the thesis to HBNI.

I/We hereby certify that I/we have read this thesis prepared under my/our direction and recommend that it may be accepted as fulfilling the thesis requirement.

Date: **17.9.2020**

Place: **Mumbai**



Signature

Guide

Subject **Re: Final Viva for Shri. Vijay Telmore FCD. BARC**
From Charu Arora <charuarora77@gmail.com>
To <skannan@barc.gov.in>
Date 2020-09-17 18:15
Priority Normal

Logo

Dear Prof Kannan

Shri Vijay Tel more, FCD, BARC has presented the salient features of his Ph D work. Based on the research scholar's work, his presentation and also the clarification and answers by the research scholar to the questions asked by me/ audience I recommend Shri Vijay Telmore be awarded Phd degree in Chemistry. Best regards

On 17 Sep 2020 16:23, <skannan@barc.gov.in> wrote:

Dear Professor Charu Arora Madam

Thanks for conducting and participating the Final viva of Shri. Vijay Telmore, HBNI, PhD student of Chemical sciences. I need a line of recommendation from you for submitting the final documents to HBNI. Since your signature is not there in the final recommendation letter, the email recommendation is must for submitting the documents.

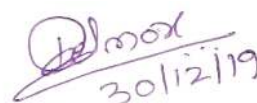
With regards

S.Kannan

STATEMENT BY AUTHOR

This dissertation has been submitted in partial fulfillment of requirements for an advanced degree at Homi Bhabha National Institute (HBNI) and is deposited in the Library to be made available to borrowers under rules of the HBNI.

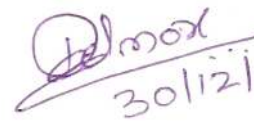
Brief quotations from this dissertation are allowable without special permission, provided that accurate acknowledgement of source is made. Requests for permission for extended quotation from or reproduction of this manuscript in whole or in part may be granted by the Competent Authority of HBNI when in his or her judgment the proposed use of the material is in the interests of scholarship. In all other instances, however, permission must be obtained from the author.



Vijay M. Telmore

DECLARATION

I, hereby declare that the investigation presented in the thesis has been carried out by me. The work is original and has not been submitted earlier as a whole or in part for a degree / diploma at this or any other Institution / University.


30/12/19

Vijay M. Telmore

List of Publications arising from the thesis

List of Publications arising from the thesis

Journal-03+1 Nos.

1. Study on complexation of palladium with thiourea based ligands and its determination in simulated high level liquid waste using solid phase extraction-electrospray mass spectrometry
Vijay M. Telmore, Pranaw Kumar, P. G. Jaison
j. Radioanal Nucl Chem **2018**,318,1249-1259
2. Separation and estimation of ^{229}Th and ^{233}U by alpha and gamma ray spectrometric technique
Pranaw Kumar, Vijay M. Telmore, P. G. Jaison, A. Mhatre, H. Naik
j. Radioanal Nucl Chem,**2016**,308,1113–1119
3. High performance liquid chromatographic separation of $^{228,229}\text{Th}$ and $^{232,233}\text{U}$ and their estimation by α - and γ -ray spectrometry
Vijay M. Telmore, Pranaw Kumar, P. G. Jaison, A. Mhatre, H. Naik
j. Radioanal Nucl Chem ,**2017**,313:319-326
4. Dual Column - HPLC method for Determination of Trace Quantity of Lanthanides in Zirconium Matrix
Vijay M. Telmore, Pranaw Kumar, P. G. Jaison, S. Kannan
Communicated to journal of Chromatography A

Symposium -04 Nos.

1. Electrospray Ionisation Mass Spectrometric Studies on Relative stabilities of Palladium Complex with thiourea, Benzoylthiourea and N,N-Diethyl N-Benzoylthiourea
Vijay M. Telmore, Pranaw Kumar, Sumana Paul, P.G. Jaison, D. Alamelu and S.K.Aggarwal
28th ISMAS-WS 2014. Page No. 234. CP No. 31
2. Solid Phase Extraction–Electrospray Ionization Mass Spectrometric Method for the Determination of Palladium
Pranaw Kumar, Vijay M. Telmore, P.G. Jaison, Arnab Sarkar, D. Alamelu and S.K. Aggarwal
29th ISMAS-WS 2015. Page No. 178.CP NO. 32
3. HPLC studies for the separation of Lanthanides in Zirconium matrix
Vijay M. Telmore, Pranaw Kumar P.G. Jaison
SESTEC-2018; BITS Pilani Goa Paper No. D10 (Best Paper Award)

4. Electrospray Ionisation Mass Spectrometric Studies of Zirconium with α -hydroxyl isobutric acid
Vijay M. Telmore, Pranaw Kumar, P. G. Jaison and S. Kannan
32nd ISAMS 2019, DAE Convention Centre, Mumbai
Accepted...


30/12/19

Vijay M. Telmore

DEDICATED TO...

my mother and father...

ACKNOWLEDGEMENTS

At the outset, I would like express my deepest appreciation and regards to my guide, Prof. S. Kannan, who expertly guided me as well as shared his excitement which kept me constantly engaged with my research.

Also I take this opportunity to thank the respected members of my doctoral committee Prof. S. K. Mukerjee(Chairman), Prof. A. K. Pandey (Member), Dr. Sangita D. Kumar (Member) their critical reviews and valuable suggestions.

I would like to express my sincere gratitude to my immediate superior and mentor Dr. P. G. Jaison, Who has introduced me into research field. His calm demeanor, knowledge and logical way of thinking and reasoning on scientific problems logical way of guidance, help in my research work, monitoring the progress of work, teachings about the writing of manuscript helped to bring out the proper shape of this work. I wish to record my heartfelt gratitude and indebtedness to him. His wide helped me immensely during the course of work. I am thankful to him for sharing his knowledge and scientific understanding during the fruitful discussions with me throughout the work.

My appreciation also extends to my dearest friend and mentor, Dr. Pranaw Kumar who has extended his wholehearted guidance, support, cooperation, encouragement throughout this research work.

Special thanks to Dr. H. Naik for his teaching, support and guidance for alpha and gamma spectrometric work.

I wish to record my deep sense of gratitude to my former supervisors Dr. S. K. Aggarwal and Dr. D. Alamelu, who gave the inspiration for pursuing my PhD.

I take this opportunity to thank my colleagues, Dr, Arnab Sarakar, Dr. Sumana Paul, Sh Amol Mahtre, Sh Jagdish Kumar and Smt. Preeti Goswami for their valuable suggestions and discussion in alpha and gamma spectrometric work. Also, I would like to thanks my

colleague Dr. Radhika Rao, Sh Raju Shah, K. Sasibhushan Sh Vijay Karki, Sh Manish Singh, Sh Manjeet Singh for support and helps at all stages of my work.

I would like to thanks Sh. Avinash Kanekar, Sh. Rajesh Gujar from radiochemistry division, and Dr. Vivek Mishra and Sh. M.K Das, Dr. B.K. Nagar, Sh. Uday Kumar Thakur, Smt. D. J. Shah from radioanalytical chemistry division for providing unconditional support during the research work.

Special thanks to administrative staff of Fuel Chemistry Division for their help and support. And finally, I would like to express my endless thanks to my wife and kids for their unconditional love and support.

CONTENTS

	Page No.
SUMMARY	I
LIST OF FIGURES	IV
LIST OF TABLES	VII
CHAPTER 1 Introduction	
1.1 Three Stage Nuclear Programme of India	2
1.2 Nuclear Materials	3
1.3 Nuclear Fuel Cycle	3
1.4 Types of Nuclear Fuels	4
1.5 Trace elemental determination in nuclear industry	5
1.5.1 Trace Metallic Impurities	5
1.5.2 Trace Non-metallic Elements Impurities	7
1.6 Techniques used for Trace Elemental Determination	10
1.7 Role of Chromatographic Methods in Nuclear Industries	11
1.8 Role of Electrospray Ionization Mass Spectrometry (ESI-MS) in Separation Science.	12
CHAPTER 2 Instruments and Techniques	13
2.1 Chromatography	14
2.1.1 Different Types of Chromatography	14
2.1.2 Theory of chromatography	16
2.1.3 Chromatographic Parameters	17
2.1.4 Band Broadening Parameters	19
2.1.5 Van Deemter Plot	21
2.1.6 Instrumentation of HPLC	22

2.1.6.1	HPLC Detector	25
2.1.7	Liquid Chromatographic Technique for Separation of Rare Earth Elements	30
2.2	Mass Spectrometry	40
2.2.1	Processes in Mass spectrometry	40
2.2.2	Instrumentation	41
2.2.3	Electrospray Ionization Mass Spectrometry	46
2.3	Gamma Ray Spectrometry	51
2.3.1	Interaction of Gamma Ray with Matter	51
2.3.2	Instrumentation of Gamma Ray Spectrometry	54
2.3.3	Applications of Gamma Ray Spectrometry	59
2.4	Alpha Spectrometry	60
2.4.1	Theory of Alpha Decay	61
2.4.2	Alpha Source Preparation	62
2.4.3	Instrumentation of Alpha Spectrometer	64
2.4.4	Applications of Alpha Spectroscopy	67
CHAPTER 3	Dual Column HPLC method for Determination of Lanthanides in Zirconium Matrix	71
3.1	Introduction	72
3.2	Experimental	75
3.2.1	Instrumentation	75
3.2.2	Reagents	76
3.2.3	Pre-concentration	76
3.3	Results and Discussions	77
3.3.1	Chromatographic Behavior of Zirconium and Lanthanides	77

3.3.2	Studies of Zirconium Species by ESI-MS	80
3.3.3	Optimization of Acidity	82
3.3.4	Preconcentration Study	83
3.3.4.1	Effect of Flow rate on Pre-concentration	83
3.3.4.2	Effect of Volume	84
3.4	Individual separation of pre-concentrated lanthanides	84
3.5	Quantification of Lanthanides	85
3.6	Conclusions	86
CHAPTER 4	Study on complexation of palladium with thiourea-based ligands and its determination in simulated high-level liquid waste using solid phase extraction-electrospray mass spectrometry	87
4.1	Introduction	88
4.2	Experimental	90
4.2.1.	Chemical and Reagents	90
4.2.2	Instrumentation	91
4.3	SPE procedure	92
4.4	Results and Discussion	92
4.4.1	ESI-MS Studies of Pd-thiourea Derivatives	92
4.4.2	Optimization of Instrumental Parameters	97
4.4.2.1	Quadrupole Energy	97
4.4.2.2	Collision cell Energy	99
4.4.2.3	Tandem Mass Spectrometric Study	101
4.4.3	Intensities of PdL ₂ Species	104

4.5	Development of auto-SPE Method for Palladium Determination	105
4.6	Comparison with other Techniques	110
4.7	Conclusions	110
Chapter 5	Separation and estimation of ^{229}Th and ^{233}U by alpha and gamma ray spectrometric technique	111
5.1	Introduction	112
5.2	Experimental method	114
5.3	Calculation and Results	119
5.4	Discussion	122
5.5	Conclusion	125
Chapter 6	High Performance Liquid Chromatographic Separation of $^{228,229}\text{Th}$ and $^{232,233}\text{U}$ and their Estimation by α- And γ-Ray Spectrometry	126
6.1	Introduction	127
6.2	Experimental Details	129
6.3	Results and Discussion	134
6.4	Conclusions	137
Chapter 7	Summary and Future Outlook	138
	REFERENCES	141

Summary

The presence of trace elements in nuclear materials can affect their performance during nuclear reactor operations. Trace elemental determination is also important in post-irradiation examination of spent fuels and in nuclear waste management. Trace elemental analysis generally encounters interferences from matrix elements and other accompanying elements. This problem can be circumvented by using suitable separation techniques. Chromatographic techniques, especially, high performance liquid chromatography (HPLC) can play an important role in the separation and determination of trace elements in different nuclear fuel and nuclear materials.

Zirconium and its alloys are extensively used for the fabrication of nuclear reactor's structural materials such as clad, pressure tubes and reactor core, etc. Some of the lanthanides like Gd, Sm, Eu, and Dy have very high neutron absorption cross-sections and their presence in zirconium and its alloys would adversely affect the overall neutron economy of the nuclear reactor. Separation of individual lanthanides are difficult by classical separation methods due to the similarities in chemical properties. Therefore, the determination of individual lanthanides in the zirconium matrix is a challenging task. The present thesis deals with the separation and determination of individual lanthanides in the presence of a large amount of zirconium using HPLC. Zirconium does not show any retention on the stationary phase whereas lanthanides get pre-concentrated under the optimized conditions. Gradient of high pH eluent, α -HIBA, is used for the individual separation of lanthanides. Pre-concentration and quantification of lanthanides in the concentration range from 2 ppb to 100 ppb can be achieved by this method. Identification of Zr species $[\text{Zr}(\text{NO}_3)_5]^-$ using ESI-MS was helpful in designing the strategy for the effective pre-concentration of lanthanides.

Because of the increasing applications and limited availability of palladium (Pd), separation and determination of palladium from spent nuclear fuel are very important. Thiourea and its

derivatives are used for the separation of palladium. ESI-MS studies of thiourea and its derivatives viz benzoylthiourea (BTU) and N,N-diethyl-N'-benzoylthiourea (DEBT) with palladium is carried out to identify the species. Tandem mass spectrometric (ms/ms) studies are carried out to investigate the relative stability of various Pd species in the gas phase. Based on these studies, an automated solid-phase extraction method is developed for the separation of Pd using DEBT, followed by its determination using ESI-MS. The developed method is used for the determination of Pd in simulated high-level liquid waste.

^{233}U and ^{229}Th are used as a spike for isotope dilution thermal ionization mass spectrometric determination of thorium. ^{229}Th is a daughter product of ^{233}U and the determination of ^{229}Th in presence of ^{233}U is very important to evaluate the purity of ^{229}Th . A radiometric method based on alpha and gamma spectrometry for the determination of ^{229}Th and ^{233}U in presence of each other from a single planchated source. , This s a simple method which can be easily adopted for routine analysis.

Determination of different isotopes of Uranium and Thorium in irradiated thoria samples is very important in the nuclear industry. Determination of ^{232}U is provides shielding requirement as the daughter product of ^{232}U i.e. ^{212}Bi and ^{208}Tl emits hard gamma rays. Determination of ^{233}U in irradiated thoria gives its fissile inventory. Their fast separation minimizes the radiation exposure. An HPLC method is developed employing α -HIBA is as a complexing agent for separation of U and Th from each other as well as from other fission products. Post-separation, these isotopes were measured using alpha as well as gamma spectrometry.

Hence the objective of the present thesis is:

1. HPLC method for determination of trace quantities of lanthanides in zirconium matrix
2. Studies on complexation of palladium with thiourea based ligands and its determination in simulated high-level liquid waste using solid-phase extraction-electrospray mass spectrometry

3. Separation and estimation of ^{229}Th and ^{233}U by alpha and gamma-ray spectrometric techniques
4. High-Performance liquid chromatographic separation of $^{228,229}\text{Th}$ and $^{232,233}\text{U}$ and their determination by α - and γ -ray spectrometry

List of Figures

Fig. No.	Caption	Page No.
Fig. 1.1	Three Stage Nuclear Programme of India	2
Fig. 1.2	Nuclear fuel cycle	3
Fig. 1.3	Decay scheme of ^{232}U	7
Fig. 2.1	Chromatogram	17
Fig. 2.2	Different band broadening parameters	21
Fig. 2.3	Van Deemter plot	22
Fig. 2.4	Schematic diagram of an HPLC system	22
Fig. 2.5	Schematic diagram of injectors in [A] inject position and [B] load position	27
Fig. 2.6	Principle of diode array detector	29
Fig. 2.7	Block diagram of mass spectrometer	40
Fig. 2.8	Features of ESI-MS	46
Fig. 2.9	Block diagram of ESI-MS	50
Fig. 2.10	Photoelectric Effect	52
Fig. 2.11	Block Diagram of a HPGe detector system	56
Fig. 2.12	Typical efficiency calibration curve in gamma ray spectrometry	57
Fig. 2.13	Tunneling Effect	62
Fig. 2.14	Instrumentation of Alpha Spectrometry	67
Fig. 2.15	Energy Calibration of Detector using ^{241}Pu - ^{241}Am source	68
Fig. 3.1(a)	Retention of La, Lu and Zr on RP column in absence of IIR	78
Fig. 3.1(b)	Retention of La, Lu and Zr on RP column in presence of IIR	78
Fig. 3.2	Effect of octyltrimethyl ammonium chloride (anionic modifier) onto the retention of Zr	79

Fig. 3.3	ESI-MS spectra of Zr (5×10^{-6} M) solution in 1.5×10^{-4} M of HNO_3 in negative ion mode	80
Fig. 3.4	ESI-MS spectrum of Zr (5×10^{-6} M) and HIBA(5×10^{-5} M) in 1.5×10^{-4} M of HNO_3 in negative ion mode	81
Fig. 3.5	Effect of mobile flow rate on the pre-concentration of lanthanides	83
Fig. 3.6	Volume calibration for pre-concentration of lanthanides	84
Fig. 3.7	Pre-concentration and separation individual lanthanides in zirconium with Ln: Zr amount ratio 1: 50,000.	86
Fig. 4.1	Structures of the ligands and Pd-DEBT complex	93
Fig. 4.2	ESI-MS spectra of Pd (5×10^{-6} M) in methanol containing (1×10^{-5} M) NaClO_4 and (2×10^{-5} M) of the ligands; (a)TU, (b)BTU and (c) DEBT. (d) Expanded region of $[\text{Pd}(\text{DEBT})_2]^+$	95
Fig. 4.3	Effect of quadrupole ion energy on intensities of PdL_2 complex species of TU, BTU, DEBT	97
Fig. 4. 1 SI	Effect of quadrupole ion energy on intensities of Palladium complex species of (a) TU (b) BTU and (c) DEBT	98
Fig. 4.4	Effect of collision cell energy on the relative percentage change in intensities of PdL_2 complex species of TU, BTU and DEBT	100
Fig. 4. 2 SI	Effect of collision cell energy on intensities of Palladium complex species of (a) TU, b)BTU and (c) DEBT	100
Fig. 4.5	Collision induced dissociation as function of collision energy for Pd complexes with (a) TU, (b) BTU (c) DEBT and (d) PdL_2 species	103
Fig. 4.6	Comparison of ESI-MS intensities of PdL_2 species using Pd (5×10^{-6} M) in methanol containing ligand (2×10^{-5} M) and NaClO_4 (1×10^{-5} M)	105
Fig. 4.7	Schematic of the automated solid phase extraction process for Palladium	107
Fig. 4.8	ESI-MS response of $[\text{Pd}(\text{DEBT})_2]^+$ as a function of concentration of Pd in SHLLW solution	108

Fig. 4.9	Auto-SPE method for Pd determination in SHLW using ESI-MS	109
Fig. 5.0	Schematic diagram for the production of different isotopes of Th and U	113
Fig. 5.1	Alpha spectrum of unpurified ^{233}U activity along with its daughter products activities	115
Fig. 5.2	Gamma-ray spectrum of unpurified ^{233}U activity along with its daughter products activities	116
Fig. 5.3	Alpha spectrum of purified ^{233}U activity free from its daughter products activities	117
Fig. 5.4	Alpha spectrum of the purified ^{229}Th activity	118
Fig. 5.5	Gamma-ray spectrum of the purified ^{229}Th activity	118
Fig. 6.1	Alpha spectrum of irradiated thoria sample.	129
Fig. 6.2	Chromatogram of separation of Th and U from dissolver solution of irradiated thoria.	131
Fig. 6.3	Alpha spectrum of purified U fraction	132
Fig. 6.4	Alpha spectrum of the purified Th fraction,	133
Fig. 6.5	Gamma-ray spectrum of the purified Th activity showing the gamma lines of ^{229}Th	134

List of Tables

Table No.	Caption	Page No.
Table 1.1	Specification limits for metallic impurities for thermal and fast reactor fuels (values are in ppm _w)	8
Table 1.2	Specification for non-metals in nuclear fuels	9
Table 2.1	HPLC detectors	26
Table 2.2	Alpha Hydroxy Carboxylic Acid	30
Table 2.3	Classification of Ion Source	42
Table 2.4	Different types of mass analyzer and their characteristics	43
Table 2.5	Different Electron Multipliers Configurations	44
Table 2.6	Types of commonly observed ions in Electrospray ionization mass spectrometry	48
Table 2.7	Standard source used for energy and efficiency calibration	58
Table 3.1	Neutron absorption coefficient and equivalent boron content	73
Table 3.2	Zr (5×10^{-6} M) solution in 1.5×10^{-4} M of HNO ₃ in negative ion mode	81
Table 3.3	Zr (5×10^{-6} M) with HIBA(5×10^{-5} M) in 1.5×10^{-4} M of HNO ₃ in negative ion mode	82
Table 3.4	HPLC method for Separation of Individual lanthanides from bulk of zirconium	85
Table 4.1	Composition of simulated high level liquid waste	90
Table 4.2	Distribution of Pd species in positive ion mode	96
Table 5.1	Nuclear spectroscopic data of ^{227,228,229,230} Th and ^{232,233,234} U	120

Thesis Highlight

Name of the Student: Vijay M. Telmore

Name of the CI/OCC: Bhabha Atomic Research Center **Enrolment No.:** CHEM01201304011

Thesis Title: Chromatography based Methods for Determination of Trace Elements in Nuclear Materials

Discipline: Chemical Sciences

Date of viva voce: September 17, 2020

The presence of trace elements in nuclear materials can affect their performance during nuclear reactor operations. Trace elemental analysis generally encounters interferences from matrix elements and other accompanying elements. This problem can be circumvented by using suitable separation techniques like HPLC.

A method was developed for determination of lanthanides in zirconium matrix using HPLC where preconcentration of lanthanides as well as Zr removal take place simultaneously. High level liquid waste from fast reactor can be a good source for palladium. A method is developed for the determination of palladium in simulated high level liquid waste using Auto-SPE and ESI-MS. ^{233}U and ^{229}Th are used as a spike for mass spectrometric determination of uranium and thorium respectively. ^{233}U undergoes alpha decay to produce ^{229}Th . A radiometric method was developed for determination of ^{233}U and ^{229}Th . A radiometric method was developed for the determination of ^{229}Th and ^{233}U in presence of each other from a single planchated source. An HPLC method is developed employing α -HIBA as a complexing agent for separation of $^{233,232}\text{U}$ and $^{228,229}\text{Th}$ from each other as well as from other fission products. Post-separation, these isotopes were measured using radiometric techniques.

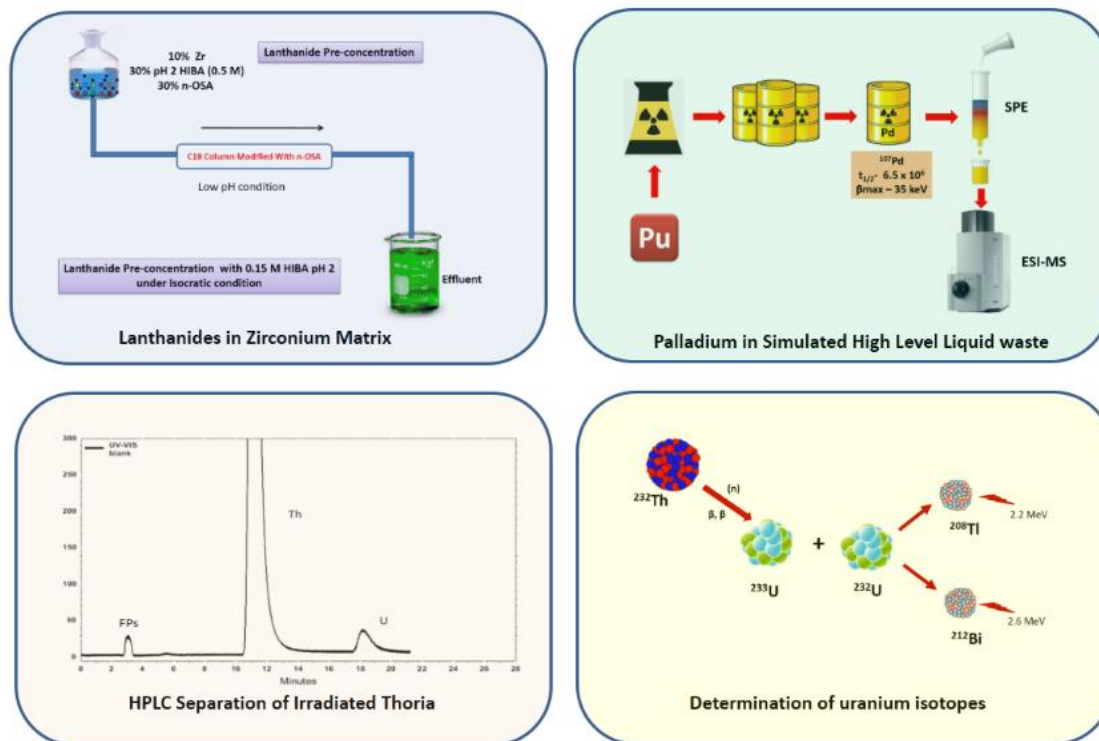


Fig. : Chromatography based Methods for Determination of trace Elements in Nuclear Materials

Chapter 1

Introduction

1.1 Three Stage Nuclear Programme of India

Per capita energy consumption has been accepted as the yard stick of development of any nation. India needs to quadruple its per-capita energy consumption to meet the rising demands and also to achieve the desired human development status. In India, electricity is produced from coal, gas, hydroelectricity, wind power and nuclear power. Nuclear power is generated by nuclear fission of fuel materials in nuclear reactors. ^{235}U , ^{233}U and ^{239}Pu are the fissile isotopes contributing towards fission in nuclear fuel materials. ^{235}U is naturally available whereas ^{239}Pu and ^{233}U are obtained from ^{238}U and ^{232}Th , respectively. Indian three stage nuclear power programme was formulated by Homi Bhabha in 1950s and is depicted in fig. 1.1. The program comprised of the first stage, focusing on the use of natural uranium for generation of electricity and the production of fissile inventory i.e. ^{239}Pu , for next generation, in thermal reactors (PHWRs). In stage two, ^{239}Pu generated in first stage will be used as a fuel core in fast breeder reactor. A blanket of ^{232}Th surrounding the fuel core will undergo nuclear transmutation to produce ^{233}U . In third stage, ^{233}U will be utilized as fuel for generation of electricity along with the production of more ^{233}U from ^{232}Th [1].

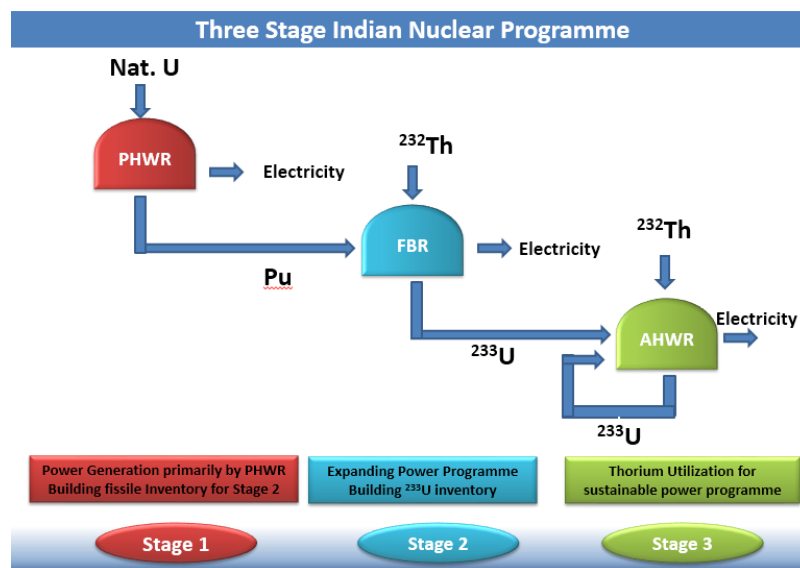


Fig.1.1: Three Stage Nuclear Programme of India

1.2 Nuclear Materials

The nuclear fuels contain fissile isotopes like uranium (^{235}U , ^{233}U) and plutonium (^{239}Pu) which on interaction with neutrons undergo fission to produce energy as well as neutrons to sustain a chain reaction. Uranium (^{235}U) is naturally available whereas ^{233}U and ^{239}Pu are formed in nuclear reactor from ^{238}U and ^{232}Th respectively. Other than actinide elements as nuclear fuels other elements like boron, cadmium, gadolinium, zirconium, graphite, alumina, aluminum oxide and beryllium oxide are also used in nuclear reactors for various applications

1.3 Nuclear Fuel Cycle

The nuclear fuel cycle consists of progression of nuclear fuels from mining, refining, purifying, utilization in the reactor, reprocessing, recycling and ultimately safe disposal of the nuclear waste generated. The nuclear fuel cycle has two parts: the front end consists from mining to fabrication of nuclear fuel and back end consists of reprocessing of the spent fuel, recovery procedures and disposal of leftover. Nuclear fuel cycle is referred as an open fuel cycle or once through fuel cycle if the spent fuel is not reprocessed. The nuclear fuel cycle is referred as a closed fuel cycle if the spent fuel is reprocessed for important elements like plutonium(Fig.1.2).

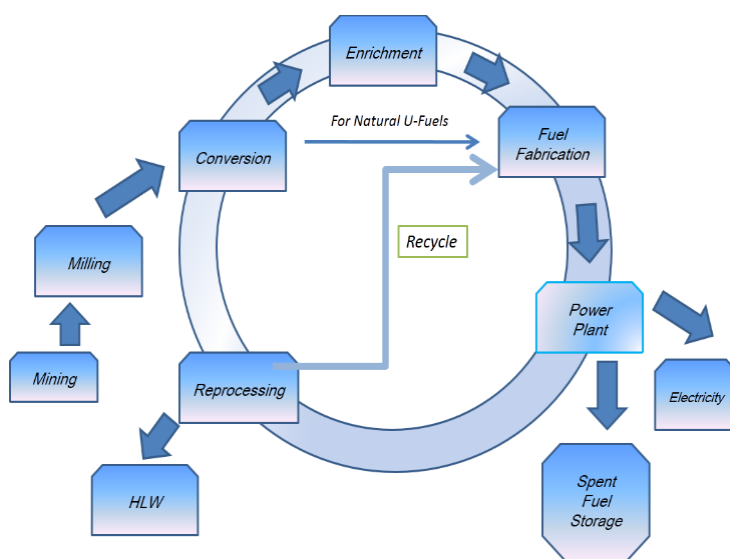


Fig.1.2: Nuclear fuel cycle [2]

1.4 Types of Nuclear Fuels

Following are the different type of fuels being used or envisaged to utilize in Indian nuclear energy programme [3].

- Ceramic Fuels

This category of ceramic fuels includes oxides of U, Th, Pu, mixed oxide of (U, Pu)O₂, (Th, Pu)O₂ and (Th, U)O₂ fuels. The Indian PHWRs utilize UO₂ (natural uranium) whereas boiling water reactor (BWR) utilizes slightly enriched UO₂ (3% enrich ²³⁵U). Mixed oxide (MOX) fuels [(U,Pu)O₂] are the preferred choice for fast breeder reactors (FBR). Proposed advance heavy water reactor (AHWR) would have a choice of Th based mixed oxide ceramic fuels viz. (Th, Pu)O₂ and (Th, U)O₂. Fuels like (U,Pu)C and (U,Pu)N come under the category of non-oxide ceramic fuels.

- Intermetallic Fuels

Uranium based fuels of the type such as U–Al, U–Si, and U–Mo are known as intermetallic fuels. They are used in research and test reactors. In case of intermetallic fuels, higher densities are achieved compare to ceramic fuels. APSARA research reactor was based on U–Al intermetallic fuel which in now modified to U–Si fuel for the APSARA-U Reactor.

- Composite Fuels

This class of fuel consist of dispersion of fissile materials in inert matrix. Composite fuels are of two types: (i) cermet fuel where ceramic fuel particles are dispersed in a metallic matrix and (ii) ceramic fuel particles dispersed in a ceramic matrix known as cer-cer fuels. They are the proposed fuels for the fast reactors in which plutonium is used as a major fissile material.

- Metallic Fuels

Mechanically bonded U-Pu fuels as well as sodium bonded U-Pu-Zr alloys are preferred choice for fast breeder reactors as they facilitate high breeding ratios. Higher densities of fissile as well as fertile materials are achieved in the category of metallic fuels.

1.5 Trace Elemental Determination in Nuclear Industry

1.5.1 Trace Metallic Impurities

Presence of trace elements (impurities) in nuclear materials may affect the neutron economy, fuel integrity and fuel fabrication process. Even after rigorous purification and separation of matrix after mining and refining, some elements may continue to accompany the nuclear materials. Further, certain impurities may be picked up during the fabrication stage from various equipment's used or from chemicals and reagents used during separation and purification steps. Fuel has many impurities which can be classified as corrosive agents, neutron poisons, metallic impurities, non-metallic impurities and daughter products formed by radioactive decay (^{241}Am from ^{241}Pu). Presence of these impurities may affect the performance of the fuel in the nuclear reactor. These impurities may affect the interaction between the fuel and clad. Impurities are also generated during fission (fission products). Fuel with minimum impurities is desirable in nuclear reactor as the fuel stays more time in the reactor and can achieve higher burn-up.

Neutron economy is very important in nuclear reactors especially in case of thermal reactors. Neutrons cause the fission and also require to sustain the chain reaction. Presence of elements like B, Cd, Sm, Eu, Gd and Dy having very high neutron absorption cross-sections, affects the neutron economy [4]. Hence their determination is very important in the chemical quality control of nuclear materials. Beta decay of ^{241}Pu gives ^{241}Am . Therefore, accurate determination of ^{241}Am in plutonium bearing materials is important as it causes increased radiation exposure [5]. Elements like Mo, W, Ta above specific limits resist the creeping of fission products and cause the pellet swelling of the ceramic fuels and this generates the stress on the clad. Elements like Fe, Cr, Ni etc. are being analyzed for checking the process pickup, to check condition of process equipment etc. Presence of non-metals like F, Cl, O, N and hydrogen, carbon in nuclear materials can cause damage to clad materials. Sulphur forms

H₂S with hydrogen leading to disintegration of fuel pallet [6,7]. Trace elemental determination is also important in back-end of nuclear fuel cycle. During the fission of nuclear fuels in reactor, different fission products are formed. Recycling of these fission products is an important aspect of Indian nuclear fuel cycle for its efficient utilization. Their abundances depend upon the nature of fuel and its resident time in the reactor. Burn-up of fuel irradiated in nuclear reactor is determined using burn-up monitors viz. ¹³⁹La and ¹⁴⁸Nd. Determination of La and Nd requires separation from U, Th and Pu matrix [8, 9]. Platinum group elements like Rh, Pd, Ru are present in high level liquid waste and can create problem during verification of nuclear waste materials. Ruthenium burdened the off-gas system, as it is volatile in nature. Palladium and Rhodium forms separate phase and may clog melting furnace. Reactor produced palladium has lot of potential applications in different industries as the radioactivity associated with it is nominal. Therefore, their determination in nuclear waste is very important. Hence determination of these PGEs in high level liquid waste is an important aspect [10, 11].

²³⁷Np is another valuable element present in nuclear waste and it is used in production of ²³⁸Pu which has application in pace-makers [12]. The fission product, ⁹⁹Tc has many medical applications [13]. Neutron irradiation of ThO₂, leads to the formation of ²³³U along with ²³²U as shown in fig. 1.3 ²³²U is short lived (t_{1/2} 68.9 years) and generates daughter products ²⁰⁸Tl and ²¹²Bi which emits hard gamma rays. This is one of the biggest challenge of Th based fuels [14,15]. Hence determination and separation of trace elements in nuclear materials is very important in view of fuel fabrication, efficient utilization of nuclear fuel and safe reactor operation. Table 1 and 2 contains list of trace elements and their specification in different nuclear fuels.

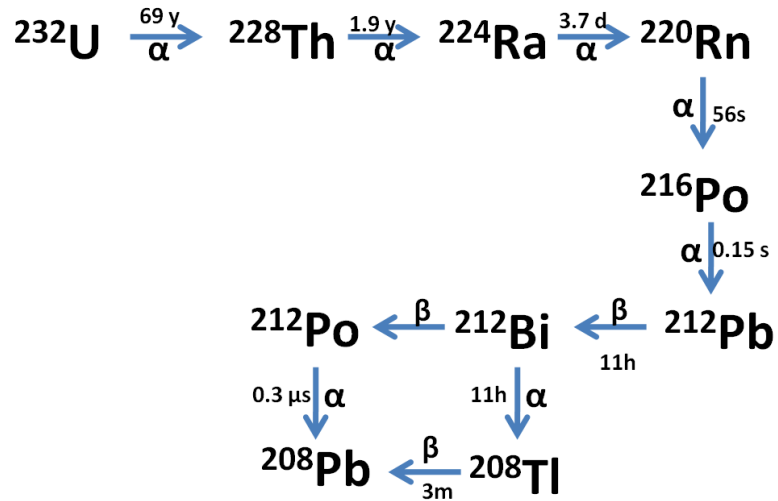


Fig.1.3 Decay scheme of ^{232}U

1.5.2 Trace Non-metallic Elements Impurities

Oxygen, carbon, nitrogen, phosphorus, sulphur, chlorine, fluorine, hydrogen, moisture, total gas content etc. are some of non-metallic trace elements analyzed in the nuclear materials. Oxygen is converted to CO by using graphite and then subsequently determined by IR spectroscopy. Carbon is converted CO₂ and purified. The concentration CO₂ is then determined using thermal conductivity detectors. Inert gas fusion technique or Kjeldhal distillation method is used for nitrogen determination. Fluorine and chlorine are determined using ion chromatography with conductivity detector after separating fluorine and chlorine from the matrix by pyro-hydrolysis. Sulphur is determined by combustion to form SO₂, followed by IR detection. Boron is determined in the nuclear materials by D.C. Arc-AES method along with other metallic impurities. Determination of boron is also carried out using curcumin based spectrophotometric based method [7].

Table 1.1: Specification limits for metallic impurities for thermal and fast reactor fuels(values are in ppm_w) [6]

Impurity	Thermal Reactors			Fast Reactors			ThO ₂
	UO ₂	PuO ₂	(U,Pu)O ₂	UO ₂	PuO ₂	(U,Pu)O ₂	
Ag	1	10	25	1	10	25	50
Al	25	250	400	25	250	500	
B	0.3	2	1	0.3	2	2	0.3
Be						10	1
Ca	50	500	250	50	500	100	200
Cd	0.2	6	1	0.2	6	1	0.1
Co		25	75		25	200	
Cr	25	200	400	15	200	300	5
Cu	20	50	400	10	50	100	50
Dy							0.2
Eu			0.2				0.08
Fe	100	500	400	100	500	1000	100
Gd	0.1	1	1	0.1	1		0.2
Mg	50	200	200	10	200	50	50
Mn	10	100	400	10	100	200	2
Mo	4	200	400	2	200	200	20
Na			400			100	
Ni	20	200	400	20	200	500	30
Pb		200	400		200	200	
Si							60
Sm							0.4
Sn						10	
V			400			100	5
W					200	200	
Zn		200	400		200	100	
Zr					100	100	

Table 1.2 : Specification for non-metals in nuclear fuels.[7]

Elements	UO ₂ (ppm)	PuO ₂ (ppm)	(U,Pu)O ₂ (Thermal) (ppm)	(U,Pu)O ₂ (Fast) (ppm)	(U,Pu)C (Mark-1)	(U,Pu)C (Mark-2)
O/M			1.98-2.02	1.98		
C/M					1.025	1.01
M ₂ C ₃					5-20%	5-20%
C	150	200	200	300	5 %	5 %
N	200	200	100	200		
O					6500 ppm	5000 ppm
O+N					7500 ppm	6500 ppm
H		1	3			
S	300	300	50			
Cl	25	50	15	25	25 ppm	25 ppm
F	25	25	10	25	25 ppm	25 ppm
H ₂ O	5000		10	30		
B	10	10	1	3	4.5 ppm	4.5 ppm
B. Eq.		2	5.5	5.5	5.5 ppm	5.5 ppm

1.6 Techniques used for Trace Elemental Determination

AES techniques provide simultaneous multi-elemental analysis. For solid and liquid samples DC Arc-AES and ICP-AES are used, respectively. These techniques also offer very wide dynamic range as the self-absorption is absent at such high temperature. This permits the analysis of major, minor and trace constituents in a same sample with very high precision. One of the drawback of ICP-AES is to interpret the complex spectra of actinides which hinders the direct trace element determination. Separation techniques like ion exchange and solvent extraction are used to remove the major matrix. DC-Arc-AES offers poor precision compare to ICP-AES. With the help of carrier distillation technique, refractory materials can be analyzed. The dynamic range in DC-Arc-AES is limited due to self-absorption of analyte [6].

Atomic absorption spectroscopy is an element specific technique therefore it has no interference from other elements. Flame or electro-thermal atomization (ETA) is used for atomization of samples. Hollow-cathode lamp is most widely used for the irradiation of the atoms.. Like ICP-AES, it also requires pre-separation of matrix.

ICP-MS is one of the most versatile techniques to carry out trace and ultra-trace level analysis in nuclear materials. It is a multi-elemental and highly sensitive technique. ICP-MS is used for quantitative determination as well as isotopic composition with good precision. Like any other mass spectrometric technique, ICP-MS also suffers from isobaric interference which can be overcome by coupling to separation techniques [16].

Thermal ionization mass spectrometry is widely used for isotopic composition of elements in nuclear fuels and other nuclear materials. It is a preferable technique due to its various advantages such as simplicity in mass spectrum, low ion energy spread, no memory effects and ease of handling radioactive elements. TIMS is famous for the precision on the isotopic

data it generates. TIMS is not a multi-elemental technique and hence rigorous separation of matrix is required in TIMS [17].

1.7 Role of Chromatographic Methods in Nuclear Industries

As aforesaid different analytical techniques like ICP-AES, ICP-MS, AAS and TIMS are reported in the literature for the determination of trace elements and isotopic composition in nuclear industry. However, most of these methods suffer various limitations such as matrix effects, spectral interference, isobaric interference etc. Traditionally, ion exchange and solvent extraction were employed in nuclear industries to take care of this problem. Both ion exchange and solvent extraction have some demerits like, generation of liquid waste, time consuming and exposure to radiation.

Chromatographic methods offer simultaneous separation of multi-elements and on-line quantification. Liquid chromatographic methods not only generate lesser liquid waste but also require shorter analysis time. HPLC is very popular due to its ability for the efficient separation of components which are having similar chemical properties. The high efficient separation is due to the small size stationary phase particles and the availability of large surface area. Low operating cost and high throughput are also the attractive features of HPLC. With the use of ion interaction reagents one can convert the reversed phase column in to cation or anion exchange column. These modified columns are known as dynamically modified column. Dynamically modified columns plays an important role in the separation of actinides and lanthanides. The dynamically modified column also offers variable capacity. Column can be easily recovered by removing the modifier by passing methanol or acetonitrile. Complete automation can be achieved using auto-sampler and fraction collectors. With the aid of fraction collector, each separated fraction can be collected for isotopic composition determination by mass spectrometry or radiometric techniques. These features result into less radiation exposure while handling radioactive materials. Reversed phase

chromatography plays very important role in the separation of lanthanides and actinides whereas ion chromatography is a useful technique for the determination of common anions and cations. Ion interaction chromatography (IIC) has been employed for determination of lanthanides, uranium, thorium and plutonium in irradiated nuclear fuel. Burn-up determination in various irradiated fuel samples like UO_2 , $(\text{U,Pu})\text{O}_2$, $(\text{Th,Pu})\text{O}_2$, ThO_2 , requires separation and quantification of La and Nd by ion interaction chromatography. Trace determination of lanthanides in Zr based materials is also possible with ion interaction chromatography [18]. Ion chromatography is routinely used for fluorine and chlorine determination in various nuclear materials [19]. Therefore, chromatographic techniques like ion chromatography, HPLC etc. are being used in the chemical characterization of trace elements in nuclear materials.

1.8 Role of Electrospray Ionization Mass Spectrometry (ESI-MS) in Separation Science.

ESI-MS is a soft ionization mass spectrometric technique. ESI-MS provides speciation information which is very valuable to identify different species required in formulating the separation schemes. Features like MS/MS can be employed for finding relative stabilities of the species under study. Though ESI-MS is mainly used for speciation studies, its applications are further extended for quantification of metal-ligand species using internal standards [20]. ESI-MS was used for studying the speciation of uranium with α -hydroxy isobutric acid which is a commonly used complexing agent for the separation of lanthanides and actinides [21]. These studies throw more light on separation mechanism which helps in designing better separation methods. This thesis also covers the work on determination of lanthanides in zirconium matrix in which ESI-MS played an important role in determining the nature of zirconium species present in the solutions.

Chapter 2

Instruments and Techniques

2.1 Chromatography

The presence of foreign or undesirable species in sample may create problems in chemical analysis. This foreign element either attenuates the signal or produces a signal which is difficult to distinguish from the signal of an analyte. This species which interferes with an analytical signal is called interference. Methods like separation, use of masking agent, matrix modification, etc. are employed to take care of the interferences. For achieving separation, techniques like chromatography, solvent extraction, precipitation, etc. are used [22]. Among different separation techniques, chromatography is a powerful analytical technique which caters to different aspects of analysis viz. separation, identification, and determination of the chemical component in a complex mixture. M. Tswett coined the word chromatography for his work on the separation of plant pigments. In Greek language *chroma* means color whereas *graph* means to write. IUPAC defines chromatography as " a physical method of separation in which the components to be separated are distributed between two phases, one of which a stationary while the other (Mobile phase) moves in a definite direction". Stationary Phase may be solid, gel or liquid. In the case of liquid as a stationary phase, it is chemically bonded to the stationary phase. The Mobile phase is a fluid percolating through the stationary bed in a definite direction. The Mobile phase may be a liquid, gas or supercritical fluid [23]. Chromatography can be classified based on the type of mobile phase used viz Gas chromatography, liquid chromatography, and supercritical fluid chromatography.

2.1.1 Different Types of Chromatography [24]

- **Adsorption or Normal Phase Chromatography**

This was the most dominating type of chromatography in the initial period of chromatography. In this mode, the stationary phase used is more polar compared to the mobile phase. The separation takes place based on the difference in the adsorption affinity of the constituents for the stationary phase. Generally, silica or alumina is used as a stationary phase. Organic solvents

like heptane to tetrahydrofuran are used as a mobile phase. In this case, non-polar analyte eluted early compare to a more polar analyte.

- **Partition or Reversed Phase Chromatography**

This is one of the most used types of chromatography. In partition or reversed-phase chromatography, mobile phase used is more polar than the stationary phase. In this mode, chemically bonded silica like C₁₈ or C₈ is used as the stationary phase. Polar compounds elute faster than the non-polar compounds. Separation in portion chromatography is achieved based on the difference in the solubilities of the components in mobile and stationary phases.

- **Extraction Chromatography**

In this mode of chromatography, non-polar extractants used conventionally in solvent extraction are immobilized on a solid support to achieve the separation..

- **Ion Exchange Chromatography**

In this case, the stationary phase consists of ionic site on its surface like $-N^+R_3$ or $-SO_3^-$. Ionic analyte interacts with this charge sites. The difference in the ionic potential of the analytes leads to separation. Generally, a styrene-divinylbenzene based stationary phase is used. Ion chromatography (IC) is the variation of ion exchange chromatography with the limited capacity column.

- **Size Exclusion Chromatography**

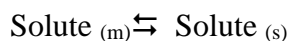
This is a special type of chromatography where samples are separated according to their size. Smaller analyte moves into the pores and spend more time in the stationary phase hence elutes later compare to larger analyte which could not enter the small pores and so elutes early. This is further divided as gel permeation chromatography (for organic solvents) and gel filtration chromatography (for aqueous solvents)

- **Affinity Chromatography**

This type of chromatography is mostly used in protein and peptide separation. The stationary phase contains a specific site which absorbs the analyte only when certain charge and steric conditions are satisfied. The retained species are eluted by using a ligand having a higher affinity for analyte compared to the stationary phase.

2.1.2 Theory of Chromatography

Differential distribution of the analytes between the stationary phase and mobile phase forms the basis of chromatographic separation. During the passage through the chromatographic bed, solute gets distributed between stationary and mobile phases. Depending upon the affinity, solutes spend more time in the stationary phase or mobile phase and an equilibrium comes into existence. The equilibrium of a solute (S) between the stationary phase (s) and the mobile phase (m) is represented below:



The distribution coefficient for solute is given by

$$K_d = \frac{\text{Solute}_{(s)}}{\text{Solute}_{(m)}}$$

$\text{Solute}_{(m)}$ is the concentration of analyte on stationary phase

$\text{Solute}_{(s)}$ is the concentration of analyte in the mobile phase

K_d is the distribution coefficient

A high value of distribution coefficient (K_d) indicates that the solute has a higher affinity for the stationary phase and should move slowly through the column, whereas a low value of distribution coefficient indicates the high affinity of solute for mobile phase and hence moves quickly through the stationary phase. With the aid of fresh mobile phase, the equilibrium gets disturbed and forms new equilibrium in the next section of the stationary phase. The mechanism of separation involves

continuous sorption and desorption along with the stationary phase. As this is repeated for more number of times, solutes having small differences in their K_d values also get separated in chromatography.

2.1.3 Common Parameters Used in Chromatographic Separation:

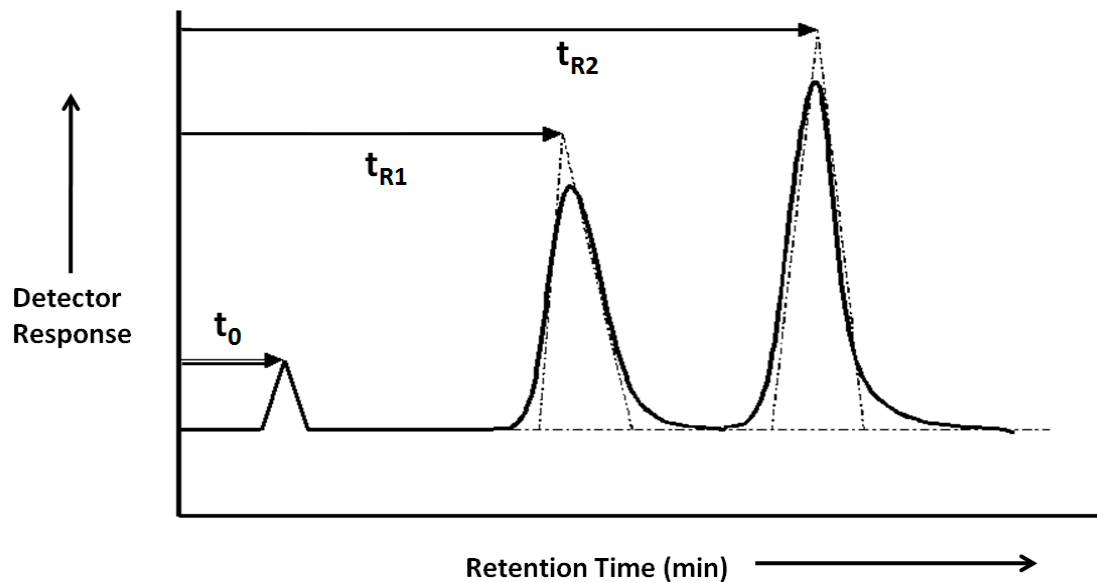


Fig.2.1 Chromatogram

- **Retention Time**

As shown in the chromatogram, (fig. 2.1) retention time (t_R) is a period between sample injection to peak maxima whereas t_0 denotes this period for an unretained species. Retention time is different for each separated species. The migration rate of the species depends upon the molecular structure, pressure, composition of the stationary and mobile phase. Retention time is a function of column length and mobile flow rate. Therefore, it is not suitable for the characterization of the compound only on the basis of the retention time.

- **Retention Factor**

As aforesaid, retention time cannot be used for characterization of the analyte. Therefore, another parameter, known as retention factor is used. Retention factor is given by

$$\text{Retention factor} = \frac{t_R - t_0}{t_0}$$

If the retention factor is very low, separation may be inadequate whereas higher retention factor results in longer analysis time.

- **Separation Factor**

The separation factor is given by the ratio of the retention factors of two different species under consideration. If the separation factor is 1, it means that the system is unable to resolve the components. The separation factor measures the ability of the chromatographic system to separate components.

$$\text{Separation Factor } (\alpha) = \frac{k_2}{k_1}$$

- **Number of Theoretical Plates(N) and Height Equivalent to Theoretical Plates (HETP)**

According to the plate theory suggested by Martin and Synge, the mechanism of separation involves continuous sorption and desorption in each plate along the stationary phase. Thus more the number of theoretical plates (N), the number of times the adsorption and desorption are repeated, better the separation among the adjacent peaks. Height equivalent to theoretical plates (HETP) is column length over each equilibration is achieved. A higher number of theoretical plates is achieved by employing a smaller particle size stationary phase. Efficiency is expressed numerically as plate count, N, or as a height equivalent to theoretical plate (HETP),

$$\text{HETP, } H = L/N$$

$$\text{Number of plates } N = 16(t_R/W)^2$$

where, L = column length,

t_R = retention time, and

W = peak width at baseline.

- **Resolution (R)**

For two neighboring peaks, resolution is the ratio of the difference in their retention times to the arithmetic mean of two peak widths. For quantitative estimations, resolution better than 1.5 is required. Resolution can be found out by using the following ways

1. Resolution based on the chromatographic data

$$\text{Resolution (R)} = \frac{2(t_{R2} - t_{R1})}{w_1 + w_2}$$

2. By using standard graphs
3. By using an equation

$$\text{Resolution (R)} = \frac{1}{4}(\alpha - 1)\sqrt{N} \frac{k_1}{1 + k_1}$$

$$\text{Where } k' = \frac{k_1 + k_2}{2}$$

2.1.4 Band broadening Parameters

Differential migration leads to the separation of different analytes in chromatography. While migrating through column molecules/ions of the same analyte may have slight differences in the time of elution which results in the broadening of peaks. This broadness of the peaks leads to loss of resolution. The different process contributing to peak broadening is mention below.

- **Eddy Diffusion**

The solute is transported through a chromatographic bed using the mobile phase. While passing through the column or chromatographic plate, solute can follow different paths. (fig. 2.2.1)

Therefore, some solute elutes before the other. This effect results in band broadening and known as eddy diffusion.

- **Longitudinal Diffusion**

While passing through the column, solute gets spread in all directions due to the concentration gradient (fig. 2.2.2). This effect is known as longitudinal effect. The broadening is a function of the mobile phase flow rate and is significant at low mobile phase flow rates. .

- **Mass Transfer**

Fig. 2.2.3 shows the mobile phase layer near the particle moves slowly as compared to the mobile phase layer passing through the center. Thus analyte moving along the central zone moves faster compared to the analyte moving along the mobile phase zone near the stationary phase particles. This effect leads to the spreading of the solute band. This is known as the mobile phase mass transfer. The stationary phase particle has channels both wide and narrow. Pores are filled with a mobile phase which does not move. Analyte moves through this stagnant mobile phase by diffusion only. Some analyte diffuse deep inside the pore of stationary phase particle whereas some analyte diffuse to very small distance and these effects lead to spread of solute band and known as a mass transfer due to stagnant mobile phase. Less viscous solvents are not effected significantly by this effect of mobile phase mass transfer. Analyte interacts with the stationary phase while passing through it. The analyte molecule gone deep inside the stationary phase particle would spend more time compare to the analyte which not diffuse inside the stationary phase. This effect leads to the spreading of the solute band and known as the mass transfer effect due to the stationary phase. All the above mentioned processes contributing to band broadening can be minimized using the stationary phase particle with small size and narrow size distribution.

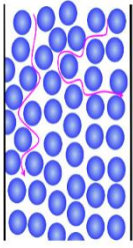
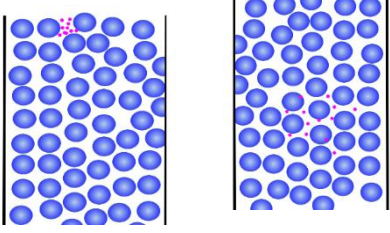
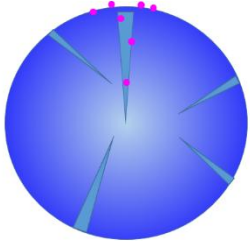
	<p style="text-align: center;">1. Eddy Diffusion</p>
	<p style="text-align: center;">2. Longitudinal Diffusion</p>
	<p style="text-align: center;">3. Mass Transfer</p>

Fig. 2.2 Different band broadening parameters

2.1.5 Van Deemter plot

Height equivalent to a theoretical plate (HETP or H) is a function of linear mobile flow velocity (u). A plot of H Vs u is known as a van deemter plot. This plot is a result of three band broadening parameters viz. eddy diffusion, longitudinal diffusion, and mass transfer. This plot (fig. 2.3) helps in finding the optimum mobile phase velocity to achieve minimum HETP and hence highest separation efficiency.

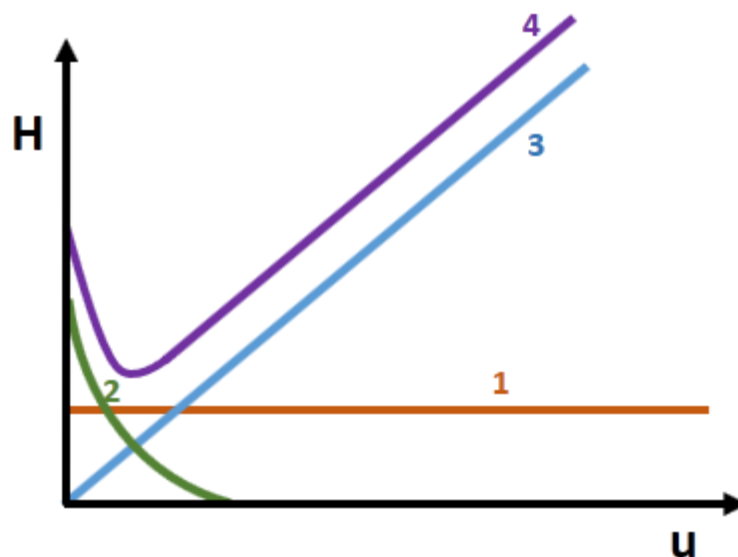


Fig. 2.3 Van Deemter plot showing the dependence of eddy diffusion (1), longitudinal mass transfer (2), mass transfers effect (3) and the cumulative factor (H) on the linear velocity of the mobile phase (u)[24].

2.1.6 Instrumentation of HPLC

HPLC instrumentation is made up of four main components: solvent delivery system; sample introduction device; column and detector. Fig. 2.4 shows a schematic diagram of a high performance liquid chromatography.

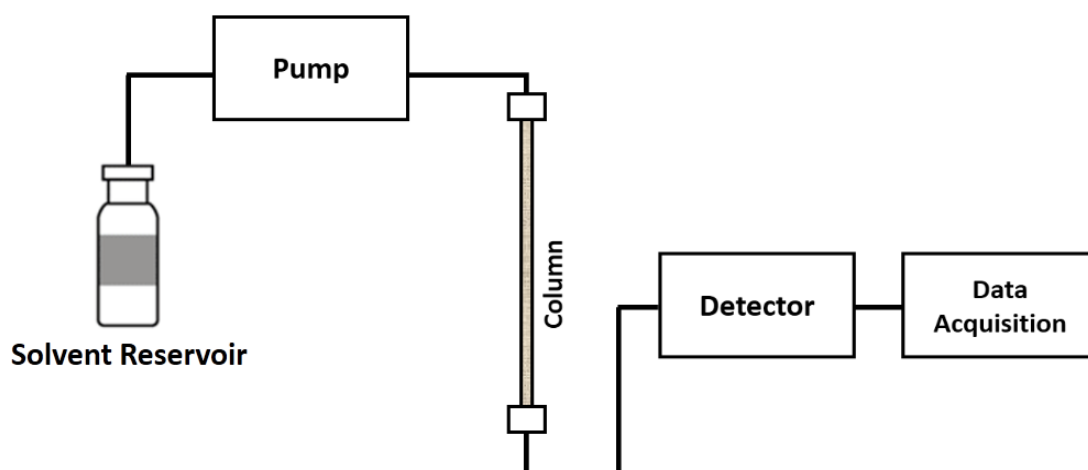


Fig.2.4. Schematic diagram of an HPLC system

- **Solvent-delivery system**

The high-pressure pump can operate at pressures from 500 to 6000 psi. The purpose of the pump is to deliver a precise, accurate, the constant and pulse-free flow of the mobile phase in to the column, in a reproducible manner. Different types of pumps used in LC are direct gas pressure system, syringe pump, pneumatic intensifier pump, reciprocating pump, etc. Reciprocating pump is the most widely used and it contains components like motor, pump are motor, ceramic piston and check valves made of a ruby ball and sapphire seat. Separations can be done isocratically, which means that the solvent composition is delivered to the column is not changing over the period. For more complex separation, gradient elution is required, which is performed by changing the proportion of eluents composition over the period. Gradient elution can be linear, stepped, or a complex sequence of each to achieve the desired separation.

- **Sample Injector**

The sample injector is one of the essential parts of HPLC. HPLC system works under high backpressures. Therefore, a special injector needed for mounting the sample on the column. Sample must be introduced as a narrow band to minimize the broadening. Sample injection with a six-port valve widely used in the HPLC system. For large number of samples, an auto-sampler is used. Fig 2.5 shows the mechanism of the injector. The loop is filled with a sample solution.

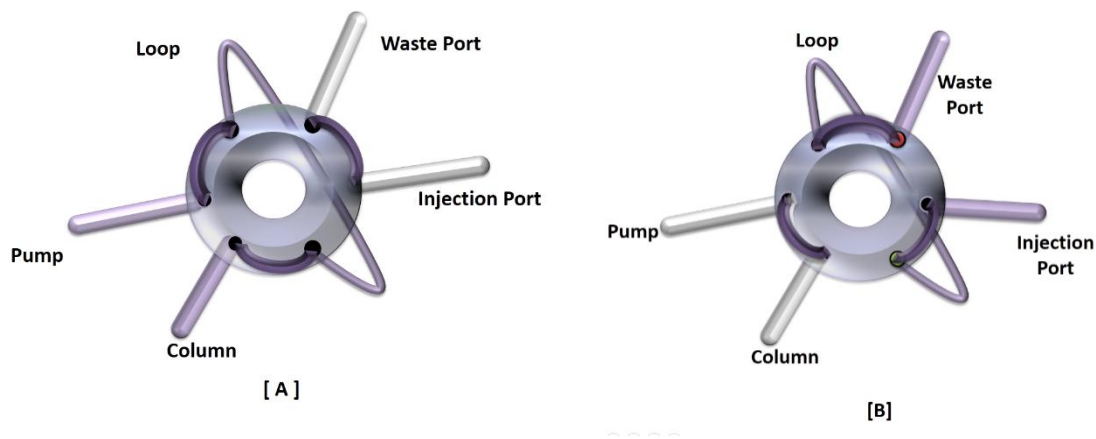


Fig. 2.5 Schematic diagram of injectors in [A] inject position and [B] load position.

- **HPLC Column**

The column is the heart of the HPLC system. Silica based column is widely used because of its good mechanical strength and high surface area. It also allows the formation of a packed bed which is stable for a long period under HPLC operating conditions. But the silica-based column has pH range restrictions. This problem to some extent is overcome by polymeric stationary phase which has a wider pH working range compared to the silica based column. Zirconia and alumina-based columns are also employed in HPLC separations. Based upon the particle types, HPLC column is classified as mentioned below

- **Totally porous silica column**

Their internal structure is totally porous. The mobile phase moves through these pores by diffusion. This type of column offers a higher column capacity. They also offer higher plate numbers (N) which results in higher separation efficiency.

- **Pellicular particle column**

Pellicular particle is made by coating a thin surface layer on a solid surface. This results in higher stationary phase mass transfer. But these particles offer less capacity due to limited surface area.

- **Superficially porous particle**

It is a hybrid of solid core with a porous outer shell. They provide much greater surface area compared to the pellicular particle resulting in higher capacity.

- **Perfusion particles**

Column contains large through-pores and diffusion-pores in a connected network. The through-pores are wide enough to allow the mobile phase to flow through it, whereas in diffusion-pores mobile phase is stagnant. The diameter of the particle is typically 20 μm . Backpressure generated here less as flow resistance is low.

- **Monolithic Stationary Phase**

It is a single piece of rod of porous materials like silica or polymer which filled the column. Their separation performance is better than the packed column. Monolith columns contain two types of pores large macropores (diameter $\sim 2 \mu\text{m}$) and small mesoporous (diameters of $\sim 10 \text{ nm}$). Therefore, the backpressure generated by this column is less compare to conventional particulate columns. A higher flow rate can be used in a monolith column without loss in column efficiency [25]. Both silica and polymer-based monolith column were employed for present work which will be described here briefly.

2.1.7 HPLC Detector

Due to the detectors used, HPLC offers quantitative information simultaneously with separation. HPLC detectors are classified as either bulk property detector of the eluent such as refractive index or conductivity, or solute property detector, which respond to the property of analyte such as UV absorbance.

Characteristics of detectors [24]

Table 2.1 HPLC Detectors

Concentration sensitive	Mass sensitive
UV-Vis	Electrochemical
Fluorescence	Conductivity
Evaporative light scattering	
Refractive index	
Mass-spectrometry	
Radioactivity	

- **Concentration or Mass Sensitivity**

Detector producing a signal proportional to a concentration known as concentration sensitive. Whereas detector producing a signal proportional to mass are known as mass sensitive detectors. Different detectors used are listed in Table 2.1.

Selectivity

Based on selectivity detectors are classified as a selective or non-selective detector. For e.g. refractive index (RI) detector which records the change in the refractive index of the eluate. It is the property of the bulk. Hence they are known as non-selective detectors. The non-selective detector is not suitable in gradient elution condition where the solution composition changes with time. In the case of the selective detector, the response of the detector depends upon the analyte property. Therefore, they are selective to the nature of the analyte and known as selective detectors. For e.g. in the case of UV detectors the analyte which absorbs the UV light only get detected. Therefore, they are selective.

- **Noise**

Noise is a baseline disturbance. Motors or other appliances operated on the same electrical circuit contribute to noise. The pump used to deliver the post-column derivatization also contributes to noise. Noise cannot be completely removed. Detector's time constant and the data sampling rate are used to reduce the noise.

- **Detection limit**

This is the limiting factor of the detector for a particular application and one of the most important aspects of the detector while developing a method for the trace elemental analysis . For qualitative analysis minimum three times and for quantitative analysis, minimum ten times height of the largest peak of the noise is recommended. In HPLC derivatization technique is used to improve the detection limit of the analyte. The detection limit can also be improved by coupling the detectors like mass spectrometers.

- **Drift**

Deviation from the baseline is known as drift. Drift is almost unavoidable in case of gradient elution which is essential for the separation of Individual lanthanides. Drift is also produced due to the change in temperature during the run. Blank run at the start of day takes care of drift to some extent.

- **Linear Range**

The linear range must be as wide as possible. The detector must produce the signal proportional to the amount of sample. The linearity range in the case of UV detector is high compare to RI detector. Mass spectrometric detectors offer very wide linearity range. High linearity range allows the measurement without dilution which avoids dilution errors.

- **UV-Detectors**

The UV-Visible detector is the most commonly used detector in HPLC. It is useful for the compounds which absorb light in the UV-Visible region. According to Beer–Lambert law, the absorption "A" of an analyte by passing the light beam through the cell is a function of molar absorptivity " ϵ ", molar concentration "c" and the path length l.

$$A = \epsilon cl$$

Analyte having double bond adjacent to an atom with a lone electron pair, e.g. bromine, iodine or sulfur, a carbonyl group, a nitro group, two conjugated double bonds, an aromatic ring, inorganic anions such as Br^- , I^- , NO_3^- can be analysed by UV detector above wavelength 200 nm. Analyte sometimes have poor or no response to UV detectors. Following methods can be used for their detection.

- **Indirect Detection**

This technique is used when a non UV absorbing species need to be analysed. In this case, mobile phase used is UV absorbing. When non-absorbing analyte pass through detector cell will give negative peak because there will be less light absorb.

- **Derivatization**

Derivatization means changing the analyte in a specific way to enhance their sensitivity. If derivatization is carried out before chromatographic injection, it is known as pre-column derivatization. Pre-column derivatization may improve the chromatographic parameters of the sample. It may also serve the purification and processing of sample. If derivatization is carried out post-separation and before detection, it is known as post-column derivatization. An additional detector can be used before derivatization. Work reported here used post-column derivatization technique for the detection of U, Th, and lanthanides using Arsanazo (III) as a derivatization reagent.

HPLC UV-Diode array detectors (UV-DAD Detector)

In case of UV-DAD detector (fig. 2.6) full light pass through the detector cell using a collimator. Therefore, sample is exposed to full range of wavelength. Subsequently this light dispersed using prism or gratings. The light then fall on diode array consist of a large number of diode arrange side by side. The output of each diode is sampled and stored by a computer.

Advantages of HPLC UV-DAD detector

1. It is possible to obtain a UV spectrum for individual peaks. UV spectra can be used for identification of a compound by comparing it with library.
2. It offers both selectivity as well as sensitivity, as monitoring individual solutes at its λ_{max} is possible.
3. A suitable wavelength can be identified using UV spectrum for quantification.
4. Peak purity can be found out.
5. Baseline drift is reduced by subtracting two different wavelengths monitored.

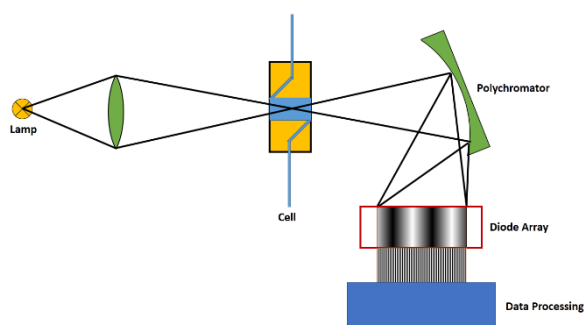


Fig. 2.6 Principle of diode array detector [24]

- **Hyphenated Detectors**

Coupling of liquid chromatography with instruments like mass spectrometer (MS), nuclear magnetic resonance (NMR), infra-red (IR), etc. is referred here as hyphenated detectors. A combination of mass spectrometers with liquid chromatography is the most widely used hyphenation technique. It is useful in providing structural information or eliminating the ambiguity for the identification of unknown.

2.1.7 Liquid Chromatographic Technique for Separation of Rare Earth Elements

Rare earth elements have become an integral part of modern era because of their wide and growing applications in different industries. The increase in demand and applications in different industries like geological, environmental, food and nuclear have enhanced the need for rapid, accurate and sensitive methods for the determination of rare earths in different matrices.

The most important feature of REE's chemistry is the similarities in their chemical properties due to very small difference in ionic size of the Ln^{+3} ions arising as a result of lanthanide contraction. Similarities in chemical properties make the separation of individual REE's a challenging task by conventional separation techniques.

Classical methods like gravimetry, complexometry and colorimetry are not selective in nature and generally used for the determination of total REE content. Techniques like mass spectrometry (MS), neutron activation analysis (NAA) and spectroscopic techniques are selective and sensitive in nature but suffer from matrix interference. This problem can be overcome by coupling these techniques with suitable separation technique. Separation techniques like chromatography, electrophoresis, solvent extraction, precipitation, gravimetric, solid phase extractions, electrochemical techniques are being employed for separation of rare earths. Separation of rare earth is generally a two-step procedure, first step being the group separation of rare earths from matrix followed by individual separation of rare earths.

Chromatography is one of the most powerful techniques for separation of rare earths because of plethora of available stationary and mobile phase combinations. Chromatography has many advantages; it can couple to suitable detection techniques to carry out sensitive analysis. Different modes of chromatography like liquid, gas and supercritical fluid chromatography are being used for separation of group as well as individual separation of REE's. Gas

chromatography as well as supercritical fluid chromatography has limited application for REE's separation due to the non-volatility of the analytes.

Liquid chromatography is the most widely used chromatographic method for the separation of rare earth. Different types of liquid chromatography like ion exchange chromatography, ion chromatography, ion-pair reverse phase chromatography, extraction chromatography are being used for separation of rare earths.

REE's can be separated by both cation and anion exchange method. Cation exchange based methods are more frequently used for separation of REEs as compared to anion exchange methods. Ion exchange chromatography exploits the differences in hydrated radii and formation constant of the complex formed between REE's for separation.

Due to high charge on REEs, they retain very strongly on the cation exchange stationary phase and cannot be eluted unless high concentrations of acids are used as eluents. It has been established that the use of chelating agents in the mobile phase is the best approach for the efficient and faster separation of REEs. On the early stage of REEs separation, glass or stainless steel column filled with Dowex 50 X 8 as a cation exchanger was used for separation of REEs using citric acid as an eluent. α -hydroxy isobutric acid (α -HIBA) has become one of the best complexing agents for the cation exchange separation of REE's till date.

Rollin et al. [26] used IonPac CS10 cation exchange column as a stationary phase and sequential elution with 1 M HCl and α -HIBA to carry out the separation of uranium, thorium and REE's elements. This method could be employed for the determination of REE's and actinide elements in nuclear materials. Schwantes et al. [27] used CS-3 cation exchange resin as a stationary phase and different concentrations & pH of α -HIBA as a mobile phase to obtain the separation of five pairs of REEs elements (Tm/Er, Gd/Eu, Eu/Sm, Sm/Pm and Pm/Nd) in 15 min. Recently, Borai et al. [28] studied various chelating agents such as (full name) DTPA, PDCA (2,6-pyridinedicarboxylic acid), (full name) NTA, α -HIBA and oxalic acid as mobile

phases, and observed that separation efficiency of the investigated eluents are mainly dependent on the number of carboxylic acid and geometrical arrangement of the chelating agent. Anion exchange resin (AG 1 X 2) in combinations with methanol-nitric acid mixtures is used for separation of Nd from irradiated UO₂ sample followed by their determination by isotope dilution based mass spectrometric method [29].

In ion chromatographic (IC) separation of REEs two columns are used. Separation takes place in the first column and the second column is used to adsorb the ions which may hinder the conductometric detection of the analytes. Earlier, IC was not suitable for rare earth separation as hydroxide based suppressor column caused the precipitation of REEs hydroxides. Development of non-suppressed IC paved the way for the analysis of rare earths by this technique. Another problem encountered in the use of IC is that the non-compatibility with gradient elution which is an essential requirement for high efficient rare earth separation. The advantage of the IC separation technique is the easiness in direct coupling to high sensitive detection systems such as ICP-MS, ICP-AES. Sevenich et al. developed a single-column method for REEs separation by using a conductivity detector and ethylenediammonium/tartrate as eluent. The substitution of tartrate with α -HIBA improved the separation [30]. Wang et al. [31] employed a non-suppressed IC for separation of the REE's using a cation exchange resin with 2-methyl lactic acid as eluent and post-column derivatization with Az (III) followed by detection at 600 nm. Dybczynski et al. [32] carried out pre- and post-irradiation group separation for the determination of individual REEs with special emphasis on Gd, Ho, Er, Tm and Lu. In this work the same separation scheme was combined with IC yielding good separation for all REEs and yttrium.

Thin layer chromatography (TLC) and Paper chromatography (PC) are basically two modes of planar chromatography. Both PC and TLC can be considered as qualitative or semi-qualitative techniques and are versatile and cost effective for REE'S separation. However,

due to dominance of HPLC in REEs separation, utilization of these techniques is very much limited.

The stationary phase of PC for separation of REEs include cellulose, inorganic or organic ions infiltrated cellulose, ion exchanger infiltrated cellulose and chelating agent infiltrated cellulose. For the separation of REEs by using PC, inorganic acid aqueous solution or its mixture with organic solvent were used as mobile phase. Complexing agents like lactic acid [33], α -HIBA [34] and EDTA [35] can be introduced into the mobile phase to improve the distribution property of REEs. However, complete separation of all the REEs is yet to be achieved by this approach. PC relies on chromogenic complexing reagents such as Alizarin Red, 8-hydroxyquinoline, Arsenazo I, II or III and pyridyl azo resorcinol (PAR) for detection. TLC is further categorized as normal and reversed phase (RP). The separation of REE's is found to be poorer in the normal phase as compared to RP. In TLC, silica gel is the most commonly used carrier whereas cellulose is found to be particularly suitable for the separation of light REEs. The Mobile phase for normal-phase thin-layer analysis of REEs is a combination of extractants, organic solvent and acid solution. For example, di(2-ethylhexyl) phosphoric acid–ether–HNO₃ and TBP–hydrocarbon–HNO₃ are preferable mobile phases in TLC. In RP-TLC, the layer is usually impregnated by extraction agents such as di(2-ethylhexyl) phosphoric acid, TBP and TOPO. Takeda and Ishida [36] used trihydroxy methyl amine and HCl-impregnated silica as stationary phase, and different alkali metal nitrate solutions as mobile phase to separate all the REEs except Pm. Later on, they used both carboxy methyl cellulose & aqueous sodium nitrate systems and carboxy methyl cellulose with aqueous sodium chloride for the separation of REEs. Soran et al. [37] studied the separation of REEs by TLC using silica and ammonium nitrate-impregnated saturated silica as stationary phase, and di(2-ethylhexyl) dithiophosphoric acid as complexing agent in the

mobile phase. In another work, [38] they also used mobile phase containing di(2-ethylhexyl) disulfophosphate and di(isobutyl) disulfophosphate to separate Uranium, Thorium and REEs. Extraction chromatography is the application of solvent extraction technique in chromatographic mode. In this technique, a suitable extractants is adsorbed on a solid support. For the separation of REEs, organophosphate based extracts are extensively studied. HNO_3 , H_2SO_4 or their combination are generally employed as mobile phase. The stationary phases loaded with acidic organophosphorus extractants viz. di(2-ethylhexyl) phosphoric acid and 2-ethylhexyl hydrogen 2-ethylhexyl phosphonate in combination with inorganic acids is the most commonly used extraction chromatography method for separating REEs.

Trace rare earth impurities were determined in high-purity Cerium Oxide and Lanthanum oxide using electro thermal vaporization (ETV) ICP-OES and ICP-MS, respectively, after HPLC separation with 2-ethylhexyl hydrogen 2-ethylhexylphosphonate resin as the stationary phase [39]. A single-step extraction chromatographic separation method for Sm and Nd isotope analysis of micro-samples of silicate rocks followed by thermal ionization mass spectrometry (TIMS) was developed by Li et al. [40]

In Capillary Electrophoresis (CE) methods, mobile phase flow is generated under the influence of applied electric field analogous to HPLC where pressure is used for same purpose. Analytes migrate through electrolyte solutions under the influence of an electric field and separation is based on the difference in the ionic motilities of the analytes.

Capillary zone electrophoresis (CZE) and capillary isotachopheresis (CITP) are the most widely used CE modes in REEs separation and analysis. REEs are not well separated with conventional CE as the mobility difference among REEs is very small owing to the small difference in their charge to radius ratio. Addition of complexing agents helps in enlargement of the differences in mobility of REE. CE provides separation of rare earths in shorter times with higher peak capacity than conventional liquid chromatographic techniques.

First CE separation of all the REEs in 15–20 min was achieved by Korchemmaya in 1970. Later on Foret et al. [41] had separated 19 metal ions including 14 REEs in 5 min. Subsequently, Jandick et al. [42] had carried out the separation of 24 ions, including REEs in 5 min. Chen and Cassidy [43] compared the CE separation of REEs with different capillary coatings. With benzyl amine amino toluene and α -HIBA as complexing agents, 14 REEs could be separated in 6 min by using Cl-coated capillary, while the separation time was 8 min when C18-coated capillary was employed. Post- separation, UV spectrometry was used for the detection of REE's . Laser-induced fluorescence (LIF) was used as a detector for the CE separation of the complexes of REEs with fluorescein-thiocarbamyl-1-(4-aminobenzyl) ethylenediamine-N,N,N',N'-tetraacetate by Saito et al. [44] to improve the detection limits. ESI-MS and ICP-MS are also employed as detectors in CE for the analysis of REEs.

Supercritical fluid chromatography (SFC) uses supercritical fluid as a mobile phase. β -diketonates complexes of REE's were separated using CCl_2F_2 and CO_2 mobile phase. Separation of REEs chelates of acetylacetone (ACAC), trifluoroacetylacetone, thenoyltrifluoroacetone, dipivaloylmethane, and octanedione derivative were investigated with ethanol-modified inert silylated column [45]. SFC instruments are relatively complex due to high pressure and temperature requirements and hence not popular as HPLC. SFC are rarely used for REEs separation.

- **Dynamic ion exchange HPLC method for REEs separation**

Dynamic ion exchange method (also known as ion-pair/ion-interaction) is one of the best methods for the separation of individual REE's (Fig.01). In dynamic ion-exchange technique, a reversed phase column coated with suitable ion interaction agent (IIR) like octane sulfonate to convert the conventional reversed phase column into cation exchange column. IIR has a long hydrophobic tail and a charge which is opposite to the charge of the analyte to be separated. The IIR imparts a charge to the surface of stationary phase. As IIR is continuously

passed through the column, constant interchange of the surfactant happens between mobile phase and stationary phase. The important advantages of this approach over conventional bonded ion exchangers are higher efficiency of separation and variable capacity. The reversed phase column can be easily recovered back by just flushing the column with methanol and this feature is especially important in case of separation of radioactive samples. During separation of radioactive elements by conventional ion exchange, the surface gets damage due to radiations emitted by radionuclides whereas in case of dynamic modification, the surface can be easily replenished. After precondition of the column with IIR, separation of individual REE's are achieved using suitable complexing agent like α -HIBA. For individual separation of REEs a concentration gradient of α -HIBA is applied.

Different models are proposed to explain the mechanism involved in dynamic ion exchange separation. One model suggests that the analytes gets exchanged between the stationary phase and mobile phase by ion exchange mechanism. In another model, an ion pair is formed between analyte and IIR. This ion pair gets partitioned between reversed phase surface of the stationary phase and the mobile phase. The third model, ion interaction model encompasses the features of both ion exchange and ion pair models.

Dynamic ion exchange method was used for separation of individual REEs for burn-up determination from spent fuels [46,]. Cassidy et al. established this method for the determination of fission in irradiated (Th,U)O₂ and UO₂ samples [47,48]. Elchuk et al. used this technique for the determination of ¹⁴⁷Pm in urine sample [49]. Barkley et.al. determined REEs and thorium in samples from uranium ore refining process using dynamic ion exchange method [50].

- **α -Hydroxy isobutric acid as a complexing agent for REEs separation**

Aqua complexes of REE's have very small difference in their stability constants. Separation factor values between the adjacent pair are very small for analytical applications. This limitation of ion exchange led to the development of a procedure for separation using aqueous chelating agents. Addition of complexing agent helps in alteration of selectivity of REE's to the ion exchanger. In addition to the primary equilibrium between the REE's and the ion exchanger, a secondary equilibrium established between ion exchanger and the REEs which results in the change in selectivity. The difference in the stability of the REEs complexes and the affinity of the complex to the stationary phase decides the separation.

REEs are hard acids and have strong preference for complexing agents having oxygen donor atoms. The most efficient separations will be achieved when the REEs is more strongly transported to the counter phase and more weakly complexed by the aqueous complexant (or vice versa). Oxygen donor weak organic acids are preferred for this purpose as they form complexes with REEs even at low concentrations. Different complexing agents like citric acid, lactic acid, EDTA are studied for separation of REE's [51]. Though these chelating agents showed some success, they suffered many limitations and reduce their utility. Amino poly carboxylate like EDTA, DTPA are better for separation of individual REE's, however, utilization is limited because of their excessively slow kinetics.

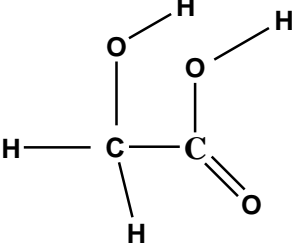
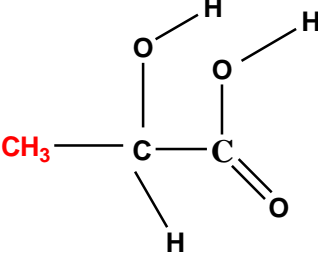
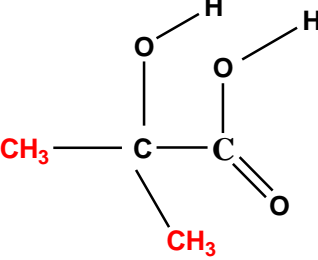
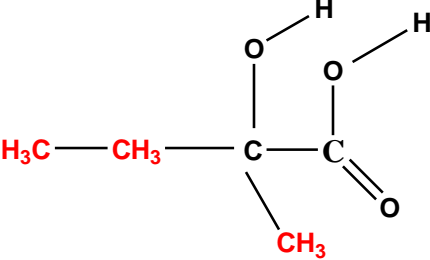
Thermodynamic study of REE's with α -HIBA and structural analog of α -hydroxy carboxylic acid without OH at alpha carbon position reveals that REEs complex formation favors in case of α -hydroxy carboxylic acid [52]. Among the different carboxylic acid eluents, a hydroxide group on the α -carbon atom creates the possibility of simultaneous coordination of both a carboxylate oxygen and the hydroxide, thus creating a chelate complex of enhanced stability. However, the oxygen donor group at α position does not necessarily translate into consistent variation of stability of REE's complex. Oxalic acid, glyoxylic acid, and malonic acid also

exhibit consistent trend in the stability of their REE's complexes as in case of α -HIBA. The polydentate α -hydroxy complexant, citric acid does not exhibit as consistent trend across the series of lanthanides as α -HIBA. An ether oxygen in the α -position (bridging a second carboxylate group- diglycolic acid) is likewise a poor reagent for a complete separation when compared to α -HIBA [53].

Among lactic acid, α -HIBA and glycolic acid and α -H- α -MBA (Table 2.2), we found that substitution of methyl group plays a very important role, which reflects in stability constants of REE's. Addition of methyl group increases the electron density around the oxygen atom of both hydroxy as well as carboxylic group and this makes it a weak acid. Therefore, strength of acid decreases from glycolic acid to α -H- α -MBA. It may have happened that the α -HIBA offer enough acidic strength which forms complex with all the lanthanides ligand and offers small but consistent variation among all the lanthanides.

Therefore, in chromatography α -HIBA remains as the most popular eluent. α -HIBA was first reported by Choppin et. al. for separation of individual members of the REE's series from a mixture using column chromatography on Dowex 50 cation-exchange resin. Its practicality is due to the stability of REE- α -HIBA complexes which is different for individual REE and steadily decreases from Lu-La. Chromatographic methods that employ α -HIBA, display the greatest separation efficiency for individual separation REE.

Table 2.2: Alpha hydroxy carboxylic acids [54]

<p>Glycolic acid pka – 3.83</p>	 <p>The structural formula of glycolic acid shows a central carbon atom bonded to a hydrogen atom on the left, another hydrogen atom below, and a hydroxyl group (-OH) above. This central carbon is also bonded to a carboxyl group (-COOH) on the right, which consists of a carbon atom double-bonded to an oxygen atom below and single-bonded to a hydroxyl group (-OH) above.</p>
<p>Lactic acid pka – 3.86</p>	 <p>The structural formula of lactic acid shows a central carbon atom bonded to a methyl group (-CH₃) on the left, a hydrogen atom below, and a hydroxyl group (-OH) above. This central carbon is also bonded to a carboxyl group (-COOH) on the right, which consists of a carbon atom double-bonded to an oxygen atom below and single-bonded to a hydroxyl group (-OH) above.</p>
<p>α-HIBA pka – 3.97</p>	 <p>The structural formula of α-HIBA shows a central carbon atom bonded to a methyl group (-CH₃) on the left, another methyl group (-CH₃) below, and a hydroxyl group (-OH) above. This central carbon is also bonded to a carboxyl group (-COOH) on the right, which consists of a carbon atom double-bonded to an oxygen atom below and single-bonded to a hydroxyl group (-OH) above.</p>
<p>α-H-α-MBA pka – 4.05</p>	 <p>The structural formula of α-H-α-MBA shows a central carbon atom bonded to two methyl groups (-CH₃) on the left, another methyl group (-CH₃) below, and a hydroxyl group (-OH) above. This central carbon is also bonded to a carboxyl group (-COOH) on the right, which consists of a carbon atom double-bonded to an oxygen atom below and single-bonded to a hydroxyl group (-OH) above.</p>

2.2 Mass Spectrometry

Mass spectrometry is a powerful analytical technique used in obtaining qualitative and quantitative information of trace, ultra-trace levels of organic compounds and inorganic elements. It covers the applications like identifying the unknown compounds by determining the molecular weights and providing information on fragmentation pattern, bulk surface and depth analysis etc. Mass spectrometry provides sensitivity, selectivity and specificity and therefore finds applications in different areas such as biological, nuclear technology, chemistry, physics, medicine, materials science, environment, forensic, astronomy, archaeology and many more.

2.2.1 Processes in Mass spectrometry

Three processes that occur in mass spectrometry are ionisation, sorting of ions and detection. Therefore, mass spectrometric instrument contains following parts. (Fig 2.7)

1. Sample Introduction
2. Ion Source
3. Mass Analyser
4. Detectors
5. Data Acquisition and Processing System.
6. Vacuum

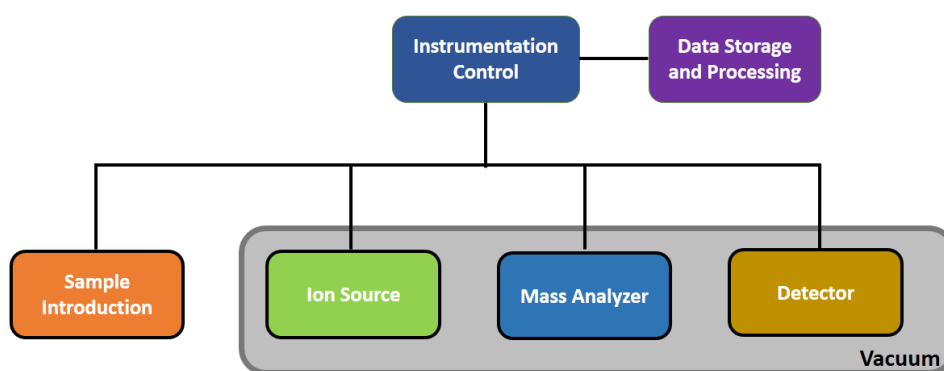


Fig. 2.7 Block diagram of mass spectrometer

Depending upon the type of ion source, solid, liquid, or gaseous sample is introduced in the ionisation source to convert into ions. These ions are then extracted and sorted in mass analyser

according to their mass to charge ratio (m/z). In special cases, fragmentation of separated ions is carried out to extract more information on the analytes. These sorted ions then detected simultaneously or sequentially by using suitable detectors. As in all these processes gaseous ions are involved, their mean free path must be maintained and hence vacuum becomes an essential part of the mass spectrometry. Finally, data storage and data processing is carried out using a computer [55].

2.2.2 Instrumentation

- **Ion Sources [56]**

Neutral analytes cannot be manipulated by electrical or magnetic fields. Therefore, neutral analytes are first convert into charged species by ionisation in the ion source. Ionization of analytes is carried out by using different methods such as electron removal, protonation, electron capture, adduct formation or transferring the charged ions from the condensed phase to the gas phase. The process of ionization adds energy to the analyte molecules. Depending upon the amount of energy acquired by analyte during ionisation, ions remain intact or fragment into smaller pieces. During ionization, if the energy acquired by the analyte is sufficient for its ionization but prevents further fragmentations then it is termed as soft ionisation. If energy acquired by analyte causes the fragmentation of the analyte into smaller pieces, the ionisation process is termed as hard ionisation. Selection of ion source depends upon the application as well as on type of information required. Ion sources are classified based on hard and soft ionisation (Table 2.3).

Table 2.3: Classification of Ion Source

Hard Ionisation	Soft Ionisation
Electron Ionisation (EI)	Matrix Assisted Laser Desorption (MALDI)
Chemical Ionisation (CI)	Atmospheric Chemical Ionisation
Laser Ion Source (LIMS)	Electrospray Ionisation (ESI-MS)
Spark ion source (SSMS)	
Glow Discharge Source (GDMS)	
Secondary Ion Source (SIMS)	
Thermal Ionisation Mass Spectrometry (TIMS)	
Inductively Coupled Plasma (ICP-MS)	

- **Mass Analyser**

The mass analyser is the heart of all mass spectrometers. The role of the mass analyser is to separate ions according to their m/z values. Mass analysers separate ions in time or in space. Scanning analysers like magnetic field or quadrupole transmit the ions along a time scale. However, the mass analysers like time of flight (ToF) and ion traps allows the simultaneous transmission of all the ions. Magnetic analyser when coupled with multiple detectors, provides for the simultaneous transmission of different ions based on their m/z .

The main characteristics for comparing the performance of a mass analyser are the mass range limit, the analysis speed, the transmission, mass accuracy and the resolution (Table 2.4).

In order extract more information, different mass analysers may be coupled in different combinations. This feature increases the versatility and allows for performing multiple experiments. Tandem mass spectrometry refers to mass spectrometer/mass spectrometer (MS/MS) for e.g. Q-q-Q and ToF-ToF. Hybrid mass analyser combines two or more dissimilar

mass analysers for e.g. Q-ToF. MS/MS analysis facilitates the structural information through the identification of unknown from fragmentation pattern.

Table :2.4 Different types of mass analyser and their characteristics [56,57]

Mass Analyser	Magnetic Analyser	Quadrupole	Time of flight	Orbitrap	FT-ICR
Ion Beam	Continuous	Continuous	Pulsed	Pulsed	Pulsed
Separation Mechanism	Momentum	Stable trajectory	Flight time of ions	Resonance frequency	Rotation
Detection	Ion current	Ion current	Ion current	Image current	Image current
Resolution (m/Δm)	1000	Unit	20000	50000	1000000
Mass Accuracy	< 10 ppm	100 ppm	10 ppm	< 5 ppm	< 5 ppm
Mass limit	20000	3000	< 500000	50000	500000
Pressure (Torr)	10 ⁻⁵	10 ⁻⁵	10 ⁻⁷	10 ⁻¹⁰	10 ⁻¹⁰
Benefits	High precision	Scanning , SIM, sensitivity	High Mass Resolution spectra Highest Mass range Simultaneous monitoring of different ions	High Mass Resolution	Highest Mass Resolution
Limitations		Nominal Mass Only	No SIM	Resolution drop with mass collection speed	Resolution drop with mass collection speed

- **Detector**

The ions separated in mass analyzer are allowed to get detected by a suitable detector. Detector produces electric current proportional to the abundance of the ion detected. Type of detectors used depend upon the combination of ion source and mass analyzer used and application. Since the amount of ions coming out from the analyzer is generally quite small, amplification of signal is required for usable signal. Except faraday cup and image current detection other detectors amplify the signal output by cascade effect. Mass spectrometric detectors are classified as point ion

collectors and array collectors. In point ion collector's detectors, the ions are monitored sequentially. In the case of array detectors, all the ions are monitored simultaneously.

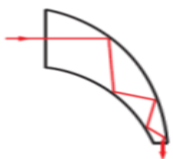
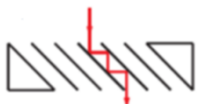
- **Faraday Cup**

Initially this was the commonly used detector in mass spectrometry due to its simple, precise and robust operation. It is a metal container in which ions sorted from mass analyzer get discharged and generate current. It does not provide any amplification and used only when sufficient quantities of sample is available. It is slow and hence not appropriate for scanning mode. It is now used only for isotope ratio measurement.

- **Electron Multipliers**

Fundamental mechanism of the all type of electron multipliers are the same. Ions from the mass analyzer interact with the surface of the detector and produce electrons. With cascading effect of the other dynodes, electrons get multiplied. Electron multipliers comes in a variety of forms.

Table 2.5: Different Electron Multipliers configurations

Discrete dynode electron multiplier	
	It is composed of a series of copper beryllium plates between which electrons cascade.
Continuous dynode electron multiplier	
	It consists of leaded glass funnel coated inside surface with semiconductor materials.
Multichannel plate detector	
	It is a porous glass plate in which each pore acts as a mini electron multiplier

- **Discrete dynode electron multiplier**

Primary electron is produced using conversion dynode. Electron get multiplied between a series of copper beryllium plates acting as a mirror reflecting the electrons and there by amplifying the signal at each step.

- **Continuous dynode electron multiplier**

A glass funnel is used where a voltage gradient is provided on a resistive surface. Electron enters the funnel and gets amplified to produce enhanced sensitivity.

- **Multichannel plate detector**

It consists of a plate containing parallel cylindrical channels. This channels are coated with semiconductor layer to perform multiplication of electrons. Each channel works like individual electron multiplier.

- **Daley Detectors**

Ions interact with the plate of Daley detector coated with the scintillator to produce photons. This photon then amplified using photomultiplier tube.

- **Vacuum system**

Ions while migrating through different sections of mass spectrometer may collide with other gaseous molecules or wall of the container. To increase their mean free path, vacuum is employed. Further in LC-MS, ionisation takes place at room temperature. While extracting the ions inside the mass spectrometer, large volumes of other gaseous cause heavy load on vacuum system. Hence differential pumping is provided to achieve better ion transmission efficiency . Generally, combination of pumps is used to active the desired vacuum. Based on the mechanism of pumping, vacuum pumps can be classified as

- **Positive displacement pump**

This type of vacuum pump expands a cavity and allows the gases to flow out of the sealed chamber. Then the cavity is sealed and causes it to exhaust in to the atmosphere. Rotary pumps work on this principle. These type of pumps are used to generate low levels of vacuum.

- **Momentum transfer pump**

In momentum transfer pump gas molecules are accelerated from the vacuum side to the exhaust side. They impose a net directional motion to the residual gases. Turbo molecular pump and diffusion pump work on this principle.

- **Entrapment pumps**

Entrapment pumps work by way of chemical reactions and are placed inside the chamber to be vacuumed. The molecules in the air are made to chemically react with the internal surfaces of the pump. Cryo pump and ion getter pump work on this principle.

2.2.3 Electrospray ionization Mass spectrometry

Electrospray ionization technique comes under the category of soft ionization. In electrospray ionization technique, ions are produced from liquid phase with the aid of high voltage at atmospheric pressure. As ions are produced directly from solution phase at atmospheric pressure, liquid phase separation techniques like LC and capillary electrophoresis can be

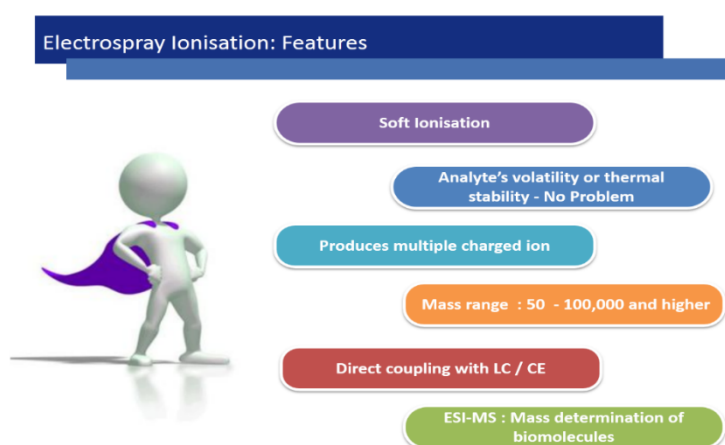


Fig 2.8 features of ESI-MS

connected to ESI-MS for separation and purification of analyte prior to mass spectrometric analysis. In ESI-MS, multi-charged species are formed which allow the measurement of very high molecular species with mass analysers with limited mass range. Although the ESI-MS has major impact in biology and proteomics, its applications have been extended to inorganic and metal-organic complexes also. Though the flexibility and simplicity are attractive features of ESI-MS, the main limitation of the techniques is interpretation of the complex ESI spectrum due to the adduct formation, multiply charged species etc. (Fig. 2.8)

- **Electrospray Ionisation Mechanism [58]**

Sample solution is passed through metal capillary at low flow rates (0.1 to 10 micro L/min). High voltage (2 – 5 kV) is applied between the capillary and a counter electrode. The strong electric field charges the surface of the liquid emerging from the capillary and forms a fine spray of charged droplet. Nebuliser gas further assists the droplet formation. As a result of this, liquid coming out from the capillary forms Taylor cone. When coulombic repulsion of the surface charge overcomes the surface tension of the sample solution (Rayleigh limit), droplets containing excess charge are formed. While the droplets move towards the mass spectrometer they shrink in size. This shrinkage of droplets in size is facilitated by the curtain gas which is flowing in opposite side at elevated temperatures. Finally, ions come out of droplet and get extracted into the mass spectrometer. Two mechanisms are proposed to explain the ion formation in electrospray viz. ion evaporation and coulombic explosion. (Table 2.6)

Table: 2.6 Types of commonly observed ions in Electrospray ionization mass spectrometry [28]

Cation	$[M + H]^+$	Positively charged ion
Anion	$[M - H]^-$	Negatively charged ions
Protonated Molecule	$[M+H]^+$	Positive ion formed by addition of proton
Deprotonated Molecule	$[M-H]^-$	Negative ion formed by removal of proton
Adduct ion	$[M + Na]^+$ $[M + Cl]^-$ $[M + NH_4]^+$	Ions formed by the addition of an ionizing species to a molecule
Multiply charged ion	$[M + nH]^{n+}$ $[M - nH]^{n-}$	Species containing multiple charge generally observed in analysis of protein and peptides

- **Instrumentation of Electrospray ionisation mass spectrometry (Fig. 2.9)**

Electrospray ionization takes place in ion-source. It consists of a two concentric capillary tubes. The solution is infused through a syringe pump at a low flow rate (0.1-10 μ L/min) into the capillary. High voltage (2-4 kV) is applied between the capillary and the spray shield. Nitrogen is used as an auxiliary gas and curtain gas. Auxiliary gas assists in droplet formation. Curtain gas at elevated temperatures passed from opposite direction assist in solvent evaporation. Under high voltages, formation of charged droplets takes place. Depending upon the nature of the analytes, positive or negative potential is applied. In ESI-MS, ions are formed at atmospheric pressure whereas mass spectrometers work in vacuum. Therefore, differential pumping is required to effectively extract the ions from atmospheric region to low pressure region.

Ions formed in ion-source get extracted to the ion optics inside the mass spectrometer through a glass capillary. Capillary also isolates the high voltage zone and low voltage ion optics. Ions

coming out from the glass capillary enter into the next compartment consisting of two funnel and hexapole. Ion-funnels are closely spaced rings with decreasing diameters where RF and DC potential are applied. Ions coming out from capillary also accompanied by solvent cluster, curtain gas and other neutral are taken care by the dual funnel assembly. The variation of the DC potential of funnel is used to carry out the in source collision induced dissociation studies. After dual-funnels, ions are extracted into a hexapole where ions are focussed on a hexapole axis using RF voltage.

Ions then enter into Q-q stage. The first quadrupole acts as a mass filter allowing ions of certain range to pass through it (ms/ms mode) or acts as a simple ion transmitter (MS mode only). The selected ion enters in to collision cell, filled with a collision gas (Ar gas). Inside the collision cell, the ion can be accelerated to different energies and allowed to collide with the collision gas leading to fragmentation of the ions. Fragmented products along with un-dissociated parent are then analysed by a second mass analyser i.e. time of flight. ToF mass analyser are worked in pulse mode. Here ion beam is chopped into bunches and gets accelerated into flight tube. In ToF heavier ions moves slowly compare to the lighter ions under identical potentials. The ions accelerated in flight tubes have small differences in their kinetic energy which is taken care by ion-reflectors. Finally separated ions are get detected by microchannel plate (MCP) detectors.

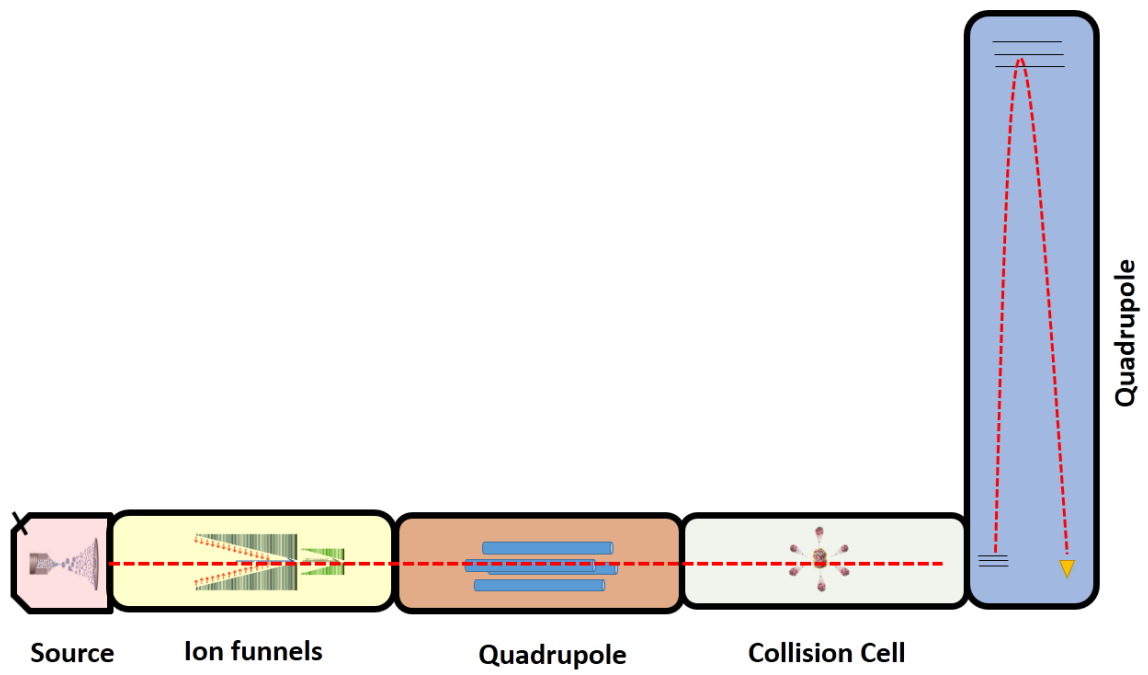


Fig. 2.9 Block diagram of ESI-MS

2.3 Gamma Ray Spectroscopy

Gamma spectroscopy is powerful radioanalytical technique for simultaneous multi-element analysis with high sensitivity, low detection limits and non-destructive analysis capability. Radionuclide with nuclear instability undergo emission of alpha or beta decays to achieve more stability. The parent radionuclide undergoes alpha and beta decay, leave the daughter radionuclide most of the time in excited state. Excited state may also result from nuclear reactions and direct excitation from ground state. An excited state radionuclide comes to lower energy state or ground state by emission of energy in the form of electromagnetic radiation known as gamma rays. Gamma rays has energy range from few KeV to MeV. Gamma ray count rate can be correlated to parent's disintegration rate. Gamma ray spectroscopy can be used for qualitative or quantitative estimation of elements, to study nuclear reactions, in separation science as a radiotracer and also for isotopic composition determination.

2.3.1 Interaction of gamma ray with matter [59]

Gamma ray interact with material in following three ways.

- **Photoelectric Effect**

In photoelectric effect the gamma ray interacts with an atom of an absorbing material. After absorption of energy, photoelectron is produced from one of the bound shell of the atom of absorbing material (Fig.2.10). The kinetic energy of the photoelectron thus produced is given by

$$E_e = E_\gamma - E_b$$

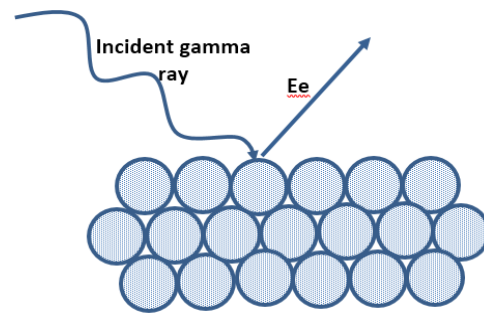
Where,

E_e = Energy of photoelectron

E_γ = Energy of incident gamma ray

E_b = Binding energy of electron in original shell

Fig. 2.10: Photoelectric Effect



The vacancy created in the electron shell due to photoelectric effect is filled by electronic rearrangement. This electronic arrangement leads to emission of X-ray or auger electron which again is absorbed by the medium. Therefore, all the energy of the incident gamma ray is deposited in the medium. Photoelectric effect depends on the gamma energy as well as atomic number of absorbing medium. Photoelectric is the dominating mode of interaction for gamma rays with energy less than 1 MeV. The cross section of photoelectric effect is given by

$$\sigma_{PE} \propto \frac{Z^{4.5}}{E_Y^{4.5}}$$

Where

σ_{PE} = Cross section of photoelectric effect

Z = Atomic No of the medium

E_Y = Energy of gamma ray

• Compton Scattering

In Compton scattering, the gamma ray transfers its partial energy to the loosely or weakly bound electron and itself gets scattered through an angle θ . The relation between energy of scattered photon and angle of scattering is given by

$$h\nu' = \frac{h\nu}{1 + \frac{h\nu}{m_0c^2}(1 - \cos \theta)}$$

Where

$h\nu'$ = Energy of scattered photon

$h\nu$ = Energy of incident gamma ray

m_0 = Rest mass of electron

C = Speed of light

θ = Angle of scattering

Kinetic energy of electron ejected is given by

$$KE_e = h\nu - h\nu'$$

From above discussion, energy of electron produced in Compton scattering is angle dependent.

This results in continuous response of the detector and hence it is not useful in γ -ray spectrometry. This mode is dominating in the gamma ray energy of 1 -5 MeV for high atomic number elements whereas for low Z elements over a wide range of energy.

$$\sigma_{CS} \propto \frac{Z}{E_\gamma}$$

• Pair production

For γ -rays having energy more than twice the rest mass of the electron (1.02 MeV) can produce positron-electron pair in the vicinity of nucleus. This effect is called pair production. Post event, the excess energy is shared between positron and electron pair in the form of their kinetic energy. Both positron and electron loss their energy in the medium and cause ionization and excitation. Positron produced can get annihilated with electron of the medium and produce two photons of energy 511keV each at 180° angle to each other. Depending upon the size of the detector this 511 keV photons can escape from the medium giving rise to double or single escape peak in the gamma spectrum.

The cross-section of the pair production is given by

$$\sigma_{CS} \propto Z^2 \ln E_{\gamma}$$

Pair production is low near its threshold but increase with energy of gamma rays and becomes the dominating mode at high energy region.

2.3.1 Instrumentation of Gamma Ray spectroscopy [60]

2.3.2.1 Detector

There are two types of detectors generally used for gamma ray spectroscopy viz. scintillation based e.g. NaI(Tl) and semiconductor based e.g. High Purity Germanium Detector (HPGe). HPGe based detector has better resolution compare to NaI(Tl) detector. But Efficiency of NaI(Tl) detector is better compare to High Purity Germanium Detector (HPGe). In the present work semiconductor based HPGe was used.

2.3.2.2 High Purity Germanium Detector (HPGe)

High purity germanium is produced by zone refining process. Depending upon the kind of impurity added, it can be p-type or n-type detector. This HPGe detector can be planar or co-axial. Under reversed bias conditions, when gamma ray interacts with depletion region of the detector, charge carriers are produced which are swept by applied electric field. This charge is proportional to energy deposited by gamma ray in the detector and is converted into proportional signal. The schematic of the detector along with electronic components is shown in Fig. 2.11. HPGe is kept under liquid nitrogen temperature (B.P. 77.3 K) to minimize the thermal generation of charge carriers. When not in use, detector can be stored at room temperature.

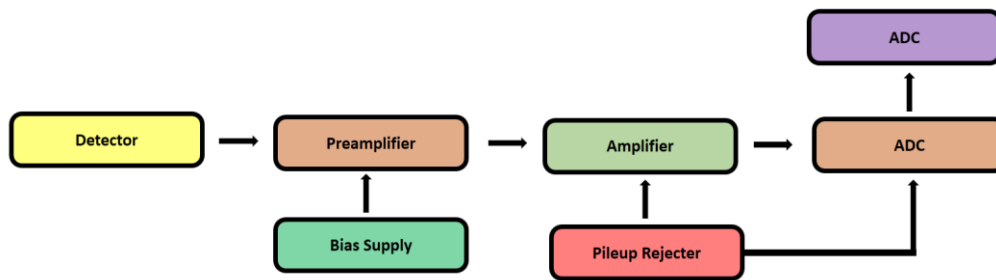


Fig.2.11 Block Diagram of a HPGe detector system

2.3.2.3 Bias voltage

It is required to collect the charge produced in the active volume of the detector. The voltage must be high enough to collect all the charges produced and low enough to avoid breakdown. Generally, 3000 to 4000 volt is applied depending upon the detector volume.

2.3.2.4 Preamplifier

Charge sensitive preamplifier are used in HPGe. Preamplifier is kept very close to detector to minimize the noise. Charges produced in active volume of the detector is converted into a voltage pulse by preamplifier. The voltage pulse produced by amplifier is proportional to energy deposited by gamma ray.

2.3.2.5 Amplifier

Amplifier serve to shape the pulse as well as amplify the signal received from preamplifier. Signal produced by preamplifiers are of low voltage. They need to be amplified before counting. Long tailed pulse produced from preamplifier is adjusted by amplifier.

2.3.2.6 Pole zero compensation circuit

It improves the performance of the analyzer at high count rates. Properly pole zero adjustment results into smooth return of the amplifier output to baseline with minimum possible time. If pole zero is not adjusted properly, Output pulses are followed by a long undershoot or overshoot that disturbs the output pulse at high count rates and peaks become broader with low or high energy tails.

2.3.2.7 Pile-up Rejection Circuit

It is a part of the amplifier. A pile-up rejection circuit is added to amplifier circuit to improve its performance at higher count rates. There are two types of pulse pile up. First tail pile-up where superposition of pulse on long duration tail or undershoot from preceding pulse.

Second peak pile up, when two pulses are so close to each other that they are considered as a single peak. The pile up effects can be minimize by making the width of the pulse as narrow as possible. It also improves the resolution and lower background.

2.3.2.9 Multi-Channel Analyzer (MCA)

It performs the important functions like collecting the data, producing output data for later analysis and providing a platform for visualization of the spectra. The main components are MCA analog to digital converter (ADC) along with control logic, memory and display. The pulse height distribution coming from amplifier is measured by means of ADC. This ADC converts the analog voltage pulse from amplifier to a digital quantity known as channel. The ADC sorts the amplifier output pulses according to voltage which is proportional to the energy deposited by gamma energy. Using MCA unwanted low or high energy events can be rejected.

2.3.3 Efficiency Calibration: For quantitative estimation, absolute efficiency of the detector required. The efficiency of detection depends upon the detector type, size, gamma energy and source to detector distance. Absolute efficiency is estimated by counting a source of a known activity. Typical efficiency curve of HPGe is shown in Fig.2.12. Absolute efficiency of the detection system is calculated by using standard source having multiple gamma rays like ^{152}Eu . Efficiency, ϵ is calculated using following formula

$$\epsilon = \frac{CPS}{dps \cdot a_{\gamma}}$$

Where

ϵ = Efficiency

CPS = observed counts per second

dps = disintegration per second of the standard

a_{γ} = Gamma ray abundance

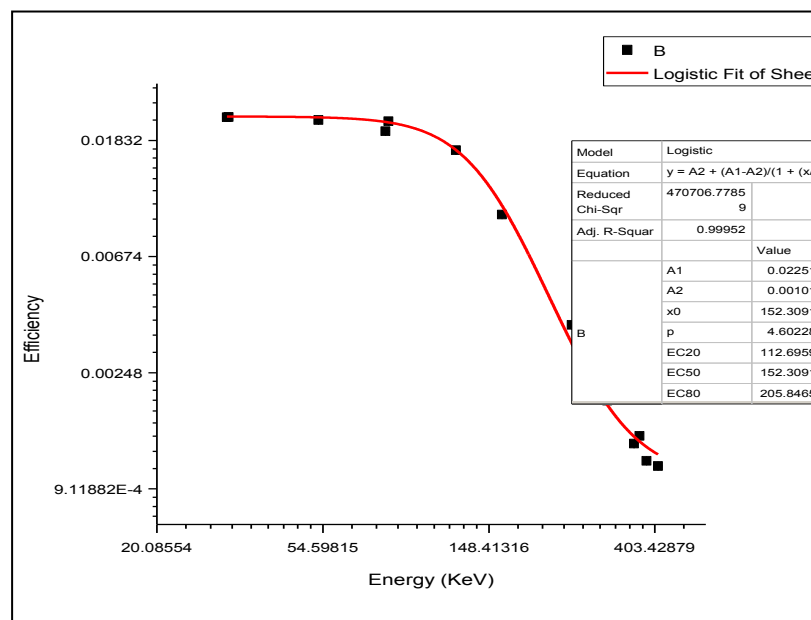


Fig. 2.12 Typical efficiency calibration curve in gamma ray spectrometry

2.3.4 Energy Calibration

Table 2.7: Standard source used for energy and efficiency calibration

Source	Energy (KeV)
^{152}Eu	121.785759
	244.6995544
	295.9490662
	367.7828979
	411.0716248
^{133}Ba	30.63414574
	30.98297882
	53.16923141
	79.62529755
	81.00393677
	160.6012115
	276.4086609
	302.8474121
	356.0100708
	383.8495483

The energy calibration involves assigning each channel, for a specific gamma energy. This involves fitting of channel numbers and gamma ray energies into a linear equation covering entire range of interest. Standard sources such as ^{152}Eu and ^{133}Ba having multiple gamma rays used for this purpose (Table 2.7). Typically, a 4K channel is calibrated to 2 MeV where the slop is about 0.5 keV per channel.

2.3.5 Resolution

Resolution refers to the ability of the detector to discriminate two radiations of nearby energies. Resolution of the detector indicates the performance of the detector. Any malfunction of the detection system can be find out by change in resolution. Resolution of the gamma ray spectroscopy is express in terms of Full width at half maxima.

$$Resolution = \frac{FWHM}{E}$$

2.3.6 Applications of Gamma Spectroscopy

2.3.6.1 Isotopic composition and concentration determination of Plutonium: Isotopic composition of solid samples of plutonium is routinely done using gamma ray spectroscopy. Gamma ray spectroscopy employed for determination of the isotopic compositions and concentration determination by using purified plutonium solutions.[61]

2.3.6.2 Neutron activation analysis (NAA): This is one of the most important methods for trace element determination in different nuclear materials. Species which are not gamma active can be made gamma active by irradiation in nuclear reactor.[60] One of the setbacks of this technique is requirement of a nuclear reactor.

2.3.6.3 Tracer Techniques: The advent of carrier free tracers led to extensive application of tracers for the study in separation, pre-concentration and extraction. Tracers are any radioisotope emitting alpha, beta or gamma ray. in development and standardization of separation and extraction studies. [62] Gamma emitting radionuclides are preferred for separation studies. In gamma ray spectrometry no sample preparation and no radiochemical purity is required.

2.3.6.4 Post irradiation Examination of fuel: Burn-up determination: Gamma scanning of irradiated fuel is carried out to find the burn-up of spent fuels using gamma rays of ^{134}Cs and ^{137}Cs . Gamma scanning of pressure tube i.e. Zircaloy-2 is done to find the activation product formed due to alloying impurity. [63]

2.4 Alpha Spectrometry

Nuclear instability of the nucleus causes spontaneous decay of radionuclides to achieve stability. The number of alpha particles emitted can be correlated to the decay rate of parent radionuclide. Alpha Spectrometry or alpha-particle spectrometry is an important radio-analytical technique used for the qualitative as well as quantitative determination of α -particle emitting radionuclides in nuclear, environmental and biological samples. Alpha spectrometry involves the measurement of alpha particle energy emitted by a radionuclide which is characteristic of that particular radionuclide. It has secured its place in the radiological laboratory over nine decades due to its features like simplicity, low-cost instrumentation, less operating cost, high sensitivity achieved due to very low background, accuracy, simple spectrum [64] Extent of peak degradation depends upon several factors viz. size and type of the detector, alpha activity ratio of high to low energy peak, energy resolution, source to detector distance, detector collimation, pressure inside chamber, peak analysis window size, thickness and homogeneity of the sources. Peak degradation is severe in case of environmental samples where inactive contaminants are also present with radionuclides. Therefore, in alpha spectrometry, it is a prerequisite to have good radiochemical purity and hence it depends upon radiochemical separations. Alpha source and the detector has to place in a chamber having a vacuum to minimize the alpha energy degradation. Mathematical calculations are required to take care for the tail contribution of high energy peaks at low energy peaks.

Theory of alpha decay [35]

Nucleus of any element has protons and neutrons. There is a strong repulsive force between the protons. This is balanced by nuclear force which is very strong, attractive and short range in nature. To escape from nucleus, alpha needs to acquire extra energy to overcome these forces. Hence alpha decay from radionuclides cannot be explained by simple classical mechanics. Gamow and team have explained the alpha decay using quantum mechanics. They have assumed that alpha particle is pre-formed inside the nucleus before emission from radionuclide. As shown in the Fig.2.14 the wave function associated with alpha particle does not go to directly zero at the wall of the potential barrier and have a finite but very small value outside the potential wall. This effect is known as tunneling effect. The probability (P) of the alpha particle cross the potential barrier is given by following equation

$$P = \exp\left(-\frac{4\pi}{h}\sqrt{2\mu} \int_{R_1}^{R_2} \sqrt{U(r)-T} \, dr\right)$$

Where μ is reduced mass $\mu = (M_\alpha M_R) / (M_\alpha + M_R)$

$U(r)$ = Potential energy as a function radial distance r

T = Total kinetic energy ($E_\alpha + E_R$)

h = Planks Constant

From above expression it is clear that higher the kinetic energy, higher will be the probability of alpha particle to cross the potential barrier

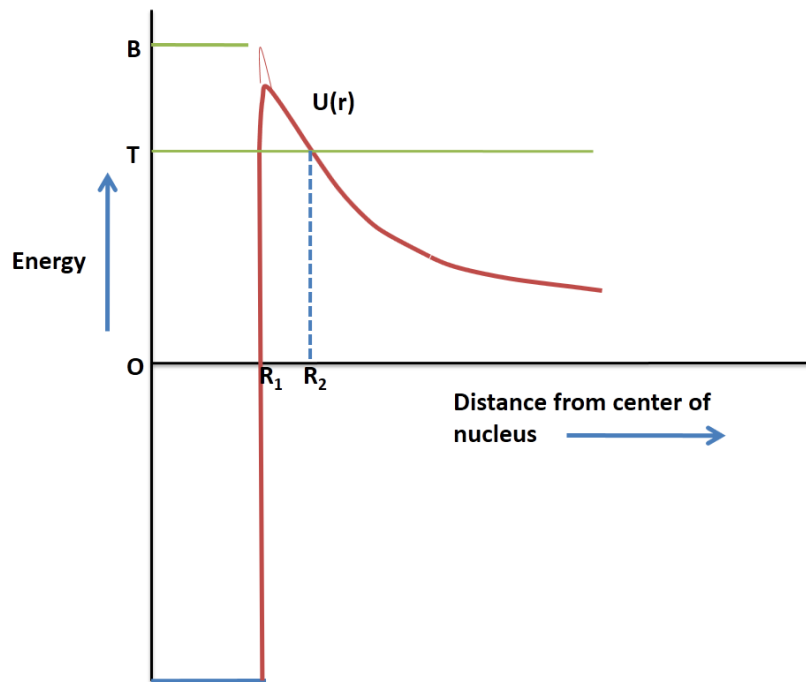


Fig.2.14: Tunneling Effect [65]

2.4.2 Alpha source Preparation

Alpha particle can travel only very short range and loses its energy very fast in materials as well as in air. Therefore, the source has to be uniform, thin and weightless to preserve the original energy as well as the mono-energetic nature of the alpha particle. Uniform, thin and weightless alpha sources minimize alpha energy degradation, lead to a high-resolution alpha spectrum. A suitable backing material with very smooth surface is required for getting good alpha spectrum. The smooth surface prevents alpha energy loss due to the roughness of the surface. Stainless steel with mirror finish is routinely used as backing material in our laboratories. Tantalum is used when HCl solutions are used whereas for high-resolution, Pt is used. Ni and Al are also used for the same purpose. Nowadays thin-film membranes are used for extraction of a radionuclide which can be directly loaded on these backing materials (38). The source preparation method must minimize the wastage and facilitate preferential

deposition of a particular radionuclide from the mixture of radionuclides. Following are the different methods for source preparation.[64]

2.4.2.1 Direct Deposition

A direct deposition is the simplest method for source preparation and is used in our laboratories on routine basis. A direct deposition is rapid and used for qualitative or semi qualitative analysis. A drop of sample is deposited on a solid substrate. Evaporation of sample is carried out using heat of an IR lamp. This source then fired to fix the activity deposited on it. Source is then allowed to cool. Generally, direct evaporation method yields non uniform sources. This results in poor alpha spectrum. This problem, to some extent, is resolved by using spreading-reagents such as tetraethylene glycol (TEG).

2.4.2.2 Electrodeposition

In Electrodeposition, a thin, uniform layer of sample is deposited on a stainless steel planchet. Set up consist of high voltage unit, cathode and anode. The actinides are co-precipitated with platinum from the cathode as hydroxides. The detailed study required to obtained electrodeposition of any element. Quality of the source depends upon the volume of the cell, current density, distance between anode and cathode voltage and shape of the anode. Ammonium sulfate, ammonium nitrate, ammonium chloride, ammonium oxalate, ammonium formate, and their mixtures are employed as electrolyte for electrodeposition.

2.4.2.3 Vacuum Sublimation

Vacuum sublimation needs an elaborate setup. As the name suggests, sample is heated to very high temperatures. The sample is vaporized using tungsten (platinum, tantalum) filament and can be sublimed to a substrate. The best quality source is produced by this method but with poor deposition yield. The vacuum sublimation method generally used for nuclear data measurements.

2.4.2.4 Micro Precipitation

In this method, actinides are precipitated as hydroxide fluoride or sulphate. Sequential precipitation helps in elimination of interfering elements. Small amount of lanthanides and hydrogen fluoride is added to a mixture of La (or Ce) and the sample to enhance the co-precipitation of actinides. Precipitate formed is filter through filter paper and mounted on a counting tray after drying.

2.4.2.5 Electro-spraying

The sample is dissolved in organic solvents like ethyl alcohol, methanol or acetonitrile. Sample is then transfer to a capillary tube. An anode is inserted into the sample. A potential of around 8 kV is required to generate a spray of a sample from anode to cathode. Sample with 100% water is difficult to generate electrospray. Before reaching to opposite electrode, the solvent evaporates.. Rotating cathode is use to get uniform deposition of sample.

2.4.3 Instrumentation of Alpha Spectrometer (Fig.2.15)[67]

• Vacuum System

Alpha particle losses its energy while travelling through any medium. To avoid energy loss, detector and sample are placed in vacuum chamber. This prevention of energy loss result in improved resolution. 10^{-2} to 10^{-3} torr is suitable to carry out analysis. Generally rotary pumps are employed to maintain the vacuum inside the vacuum chamber. Vacuum chamber has to be large enough to accommodate sample source as well as the detector. Space inside the vacuum would also make it possible to change distance between source and detector to measure the sample with different activities.

• Detectors for Alpha Spectrometer

Alpha spectroscopic analysis can be performed using ionization chamber, proportional counters, plastic and liquid scintillation detectors, magnetic spectrometers and semiconductor

detectors. Ionization chambers have high efficiency but resolution is very poor. Proportional counters as well as liquid and plastic scintillators have advantage that the radionuclide can be placed inside the counter thereby achieving good efficiencies. Alpha liquid scintillation counting most widely used in laboratory for gross alpha counting due to its low cost and simplicity. Semiconductor detectors are very good detectors for alpha energy measurement as they provide high resolution.

- **Silicon Surface Barrier Detectors**

It is a semiconductor type of detector. An electron rich (n-type) semiconductor material, mostly silicon, is used in surface barrier detector. Surface of the detector is etched. Gold is evaporated and thin layer is deposited on this etched surface in such way that an oxide layer is formed between gold and silicon. This thin layer of oxide acts as a p-type of material. As this oxide layer acts as a barrier this detector is called as surface barrier detector. Diffusion of charge particle result in formation of a depletion region with depth of 0.1 to 2 μm . Depletion depth of 2-3 mm is achieved by applying a bias voltage. Charge particle interact with detector and produce electron hole pair in this depletion region. These electrons and holes are attracted by opposite charged detector contacts. The integrated charged produced is directly proportional to the energy loss of alpha particle in the detector. Surface detector can also be produced by starting material of p-type and a thin layer of aluminum is deposited on it to form equivalent n-type of the contact. This surface barrier detector is not only used for alpha spectrometry but can also be used for other charge particle.

- **Passivated Ion Implanted detector (PIPS)**

Impurities are added to semiconductor material to convert it to either electron deficient (P-type) or electron rich (n-type). These impurities can be introducing in the semiconductor material by exposing semiconductor material to beam of ions produced by ion accelerator. Therefore, the

name is passivated ion implantation. Both p-type and n-type detectors can be fabricated using this method. A well defined profile of impurities added to the semiconductor is achieved with this technique as mono energetic incident ions are produced. Compare to surface barrier detectors, passivated ion implanted detectors are more stable and less susceptible to ambient conditions. In PIPS detector better resolution is obtained compare to surface barrier detectors.

- **Preamplifier**

It is the first interface between the detector and the rest of the system. Main function of preamplifier is to convert charge produced in active volume of the detector to proportional signal. It prevents the signal degradation by physical proximity to the detector. It produced long tailed output pulse. In case of semiconductor based detector capacitance is not constant. Therefore, a charge sensitive preamplifiers are used whose output voltage is independent input capacitance. It produced output signal compatible to the amplifier with maximum signal to noise ratio and proportional to the charge collected.

- **Amplifier**

Input of analyzer are required in the 0 to 10 V range whereas the output signal of preamplifier is in mV range. Therefore, signal has to amplify. The long output pulse from the preamplifier is not desirable. Therefore, before feeding the signal from the preamplifier to analyzing system, they are shaped. Both amplification and shaping of the pulse is achieved by amplifier. Care is taken while processing signal from the preamplifier to produce the output with highest signal to noise ratio.

- **Bias Voltage**

In semiconductor based detectors, due to migration of electron from n-type to p-type and hole migration from p type to n-type, result in formation of depletion region. This depletion region is charge free zone in detector and active volume of the detector. The depth of the depletion

region can be increased by application of reversed bias voltage. This applied voltage also swept the charge produced in depletion region which produces the signal proportional energy loss of an alpha particle. High voltage can cause the breakdown hence small but high enough to collect all charges produced. Reversed bias voltage applied in case of alpha spectrometer is less compare to gamma spectrometry as the detector size is smaller in case of alpha spectrometers.

- **Multichannel Analyzer**

Main function of MCA is to analyze the pulses from the amplifier, sort according to their height and then store them in different channel number by means of analog to digital converter (ADC). Two types of ADC are used viz. Wilkinson's ADC and successive approximation type ADC. Content of the channel is incremented by one. ADC also have a provision for cutting off unwanted pulses. MCA is interfaced to a computer to provide display of spectrum, recording and analysis

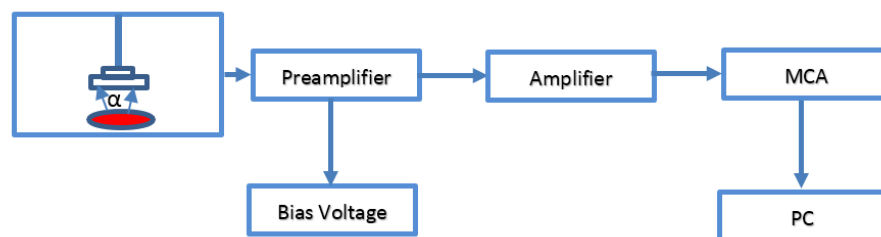


Fig. 2.15 Instrumentation of Alpha Spectrometry

2.4.4 Applications of Alpha Spectroscopy

Qualitative Analysis

For qualitative analysis, an energy calibration standard is required. For this purpose, a mixture of ^{238}Pu and ^{241}Am is used (Fig 2.16.). Once the alpha spectrometer is energy calibrated, it can

be used for unknown sample where alpha energies are unknown. In early discoveries of actinides, alpha spectrometers played very important role.

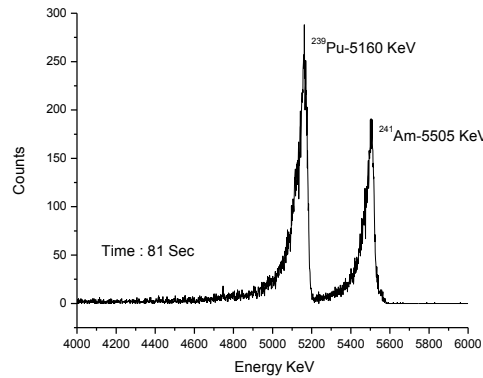


Fig. 2.16 Energy Calibration of Detector using ²⁴¹Pu-²⁴¹Am source

2.4.4.2 Quantitative Analysis

- **Using Efficiency:** For quantitative measurement, first efficiency of alpha spectrometer is find out by using standard source whose activity details are known.

$$Efficiency = \frac{CPS_{Std}}{Abundance_{\alpha} \times DPS_{Std}}$$

Here abundance is known from literature and DPS_{std} is the activity of source. CPS_{std} of standard is find out from the measurements. Theses determined efficiency is source-to-detector distance dependent. Now for analysis of radionuclides whose quantitative determination has to be done, is placed in measurement chamber and kept at the same distance as standard. Following formula is used to find the activity of sample.

$$DPS_{sample} = \frac{CPS_{sample}}{(Abundance_{\alpha} \times Efficiency)}$$

CPS_{sample} of sample is find out from alpha spectroscopy. From DPS_{sample} value, amount of a particular radionuclide can be find out. For e.g. determination of ²⁴¹Am in plutonium matrices

for quality control purpose. Alpha spectrometry is used for the determination of ^{232}U in thorium matrix in view of the potential isobaric interference of ^{232}U by ^{232}Th .

Isotope Dilution Alpha Spectroscopy

As aforesaid for alpha spectrometry, it is prerequisite to have purified sample. During separation and purification, there is chance of loss of radionuclides. This inefficient separation and purification may lead to erratic measurements. To take care of this, isotope dilution alpha spectrometry (ID-AS) is used. In IDAS standard of known alpha activity and concentration is required which also known as spike. A known amount of sample and spike are mixed together and alpha spectrometry of the mixture is carried out. Alpha spectrometry of a known amount of a sample is also carried out. Following formula is used for qualitative estimation. [66]

$$C_{Sa} = \frac{C_{Sp} W_{Sp}}{W_{Sa}} \frac{(R_{Sp} - R_m)}{R_{Sp}(R_m - R_{Sa})} + \frac{(AF_i \cdot \lambda_i)_{Sp}}{(AF_j \cdot \lambda_j)_{Sa} + (AF_k \cdot \lambda_k)_{Sp}} \frac{\langle At wt \rangle_{sa}}{\langle At wt \rangle_{sp}}$$

Where,

C_{Sa} = Concentration of sample

C_{Sp} = Concentration of spike

W_{Sa} = Weight of Sample

W_{Sp} = Weight of Spike

R_{Sp} = Ratio of Spike (i/j)

R_{Sa} = Ratio of Sample (i/j)

R_m = Ratio in the mixture of sample and standard (i/j)

AF = Atom fraction of isotopes

At Wt sa = Atomic weight of sample

At Wt sp = Atomic weight of sample

λ_i represents the decay constant of the isotope "i"

λ_j represents the decay constant of the isotope "j"

λ_k represents the decay constant of the isotope "k"

ID-AS is an important alternate to Isotope dilution mass spectrometry for the determination plutonium concentration in irradiated fuel.

Nuclear Data Measurement [64]

• Emission Probability of Alpha Particle

Vacuum sublimation method is used to determine the alpha emission probability of radionuclides. Sample with very high radiochemical purity and isotopically pure radionuclides were used for this purpose

• Half-life Measurement

Alpha spectrometry can be used for precise and accurate determination of alpha decay half-life of various actinides. There are different approaches to find the half-life of a radionuclide.

1. Parents decay method: e.g. alpha Half-life determination of ^{242}Cm
2. Daughters growth method: e.g. β decay half-life of ^{241}Pu using daughter ^{241}Am
3. Isotope dilution alpha Spectrometry. Ingrowth of ^{241}Am was determined using ^{243}Am as a spike
4. Alpha spectrometry with thermal ionization mass spectrometry

e.g. Alpha Spectroscopy is very useful in Half-life measurement of ^{232}U (70.6 years) because it has low abundance and high alpha activity and Mass spectrometric analysis suffers isobaric interference from its parent ^{232}Th

Alpha Activity Ratio Measurements

Alpha spectrometer is also employed for alpha activity ratio measurements. Isotopic composition measurement of uranium and plutonium suffers isobaric interferences in mass spectrometric analysis. For eg. ^{232}U from ^{232}Th and ^{238}Pu from ^{238}U . In such a situation, values of $^{232}\text{U}/^{233}\text{U}$ and $^{238}\text{Pu}/^{239}\text{Pu}$ are measured using alpha spectroscopy. Because of peak degradation, low energy peaks would have tail contribution from high energy alpha particle. To take care of this, geometric progression method is used. The activity ratio of alpha emitting radionuclides is determined using geometrical progression method.

Chapter 3

Dual Column HPLC method for
Determination of Lanthanides in
Zirconium Matrix

3.1 Introduction

Zirconium and its alloys exhibit exceptionally high levels of hardness and durability, low expansion and very low thermal conductivity. Due to the formation of a chemically inert and strongly adsorbing oxide film, this metal displays strong resistance to most organic and inorganic acids, strong alkalis, some molten salts etc. Zirconium products are thus used in a wide range of applications where corrosion resistance, low weight, strength or human body compatibility are important product properties. Due to these unique properties, the applications of zirconium and its alloys have increased exponentially in various technologically challenging fields. For example, zirconium based materials are used for medical implants, heat exchangers, laboratory equipment's, sporting goods etc. [68,69] It is also an excellent low-cost replacement for platinum in the manufacturing of crucible material required for fusions involving sodium carbonate or sodium peroxide.[72] Owing to the extremely low thermal neutron absorption cross-section ($\sigma = 0.18$ barns), stability at nuclear reactor conditions and high corrosion resistance, zirconium qualifies to be an excellent material of choice in the nuclear reactor arena. Zirconium and its alloys are extensively used for fabrication of nuclear reactor's structural materials such as clad, pressure tubes and reactor core etc. The metallic fuel alloys of zirconium such as U–Zr and U–Pu–Zr have received enormous importance in the recent years as candidates for fuels to be used in advanced liquid metal cooled fast breeder reactors. [71]

Zirconium invariably contains lanthanides as impurities due to the same origin of their sources. Some of the lanthanides like Gd, Sm, Eu and Dy have very high neutron absorption cross-sections and their presence in zirconium and its alloys would adversely affect the overall neutron economy of the nuclear reactor. Therefore, zirconium based materials intended for nuclear technological applications have to meet stringent specification for their lanthanide content. Neutron absorbing property of a nuclear material is often expressed as equivalent

boron content (EBC). Equivalent boron content and neutron absorption cross-section for some of the lanthanides along with zirconium and boron are given in Table 3.1 [72].

Table 3.1: Neutron absorption coefficient and equivalent boron content			
Elements	Average Atomic Weight	Average Thermal Neutron Absorption Cross section (barns)	Equivalent Boron Content (EBC)
B	10.811	764	1.00E+00
Zr	91.224	0.185	2.87E-05
La	138.91	8.97	9.14E-04
Ce	140.12	0.7	0.00007
Pr	140.91	11.5	1.15E-03
Nd	144.24	50.5	4.95E-03
Pm*	146.92	8400	-----
Sm	150.36	5670	5.34E-01
Eu	151.96	4565	0.4250
Gd	157.25	48890	4.3991
Tb	158.93	23.4	2.08E-03
Dy	162.50	940	0.0818
Ho	164.93	64.7	5.55E-03
Er	167.26	159.2	0.0135
Tm	168.93	105	8.79E-03
Yb	170.04	35.5	2.90E-03
Lu	174.97	76.4	6.18E-03

According to ASTM specification code ASTM C1065 – 08 -2015, the total equivalent boron content (EBC) should not exceed 500 $\mu\text{g/g}$ on a mass basis relative to ZrO_2 and sum of Gd, Sm, Eu and Dy contents in zirconium should not exceed 200 $\mu\text{g/g}$. [72]

Different methods based on techniques such as UV-Vis Spectroscopy, ICP-AES, ICP-MS etc. are reported in the literature for the determination of rare earths in zirconium matrix. However, most of these methods suffer from various limitations such as matrix effects, spectral interference, isobaric interference etc. [73-77]. One way to circumvent the matrix effects is the prior separation of zirconium matrix by solvent extraction or chromatographic methods. Spectral or isobaric interference in the determination of lanthanides can be overcome by their individual separation. The similarities in chemical properties have rendered the individual separation of lanthanides a challenging task.

High performance liquid chromatography (HPLC) along with different detectors offers fast and efficient separation and quantification of individual lanthanides. LC methods based on ion interaction chromatography (IIC) are widely used for the separation of lanthanides in different matrices as they provide high resolution and rapid separation of lanthanides compared to bonded ion exchangers. The improved efficiency of the IIC is attributed to faster mass transfer at the surface of the stationary phase. Thus IIC in combination with α -hydroxy isobutyric acid (α -HIBA) as a complexing agent is one of the most popular choice for the separation of lanthanides. [78-80] In HPLC, it is essential to employ either pH gradient or concentration gradient of the eluent to achieve efficient separation of individual lanthanides. However, with the increase in pH of the mobile phase, zirconium is expected to undergo hydrolysis or polymerization. Thus high concentrations of zirconium can be detrimental in the separation of lanthanides using HPLC. The present studies describe the development of a IIC method for the separation and determination of individual lanthanides in bulk of zirconium. Chromatographic behavior of lanthanides and zirconium was studied on a dynamically modified reversed phase

column using α -HIBA as a complexing agent. Nature of major zirconium species under experimental conditions was studied using liquid chromatography and by electrospray mass spectrometry (ESI-MS).

Experimental parameters such as pH of mobile phase, concentrations of eluent and ion interaction reagent were optimized for obtaining the optimum separation among the lanthanides. The influence of pre-concentration conditions such as composition, volume and loading flow rate of the sample etc. were studied for maximizing the recovery of lanthanides. Under the optimized conditions, bulk of zirconium is found to elute out from the column whereas lanthanides were quantitatively retained onto the column. Subsequently, preconcentrated lanthanides were separated on a similar modified column of larger dimension and determined using UV-Vis detector employing Arsenazo (III) as a post-column reagent. Advantages of the developed method are (i) bulk of zirconium has no interaction with stationary phase which enable the use of a low capacity column to achieve pre-concentration and (ii) on-line preconcentration procedure minimize the analyte loss and cross-contamination. To the best of our knowledge, this is the first HPLC report for the direct determination of trace amounts of lanthanides in zirconium matrix.

3.2. Experimental

3.2.1 Instrumentation

Chromatographic studies were carried out using an HPLC system consisting of low pressure quaternary gradient pump L-7100 (Hitachi Elite LaChrom) and a Rheodyne injector (Model 7725i) with a 100 μ L sample loop. Silica based C₁₈ monolithic RP columns (50 mm \times 4.6 mm ; 100 mm \times 4.6 mm, Chromolith, Merck, Darmstadt) were used. 50 mm column was used for studying the influence of chromatographic parameters on the retentions of REEs and Zr. 100 mm column was used as the analytical column for carrying out the individual separation of lanthanides. A polymeric based PRP- C₁₈ column (5 μ m, 50mm \times 4.6mm, Hamilton,

Switzerland) were used as stationary phases for pre-concentration of lanthanides. The effluents from the column was monitored employing a diode array detector (Hitachi Elite LaChrom) after reaction with a post-column reagent (PCR), which was added with a metering pump (Eldex Laboratories Inc) into a low dead volume-mixing tee (Valco). The signal from the detector was processed by EZChrom software. An isocratic pump (Model 501, Waters Corporation) was used for delivering the sample solution through the preconcentration column. pH of the samples and buffer were measured using a pH meter (CL54+, TASHCON, India). An electrospray ionization mass spectrometer (ESI-MS) consisting of hybrid quadrupole and time of flight mass analyzer (Bruker Daltonik GmbH, Germany) was used for the identification of different species of zirconium. Solution was directly introduced using a syringe pump (Nemesys, Cetrol GmbH, Korbussen, Germany) into the ESI-MS. The species formed were analyzed in negative ion mode at a capillary potential of +3800 V. Other ESI-MS conditions were similar to previously reported work. [117]

3.2.2 Reagents

All solutions were prepared using de-ionized water from Milli-Q system (Millipore) and were filtered through a 0.45 μm membrane filter (Millipore) prior to use. α -HIBA (FLUKA) was used as an eluent. Zirconium solution was prepared by dissolving zirconium oxychloride (Merck, Germany) in diluted nitric acid. ICP-standards of lanthanides (Inorganic venture, Bengaluru) were used after suitable dilutions. Sodium n-octane sulphonate (Fluka) and Octyltrimethyl ammonium chloride (Chemika) were used as the IIRs. Arsenazo (III) (Fluka) was used as the post column reagent (PCR). HNO_3 and NH_4OH (Suprapure grade, Merck) were used for adjusting the pH of the mobile phase. Isopropyl alcohol (LC-MS grade, Sigma aldrich) was used for the preparation of the PCR.

3.2.3 Pre-concentration

Known amounts of zirconium oxychloride and lanthanides from the stock solutions were diluted with a mobile phase consisting of 0.03 M of n-octane sulphonic acid and 0.15 M of α -HIBA (pH 2.0). Simulated sample solution prepared in this way was passed through a preconditioned column PRP-C18 (50 mm X 4.6 mm) at a flow rate of 2 mLmin⁻¹. The effluents from the preconcentration column were collected and weighed to determine the exact amount of sample solution passed through the column. Then washing was carried out with 10 mL of mobile phase containing α -HIBA(0.15 M, pH 2.0) to remove zirconium and other non-retained impurities. After washing step, the pre-concentration column was connected to another modified column (150 mm X 4.6 mm) in such a way that the orientation of the preconcentration column is reversed. A concentration gradient of α -HIBA (pH=6.0) with the change in the concentration from 0.0-0.2 M in 20 mins was used at 1 mL min⁻¹ flow rate. The PCR solution of Arsenazo (III) [0.15 mM Arsenazo (III), 0.01 M urea and 0.1 M HNO₃ in 20% Isopropyl alcohol] was delivered at a flow rate of 0.3 mLmin⁻¹. Blank runs were performed before and after the sample analysis under identical conditions. Quantification of lanthanides was achieved based on the area of the chromatographic peaks.

3.3. Results and Discussions

3.3.1 Chromatographic Behavior of Zirconium and Lanthanides

For this studies, monolith C18 column (50 mm x 4.6 mm) was used with α -hydroxy isobutric acid. Lanthanum and lutetium were selected as the representative elements to compare the chromatographic behavior with zirconium. The effects of ion interaction reagent (IIR) and pH of mobile phase on the retention behavior of lanthanides and zirconium were studied. As seen in Fig.3.1a, in absence of ion interaction reagent lanthanides and zirconium eluted near the solvent front. This indicates the non-hydrophobic nature of the lanthanides and zirconium species. With the increase in concentration of IIR, the retention of lanthanum and lutetium

increased whereas zirconium continued to show no retention on to the column as shown in Fig.3.1b. Increase of IIR concentration in the mobile phase resulted in enhancing the ion exchange capacity of the column which led to higher retention of lanthanides species. This affirms the cationic nature of lanthanides species. The dominating zirconium species

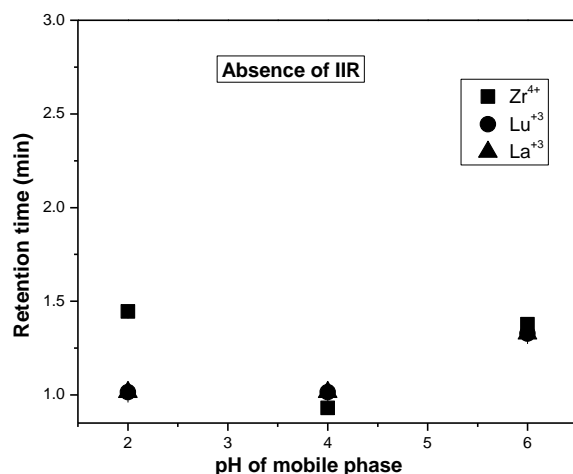


Fig. 3.1(a). Retention of La, Lu and Zr on RP column in absence of IIR

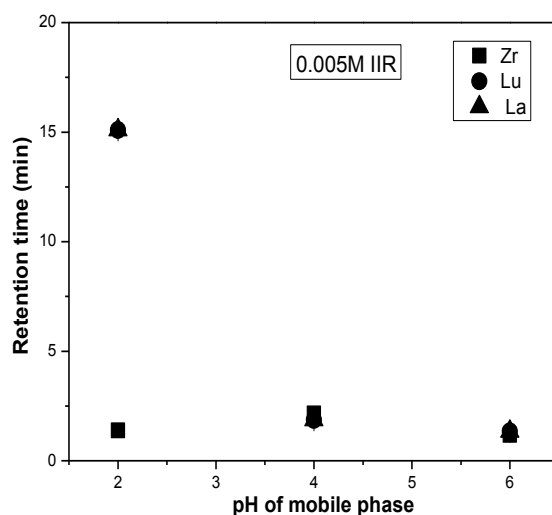


Fig. 3.1(b). Retention of La, Lu and Zr on RP column in presence of IIR

therefore must be non-cationic in nature. Non cationic nature of zirconium species was also observed by ayres et al. and Schubert et. al. [82,83] As expected, increase in the pH of mobile phase caused a decrease in retention of lanthanides as shown in Fig.3.1b This is attributed to

the increased percentage of ionized α -HIBA at higher pH, leading to increase in complexation and hence faster elution of lanthanides. Since there was no retention of zirconium on reversed phase or cation exchange column, it was felt that zirconium species might be forming predominating anionic species under these chromatographic conditions. This observation is corroborated with the literature where it is reported that when zirconium to nitrate ratio is high, zirconium forms exclusively anionic species [81]. Contrasting behaviors of lanthanides and zirconium under low pH ion interaction chromatographic conditions gave in puts to design a strategy for the preconcentration of lanthanides and preferential elution of zirconium. The lanthanides thus pre-concentrated can be individually separated using another dynamically reversed phase column. Since zirconium showed little retention onto the modified column under optimized conditions, a small capacity column can be used for preconcentration of lanthanides in presence of large proportions of zirconium. In order to ascertain the nature of the species formed between zirconium and α -HIBA, studies were carried out using an RP column dynamically modified with octyltrimethyl ammonium chloride. Fig.3.2 shows the change in the retention time of zirconium as a function of concentration of octyltrimethyl ammonium chloride in the mobile phase.

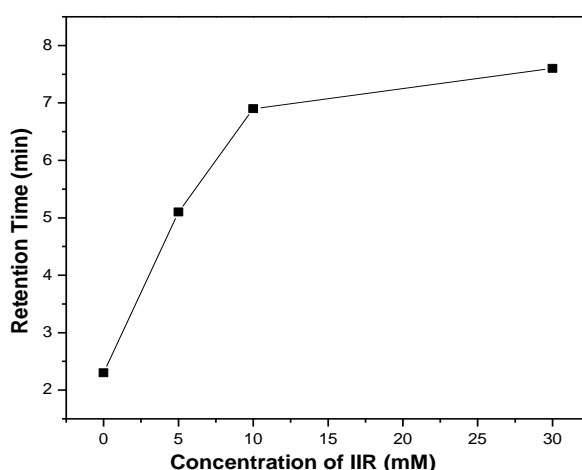


Fig. 3.2. Effect of octyltrimethyl ammonium chloride (anionic ion interaction reagent) onto the retention of Zr

It is seen that the retention of zirconium increases with the increase of the hydrophobic cation. This observation indicates that major zirconium species must be anionic in nature and hence shows little retention on cation exchange column as well as on unmodified reversed phase column. In order to identify the type of major zirconium species formed, following ESI-MS study was performed.

3.3.2 Studies of zirconium species by ESI-MS

Earlier, there was a controversy over the existence of the zirconyl ion ZrO^{2+} in solution. [84] Zaitsev et al. have shown that ZrO^{+2} does not exist in solution but presents only in solid state. Studies also have shown that zirconium under sufficiently acidic conditions exists as Zr^{+4} [85] In order to ascertain the species of Zr, ESI-MS studies were carried out. Zirconium solution prepared from 50 mM $ZrOCl_2$ in 10^{-2} M HNO_3 was diluted with methanol and HNO_3 to have a zirconium concentration of 5×10^{-6} M. This solution was directly infuses into ESI-MS and the mass spectrum obtained in the negative ion mode is given in Fig.3.3.

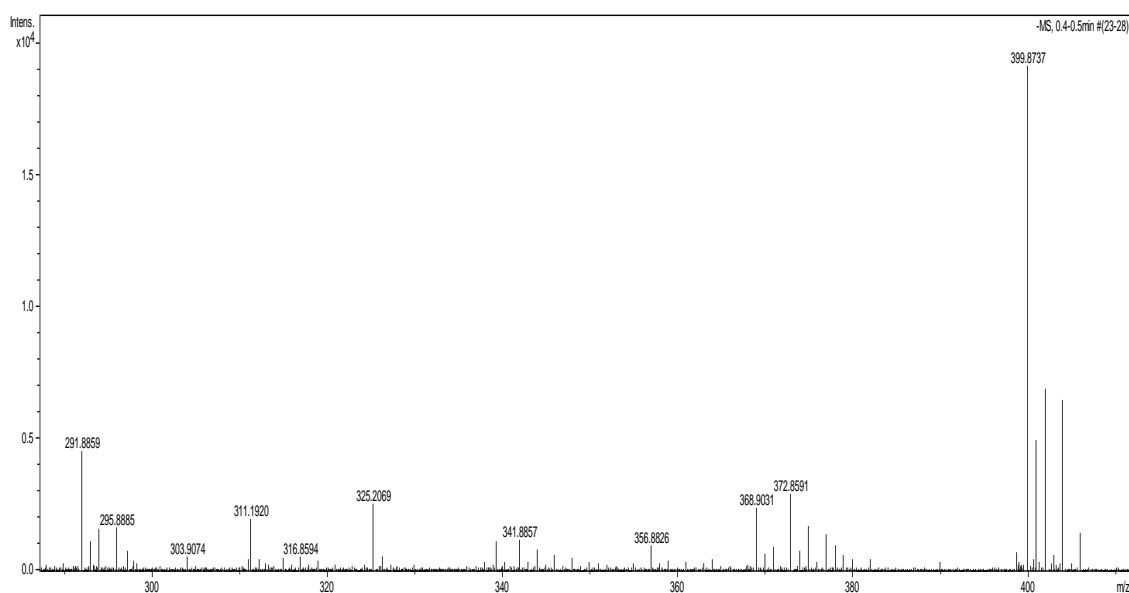


Fig 3.3. ESI-MS spectra of Zr (5×10^{-6} M) solution in 1.5×10^{-4} M of HNO_3 in negative ion mode

The different species observed in the negative ion mode were identified and are presented in Table 3.2. As can be seen, the most dominating peak is observed at m/z of 399.86 corresponding to species $[\text{Zr}(\text{NO}_3)_5]^-$. Interestingly, Zirconyl ion (ZrO^{2+}) containing species $[\text{ZrO}(\text{NO}_3)_3]^-$ (at m/z of 291.86) was also observed in the present study. Nitrate containing species were seen with higher intensity than non-nitrate containing species. Subsequently, zirconium solution mixed with HIBA was also analyzed in negative ion mode Fig.3.4 and the species observed are presented in Table 3.3.

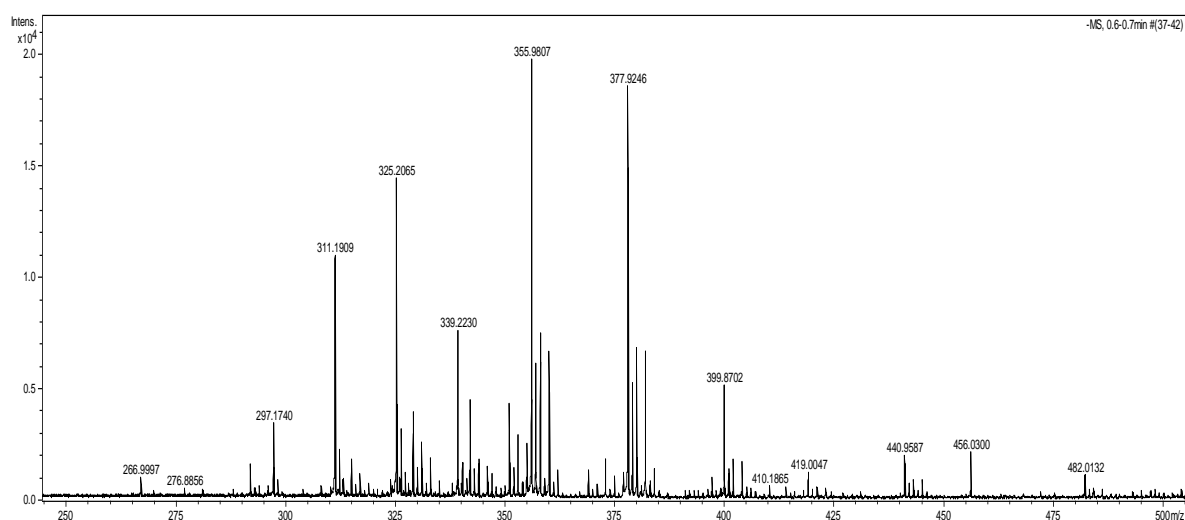


Fig.3.4 ESI-MS spectrum of Zr (5×10^{-6} M) and HIBA(5×10^{-5} M) in 1.5×10^{-4} M of HNO_3 in negative ion mode

Species	m/z	Intensity
$[\text{Zr}(\text{NO}_3)_5]^-$	399.86	30950
$[\text{ZrO}(\text{NO}_3)_3]^-$	291.86	4539
$[\text{Zr}(\text{NO}_3)_4(\text{CH}_3\text{O})]^-$	368.88	10080

Table 3.3 :Zr (5 x 10⁻⁶ M) with HIBA(5x10⁻⁵M) in 1.5x 10⁻⁴ M of HNO₃ in negative ion mode		
Species	<i>m/z</i>	Intensity
Zr(C ₄ H ₇ O ₃)(NO ₃)(OH) ₂	350.92	4498
Zr(C ₄ H ₆ O ₃) ₂ (NO ₃)	355.95	22081
Zr(C ₄ H ₆ O ₃)(NO ₃) ₃	377.92	18661

The types of species observed can be categorized as ML₁ and ML₂, where M is the metal ion and L is the ligand. All the dominating Zr-HIBA anionic species were found to contain NO₃⁻ ion also. The anionic nature of major zirconium species is responsible for the poor retention of zirconium onto the reversed phase and cation exchange stationary phases. The ESI-MS studies thus corroborate the chromatographic behavior of zirconium.

3.3.3 Optimization of acidity

Zirconium being a tetravalent ion, it is prone to hydrolysis under low acidic conditions leading to precipitation and the micro precipitate of zirconium can clog the HPLC column. The percentage of hydrolyzed and polymeric zirconium species depends upon various parameters such as composition of solution, method of preparation and aging of zirconium solution [84]. In order to minimize the chances of zirconium hydrolysis, the samples should be kept in certain acidity. At higher acidities, H⁺ ions might interact with cation exchanger causing the early elution or poor recovery of lanthanides. Higher acidities are also detrimental to silica based reversed phase column. Hence optimization of acidity of the sample solution was necessary for the preconcentration of lanthanides in presence of zirconium. In order to study the effect of acidity, simulated sample solutions with varying molarities of nitric acid viz. 0.2 M, 0.4 M, 0.6 M and 0.8 M were prepared. The minimum concentration of nitric acid required to carry out experiment using 5000 ppmw of zirconium solution was found to be 0.2 M. of nitric acid concentration above 0.2M results in poor recoveries of lanthanides.

3.3.4 Preconcentration Study

In order to carrying out the preconcentration studies, 0.15 M of HIBA (pH =2.0) and 0.03M of n-octane sulphonic acid ware used as the mobile phase. Effect of different parameters which are effecting the preconcentration such as flow rate for loading of solution, volume of the solution, amount of zirconium and lanthanides etc. on the recovery of lanthanides ware studied.

3.3.4.1 Effect of Flow rate on Pre-concentration

Flow rate studies were carried out with using a simulated sample containing 500 ppm of zirconium and 100 ppb of lanthanides. The solution was passed at different flow rates from 0.5 mL min⁻¹ to 3.0 mL min⁻¹ and the pre-concentrated lanthanides were separated as per the gradient condition mention earlier. Fig.3.5 shows the peak area of the lanthanides obtained after recovery, as a function of sample solution loading flow rates. As seen in the Fig, 3.5 the peak area of the lanthanides was constant till a flow rate of 2.0 ml min⁻¹. Further increase in flow rate led to a decrease in the peak area due to the loss of lanthanides in the preconcentration step. The optimized flow rate of 2.0 ml min⁻¹ was used for further studies.

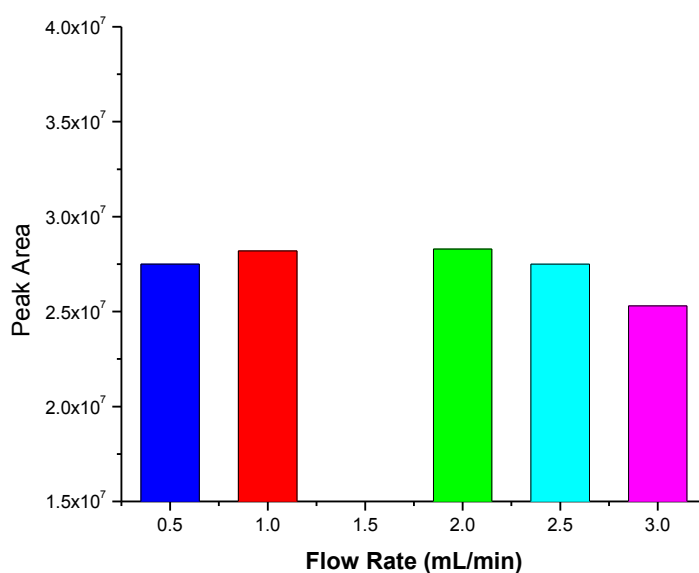


Fig. 3.5. Effect of mobile flow rate on the pre-concentration of lanthanides

3.3.4.2 Effect of Volume

In order to adopt the method for low concentrations of lanthanides, different volumes of the solution were passed through the column at the flow rate of 2.0 mLmin⁻¹ keeping the concentration of zirconium and lanthanides as 500 ppm and 100 ppb, respectively. Fig.3.6 shows the recovery of Lns/mL of sample solution as a function of sample volume introduced into the column. This study also demonstrated the adaptability of the method for carrying out the preconcentration and separation of lanthanides in presence of zirconium up to a zirconium to lanthanides amount ratio of 2, 50,000.

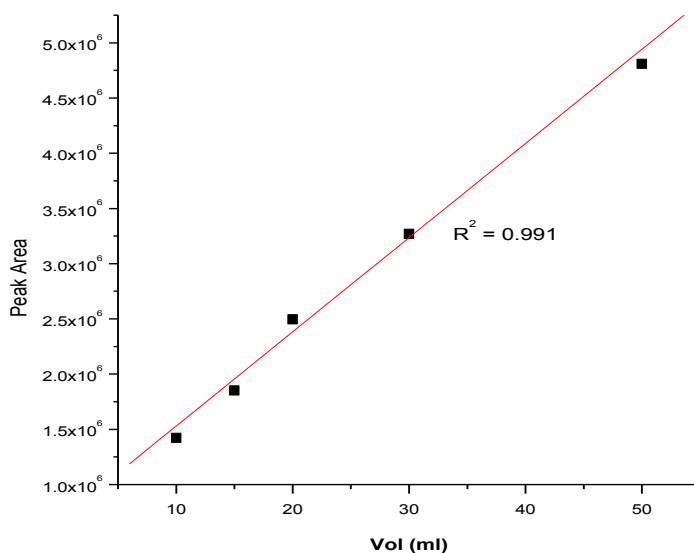


Fig. 3.6. Volume calibration for pre-concentration of lanthanides

3.4 Individual separation of pre-concentrated lanthanides

In order to ensure complete removal of zirconium left over in preconcentration column, washing of the column with low pH α -HIBA was carried out prior to the individual separation of lanthanides. The individual separation of lanthanides was achieved with the change in pH of the mobile phase. The separated fraction from the analytical column was mixed with the PCR at a T-junction. During the separation studies it was found that PCR was not flowing

through the detector after completion of one round of experimental. This may be due to the reason that at T connector there could be formation of zirconium hydroxide which might get coated on the inner wall of the tube or even flow cell walls. This was circumvented by introducing 30% isopropyl alcohol in post-column reagent. After the introduction of 30% isopropyl alcohol in the PCR solution, there was no instance of disruption in the monitoring of eluted species.

3.5 Quantification of Lanthanides

The method finally optimized for the Zr matrix removal cum pre-concentration followed by individual separation of lanthanides is summarized in Table 3.4. This method was validated by preparing a simulated sample of lanthanides in zirconium matrix with Ln/Zr amount ratio of 2,50,000. As shown in Fig. 3.7 all the lanthanides were separated with satisfactory resolution using the developed elution steps. Standard addition method was used for the quantification of lanthanides. A good agreement was observed between the added concentrations of lanthanides and those determined by HPLC. Linear calibration curves have been obtained for all the lanthanides with correlation coefficient of $R^2 > 99$ in the range from 0.01 to 0.1 ppm with the preconcentration based HPLC method.

Table 3. 4: HPLC method for Separation of Individual lanthanides from bulk of zirconium	
Steps	Chromatographic Conditions
Conditioning	0.15 M pH 2 α -HIBA
Loading	Approx. 500 ppm of Zirconium containing Trace Lns in 0.15 M pH 2 α -HIBA
Washing of bulk zirconium	Isocratic Elution- 0.15 M pH 2 α -HIBA
Individual Separation of Lanthanides	0.15 M pH 2 α -HIBA in 0 to 3 mins; 0 m to 0.2 M pH 6 α -HIBA from 3 mins to 20 mins

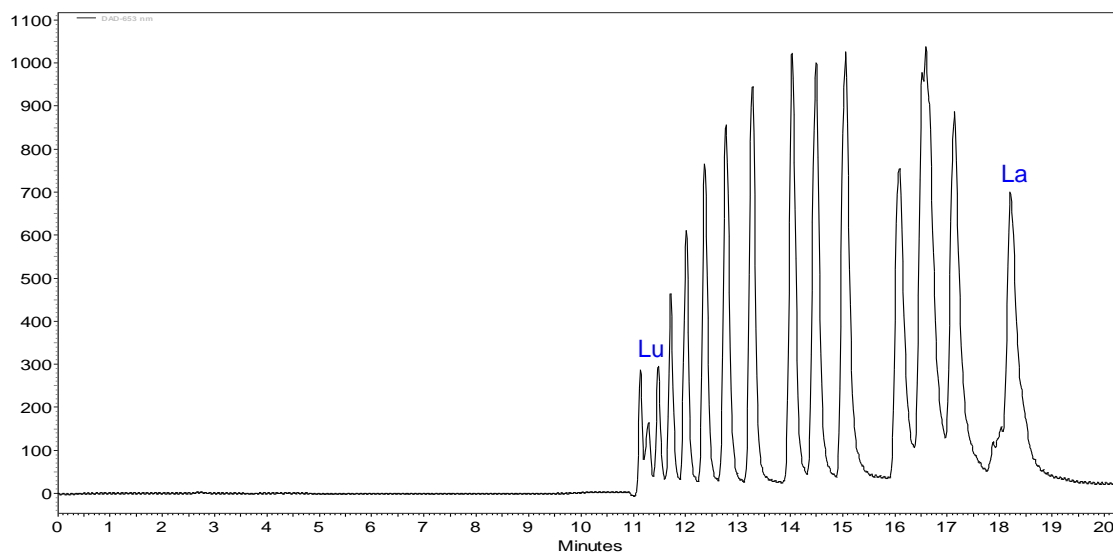


Fig 3.7. Pre-concentration and separation individual lanthanides in zirconium with Ln: Zr amount ratio 1: 50,000. Conditions: α -HIBA pH 6.0 changed from 0.025 M to 0.125 M in 25 min and then changed to 0.25 M from 25 min to 35 min

3.6. Conclusions

An HPLC based method for the preconcentration of lanthanides on modified RP column was developed. The method was found to be effective for the preconcentration and separation of trace amounts of lanthanides in presence of large excess of zirconium matrix. The developed method was used for the determination of lanthanides in a simulated sample with zirconium to lanthanide amount ratios up to 2, 50,000. Use of a single eluent, α -HIBA, at different pH was helpful in achieving the preconcentration and separation of the lanthanides large zirconium matrix. The present method obviates the need for offline removal of zirconium matrix prior to the separation of lanthanides. Hence, method offers a simple approach for quantification of lanthanides in zirconium matrix. The methodology was validated by simulated samples. Good agreement was obtained for the developed method by virtue of the selectivity and enrichment of the analyte. The methodology can be used routinely for the determination of lanthanides in zirconium matrix.

Chapter 4

Study on complexation of palladium with thiourea-based ligands and its determination in simulated high-level liquid waste using solid phase extraction-electrospray mass spectrometry

4.1 Introduction

Significant quantities of platinum group of elements (PGEs) viz. ruthenium (Ru), rhodium (Rh) and palladium (Pd) are formed in nuclear reactors as fission products [86-87]. Their limited availability and increasing global demand make nuclear reactor produced PGEs as an alternative potential source of PGEs for selective applications.

Extraction of these elements from nuclear waste is also important for better nuclear waste management as they form separate phase during the vitrification process [11]. High level liquid waste (HLLW) obtained from reprocessing of spent nuclear fuel of PHWR (burn up 6700 MWD per te) and FBTR (burn up 150 GWD per te) contains $\sim 132 \text{ ng mL}^{-1}$ and $\sim 390 \text{ ng mL}^{-1}$ of Pd, respectively. Palladium obtained from fission comprises of isotopes ^{104}Pd (17 wt%), ^{105}Pd (29 wt%), ^{106}Pd (21 wt%), ^{107}Pd (17 wt%), ^{108}Pd (12 wt%), ^{110}Pd (4 wt%). Among all isotopes, ^{107}Pd is the only radioactive isotope with a half-life of 6.5×10^6 years and is a soft β emitter with β_{max} of 35 keV. Still it finds various applications in nuclear field as the associated radioactivity of ^{107}Pd may be insignificant [87]. Several research groups are exploring the possibility of recovering Pd from high level liquid waste by methods like solvent extraction [88] and ion exchange [89]. Pd recovered from nuclear waste is proposed to use in the purification and storage of tritium [90], coating of zircaloy cladding materials [91] and nuclear fusion systems [92].

Thiourea (TU) and its derivatives offer selective binding with PGEs due to their soft nature and hence find applications in extraction and separation of these elements from different matrices [93-94]. TU is a strong nucleophile and building block of N-benzoylthiourea (BTU) and N,N-diethyl-N'-benzoylthiourea (DEBT). BTU was used for pre-concentration of Pd from simulated high level liquid waste (SHLLW) by employing disposable pipette extraction (DPX) and subsequent quantification by ESI-MS [95]. DEBT was used for the selective

preconcentration of Pd in urine and soil sample using HPLC [68-69]. Recently DEBT was used for the solvent extraction of Pd and gold (Au) from chloride medium [98]. A review on the fundamental co-ordination chemistry and analytical applications of N-alkyl- and N,N-dialkyl-N'-acyl(aryl)thiourea based ligands is available in the literature [99]. ESI-MS has emerged as an unequivocal technique to study metal-ligand equilibrium due to its capability for high sensitive detection and simultaneous determination of multiple species [100]. However, ESI-MS response of a given species can be highly influenced by the presence of matrix effect and co-existing elements. Techniques like liquid chromatography or capillary electrophoresis are reported for isolation of analyte from the matrix elements [101-102]. In solid phase extraction (SPE), a liquid sample is passed across an adsorbent bed to selectively concentrate the target analyte and this process minimizes matrix effect which may adversely affects the ESI-MS response. Automation of solid phase extraction (Auto-SPE) enables one-to-one replication of manual process steps on an automated platform. The use of Auto-SPE brings other benefits such as improved precision and reliability of the analysis, since the procedure does not rely on the experience of the user. An automated SPE methodology is especially beneficial while handling radioactive samples as it minimizes the radiation exposure. Very few reports are available for quantification of trace metals by ESI-MS [103-109]. This situation may be due to the matrix effect of co-existing ions and availability of established technique such as ICP-MS and ICP-AES. In the present report, the complexation of Pd(II) with TU, BTU and DEBT were compared using ESI-MS. In order to characterize different Pd species in ESI-MS, different instrumental parameters were optimised. Tandem mass spectrometric technique (ms/ms) was used for investigating relative stability of Pd species in gas phase. Among the three ligands, DEBT is found to form the most stable complexes based on tandem mass spectrometric results. Hence separation of Pd was carried out by auto-SPE using DEBT as

chelating agent and determination of Pd was done using ESI–MS by monitoring $[\text{Pd}(\text{DEBT})_2]^+$ species. Proposed method was then applied for determination of Pd in SHLW.

4.2 Experimental

4.2.1. Chemical and reagents

Pd, Pt, Ru, Rh, Ag, Cd and U solutions were prepared from respective ICP-MS standards (Merck, Germany) of 1000 ppm concentration. N-benzoylthiourea (BTU) and Thiourea (TU) were procured from Alpha Aesar, UK. The synthesis of DEBT was carried out according to the procedure given elsewhere [82]. Sample solutions for ESI–MS analysis were prepared by mixing palladium ($5 \times 10^{-6} \text{ M}$) and ligand ($2 \times 10^{-5} \text{ M}$) and NaClO_4 ($1 \times 10^{-5} \text{ M}$) in methanol (Sigma Aldrich, India). SPE cartridge containing C_{18} sorbent particles (3ml, 200 mg, 45 μm Gerstel, Germany) were used for the pre-concentration studies. SHLLW solution was obtained from Waste Management Division (WMD), BARC as per the composition provided in Table 4.1 [111].

Table 4.1 Composition of simulated high level liquid waste [113]

Elements	Concentration ($\mu\text{g/g}$)	Elements	Concentration ($\mu\text{g/g}$)
Ba	60	Cs	320
Fe	720	Nd	120
Cr	120	Pr	90
Ni	110	Sm	86
Mn	430	La	180
K	220	Ce	60
Na	5500	Sr	30
Mo	140	Y	60
Zr	4		

4.2.2 Instrumentation

Quadrupole-time-of-flight (Q-ToF) mass spectrometer (Bruker Daltonik, Germany) equipped with an electrospray ionization (ESI) source was used for the studies. The ESIQ-ToF was calibrated with an internal calibration standard, Tune mix. Compass isotope pattern software (Bruker Daltonik, Germany) was used to compare the isotopic patterns as well as to calculate the expected mass of the species. Samples were introduced into the ESI source using an automatic syringe pump (Cetoni GmbH, Germany) at a flow rate of 4 Lmin⁻¹. All data were collected and analyzed using Bruker Compass data analysis software for ms and ms/ms modes. Nitrogen was used as a sheath gas as well as auxiliary gas. ESI-MS analyses were performed in the positive ion mode at a capillary voltage of - 4.5 kV and at an end plate offset voltage of - 500 V. Capillary temperature of 180 °C; sheath gas flow rate of 4 Lmin⁻¹ and auxiliary gas pressure of 0.3 bar were routinely used for ESI-MS. For all the species, the identification of peaks was confirmed by accurate mass measurement and comparison of the observed m/z with the theoretically calculated data using natural isotopic abundances of the different elements. Ms/ms measurements were carried out using high purity argon as a collision gas. The species to be activated is mass selected and subjected to collision induced dissociation (CID) by increasing the collision energies up to the level where the species experience full fragmentation. All solid phase extraction studies were performed using a multipurpose sampler (Gerstel, Germany) having robotic X-Y-Z coordinate arm and the sequence of steps were controlled using Maestro software (Gerstel, Germany). The auto sampler head was equipped with a 2.5 mL syringe for all sample preparation steps. SPE cartridges having transport adapters and syringe needles were used for extraction.

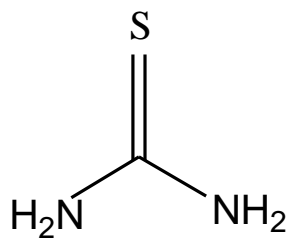
4.3 SPE procedure

DEBT was dissolved in methanol to obtain a stock solution of 0.1 M. This solution was mixed with appropriate volumes of Pd(II) solution and nitric acid to obtain the required proportions of Pd(II) and DEBT. Blank solution consisting of (2×10^{-5} M) DEBT in 0.2 M HNO₃ in 9:1 water–methanol mixture was prepared and used for conditioning as well as washing of C₁₈ cartridge. To carry out the extraction studies, C₁₈ cartridge was first washed with 2 mL methanol and then conditioned with 2 mL of blank solution. 1–4 mL of Pd(II) solution prepared in blank was allowed to pass through the conditioned cartridge. Washing was carried out with 2 mL of blank solution to remove matrix elements. Elution of Pd(II) was done with 2 mL of methanol. The fraction was mixed with 10 μ L of 10^{-3} M DEBT and then directly introduced into the ESI–MS system. A known amount of Pd was added to SHLLW and the final dilution was made to 3 M HNO₃ to maintain the SHLLW conditions

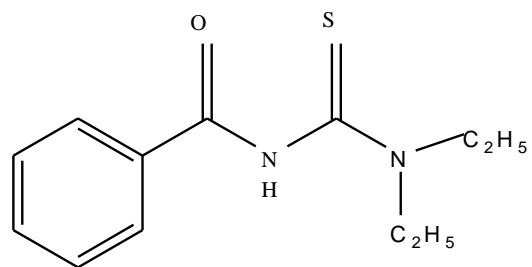
4.4 Results and discussion

4.4.1 ESI–MS studies of Pd-thiourea derivatives

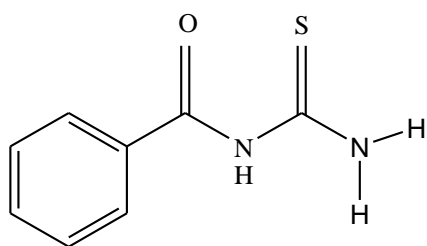
All ligands viz. TU, BTU and DEBT (Fig. 4.1) are neutral in nature and hence positive ion mode was used for ESI–MS studies. Methanol was used as a solvent as it does not form solvated species with Pd and offers better ESI–MS efficiency compared to acetonitrile [112]. Based on our previous work on Pd-BTU system [95], a metal to ligand ratio of 1:4 was used for acquiring the ESI–MS spectra. Mass spectra obtained by infusing the complexes of Pd(II) with TU, BTU and DEBT in methanol are shown in Fig. 4.2a–c, respectively. The identity of all the Pd species were verified by the isotopic pattern as well as the accurate mass data. e.g. Fig. 4.2d is the expanded region of $[\text{Pd}(\text{DEBT})_2]^+$ at m/z 577.08 confirming the isotopic pattern for Pd. Different species of Pd in positive ion mode assigned for the three ligands are presented in Table 4.2. m/z of the species reported by considering the m/z of the most abundant isotope of



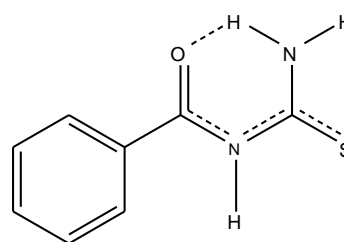
(a) Thiourea (TU)



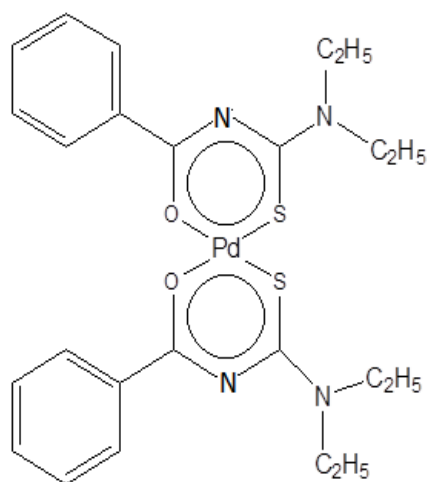
(c) N,N-diethyl-N'-Benzoylthiourea (DEBT)



(b1) Cis Benzoylthiourea (cis -BTU)



(b2) Trans-Benzoylthiourea (trans-BTU)



(d) Pd(DEBT)₂ complex

Fig. 4.1 Structures of the ligands and Pd-DEBT complex [99, 96]

each element in a species. In case of Pd-TU system, $[\text{Pd}(\text{TU})_3\text{Cl}]^+$ was the most abundant species. This species shows that TU coordinates to Pd through sulphur atom, essentially behaves as a monodentate ligand [102]. Species such as $[\text{Pd}(\text{TU})_3]^+$ and $[\text{Pd}(\text{TU})_2]^+$ were also observed with relative abundances of 96% and 53%, respectively. In Pd-BTU system, $[\text{Pd}(\text{BTU})_2]^+$, $[\text{Pd}(\text{BTU})_2\text{Cl}]^+$ and $[\text{Pd}(\text{BTU})_3\text{Cl}]^+$ were the major species observed with abundances 87%, 99% and 100%, respectively. Based on the DFT studies, we have previously reported that BTU occurs in two geometrical conformational forms viz. cis and trans [113]. In cis form, due to the possibility of coordination through both oxygen and sulphur, it behaves as a bidentate ligand and forms two six membered chelating ring with Pd. However, the trans BTU has only one sulphur donor atom available for coordination with Pd as it is forming an intramolecular hydrogen bond between the carbonyl oxygen $-\text{C}(\text{O})\text{N}$ and $-\text{C}(\text{S})\text{NHR}$ moiety. Thus trans BTU should behave as a monodentate ligand similar to TU. Due to chelate effect, complex of Pd formed with cis isomer of BTU is thermodynamically more stable than that formed by trans isomer [85]. In the case of $[\text{Pd}(\text{BTU})_3\text{Cl}]^+$, all the BTU molecules must be behaving as monodentate ligand. Similarly, in the case of the species such as $[\text{Pd}(\text{BTU})_3]^+$, one of the BTU must be behaving as a bidentate and other two as monodentate. However, in case of DEBT, it forms preferentially $[\text{Pd}(\text{DEBT})_2]^+$ with a relative abundance 100%. It behaves similar to cis BTU. As in case of DEBT, the substitution on N-moiety by two ethyl group prevents the intramolecular hydrogen bonding and thus facilitates preferential bidentate coordination with Pd. The species observed in ESI-MS supports the bonding as reported in literature. However, the dominance of species observed in mass spectra can be influenced by instrumental parameters. It was of interest to study the effect of instrumental parameter on the intensity of different Pd species.

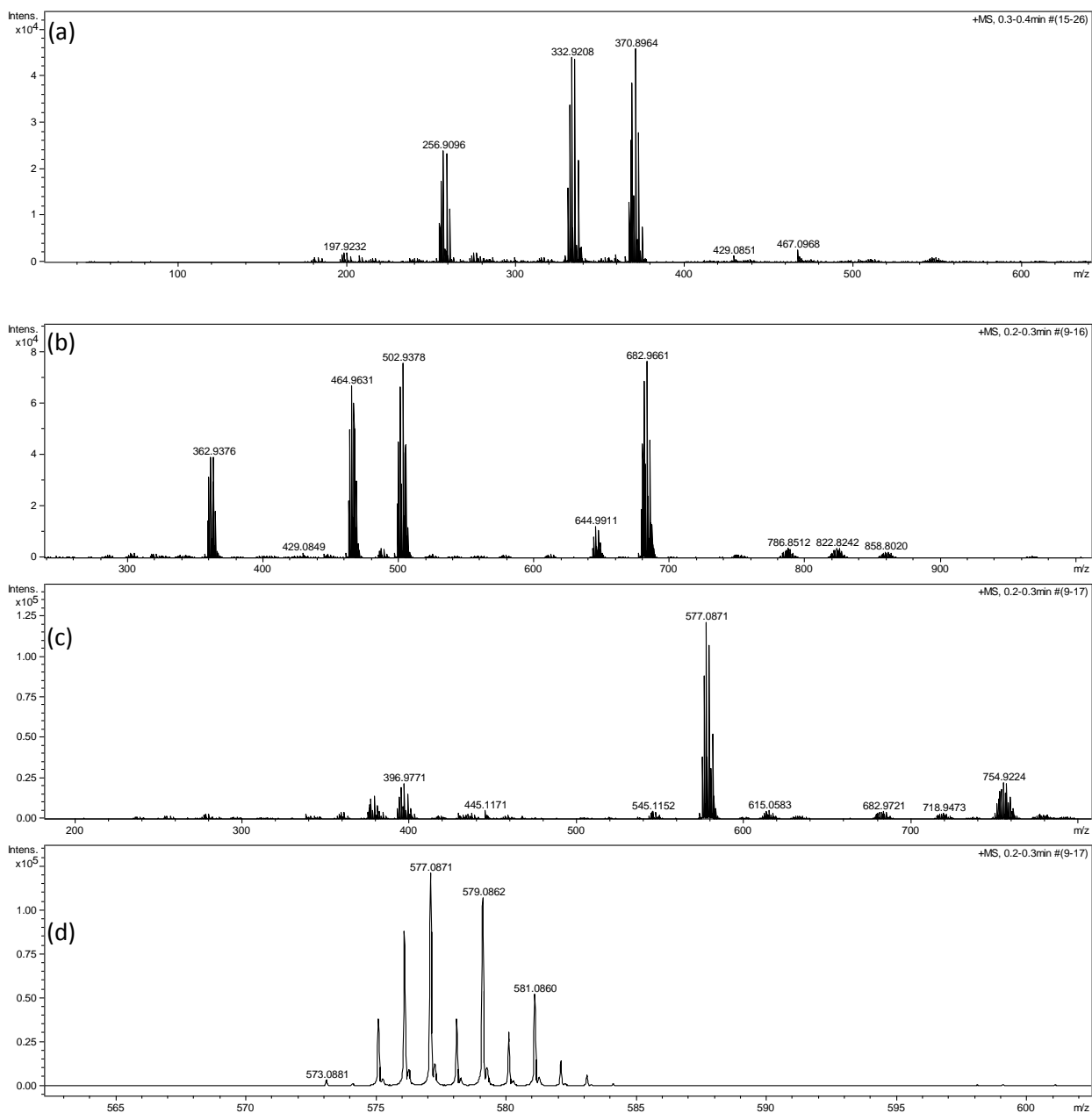


Fig. 4.2 ESI-MS spectra of Pd (5×10^{-6} M) in methanol containing (1×10^{-5} M) NaClO₄ and (2×10^{-5} M) of the ligands; (a)TU, (b)BTU and (c) DEBT. (d) Expanded region of $[\text{Pd}(\text{DEBT})_2]^+$

Table 4.2 Distribution of Pd species in positive ion mode

Assignment	m/z and relative intensity w.r.t. base peak		
	TU	BTU	DEBT
ML ⁺	-----	284.93(1.0)	340.99(3.0)
ML(OH) ⁺	197.9 (4.7)	302.94(2%)	-----
ML(H ₂ O) ⁺	-----	-----	359(3.0)
ML(OH) ₂ ⁺	-----	318.91(2.0)	-----
MLCl ⁺	-----	-----	378.96 (11)
MLCl(H ₂ O) ⁺	-----	-----	396.97(17)
ML(TU) ⁺	-----	360.93(52.0)	-----
ML(SCN) ⁺	239.88 (2.0)	-----	-----
ML ₂ ⁺	256.91 (53.3)	464.96(87)	577.06 (100)
ML ₂ Na ⁺	-----	486.94(5.0)	-----
ML ₂ (OH) ⁺	274.91 (4.4)	-----	-----
ML ₂ Cl ⁺	292.88 (1.32)	502.96(99.5)	615.05(5.0)
ML ₂ (TU)Cl ⁺	-----	578.92(2.0)	-----
ML ₂ (SCN)	314.87(2.0)	-----	-----
ML ₂ Cl ₂ Na ⁺	352.84(2.3)	-----	-----
ML ₃ ⁺	332.92(96.5)	644.99(16)	813.17(1)
ML ₃ Cl ⁺	370.89(100)	682.96 (100)	-----
M ₂ L ₂ Cl ⁺	-----	-----	718.94(3.0)
M ₂ L ₂ Cl ₂ ⁺	-----	-----	754.92(17)
M ₂ L ₃ Cl ⁺	-----	786.86 (4.0)	955.06 (11)
M ₂ L ₃ Cl ₂ ⁺	510.76 (1.47)	822.82 (5.0)	-----
M ₂ L ₃ Cl ₃ ⁺	548.73 (2.2)	858.8 (3.0)	-----
M ₂ L ₄ Cl ⁺	-----	966.88 (2.0)	-----

Abundance in parenthesis.

Palladium (5×10^{-6} M) in methanol containing 2×10^{-5} M of the ligand and 1×10^{-5} M of NaClO₄.

4.4.2 Optimization of instrumental parameters

In ESI–MS, the process of ionisation and subsequent detection of metal complexes depends on instrumental parameters [114]. Proper selection of instrumental parameters helps in circumventing problems like cluster formation under mild conditions and fragmentation under harsh conditions.

4.4.2.1 Quadrupole energy

Figs 4.1SIa, 4.1SIb and 4.1SIc show the effect of quadrupole energy on the intensities of major species of Pd with ligands TU, BTU and DEBT, respectively. During this experiment, a collision cell energy of 8 eV was employed. From Figs. 4.1SIa, 4.1SIb and 4.1SIc, it is clear that PdL₂ type species is the most dominating species in the quadrupole energy region of 6–12 eV indicating the stability of the PdL₂ species. PdL₂ type species has reported to play a pivotal role in the separation of Pd by solution based techniques when BTU or DEBT was employed as a complexing agent [95-99].

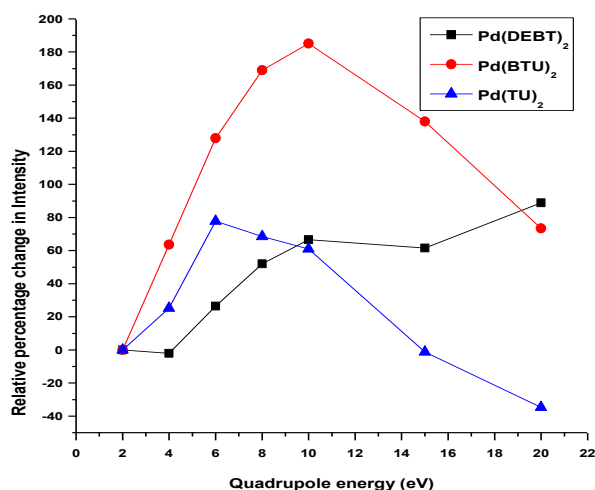


Fig. 4.3 Effect of quadrupole ion energy on intensities of PdL₂ complex species of TU, BTU, DEBT

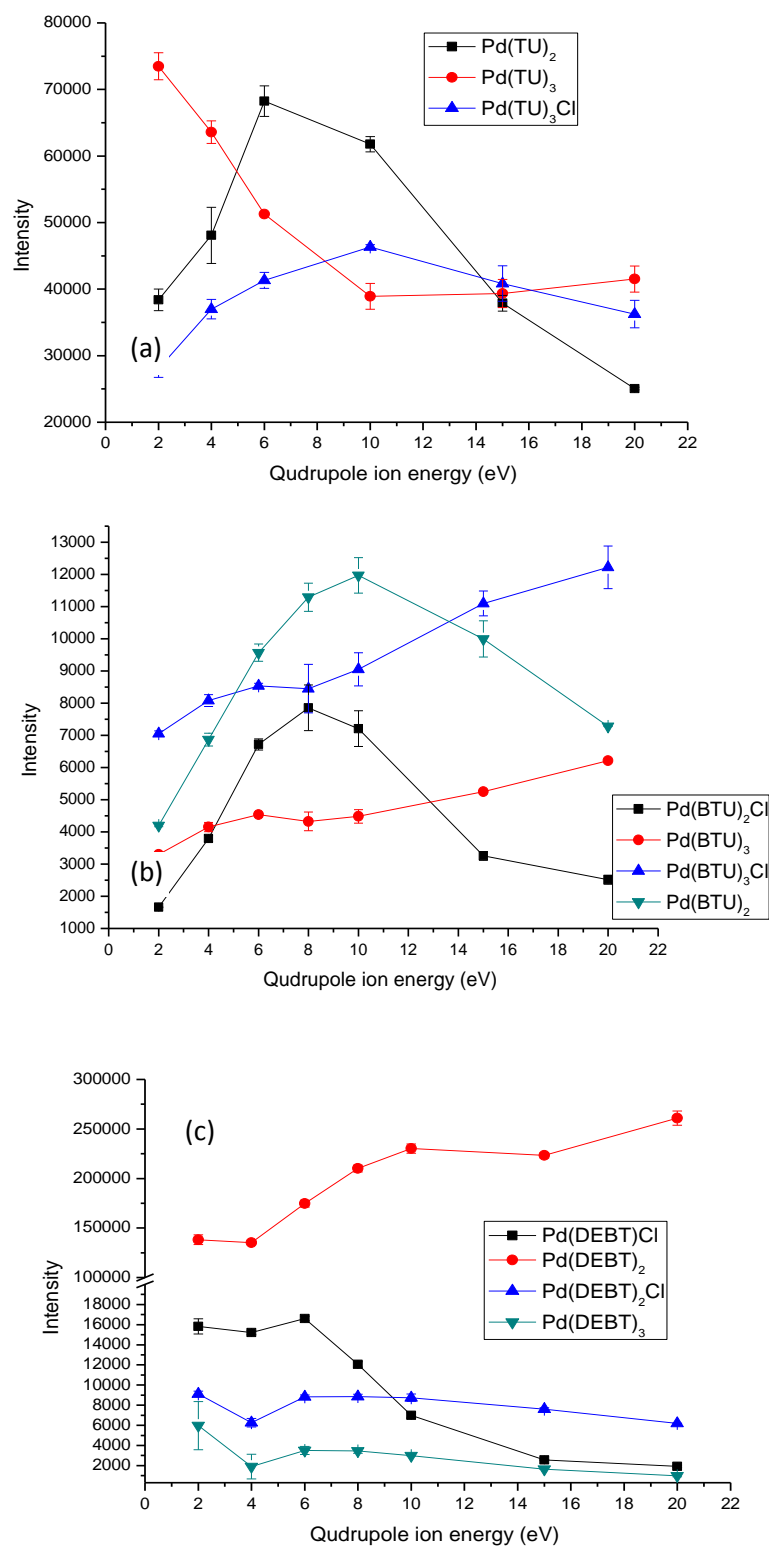


Fig. 4. 1 SI Effect of quadrupole ion energy on intensities of Palladium complex species of (a) TU (b) BTU and (c) DEBT

Fig 4.3 shows the relative percentage change in intensity of these species with respect to their original intensity.

$$\text{Relative percentage change} = [(I_i - I_r) \times 100] / I_i$$

where I_i and I_r are initial intensity and intensity at a given ion energy. When the PdL₂ type of species were compared as a function of quadrupole ion energy, it was found that with the increase in quadrupole energy, ion transmission became more effective and ion intensity was enhanced. However, at higher quadrupole energies, species may suffer fragmentation depending upon the stability of species. It is seen that relative intensities of both [Pd(BTU)₂]⁺ and [Pd(TU)₂]⁺ increase initially as a function of quadrupole ion energy but later on decrease due to fragmentation. In the case [Pd(DEBT)₂]⁺, relative intensity shows an increasing trend during the entire quadrupole ion energy range studied. The relative percentage change in intensity is minimum for [Pd(DEBT)₂]⁺. The reason for the different trend shown by the [Pd(DEBT)₂]⁺ species compared to [Pd(BTU)₂]⁺ and [Pd(TU)₂]⁺ must be attributed to the greater stability of [Pd(DEBT)₂]⁺. Based on the behaviour of the PdL₂ type ions in the above study, a quadrupole ion energy of 10 eV was chosen for further studies.

4.4.2.2 Collision cell energy

In the mass spectrometer, while proceeding from quadrupole region towards ToF region, ions are passed through a collision cell containing argon as a collision gas. In the collision cell region, the extent of fragmentation undergone by a species depends on its kinetic stability. Fig. 4.2SIa, 4.2SIb and 4.2SIc show the effect of collision cell energy on the intensities of the major species of Pd. PdL₂ is the dominating species when the collision cell energy was in the range 2–8 eV. Fig. 4.4 shows the relative change in intensities of PdL₂ type species formed with ligands is TU, BTU and DEBT as a function of collision cell energy. When the relative change in intensities is compared, unlike in quadrupole ion energy studies, all species show decreasing

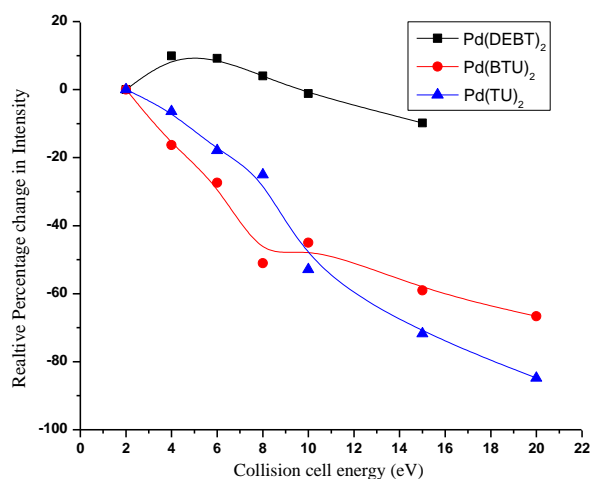


Fig. 4.4 Effect of collision cell energy on the relative percentage change in intensities of PdL₂ complex species of TU, BTU and DEBT

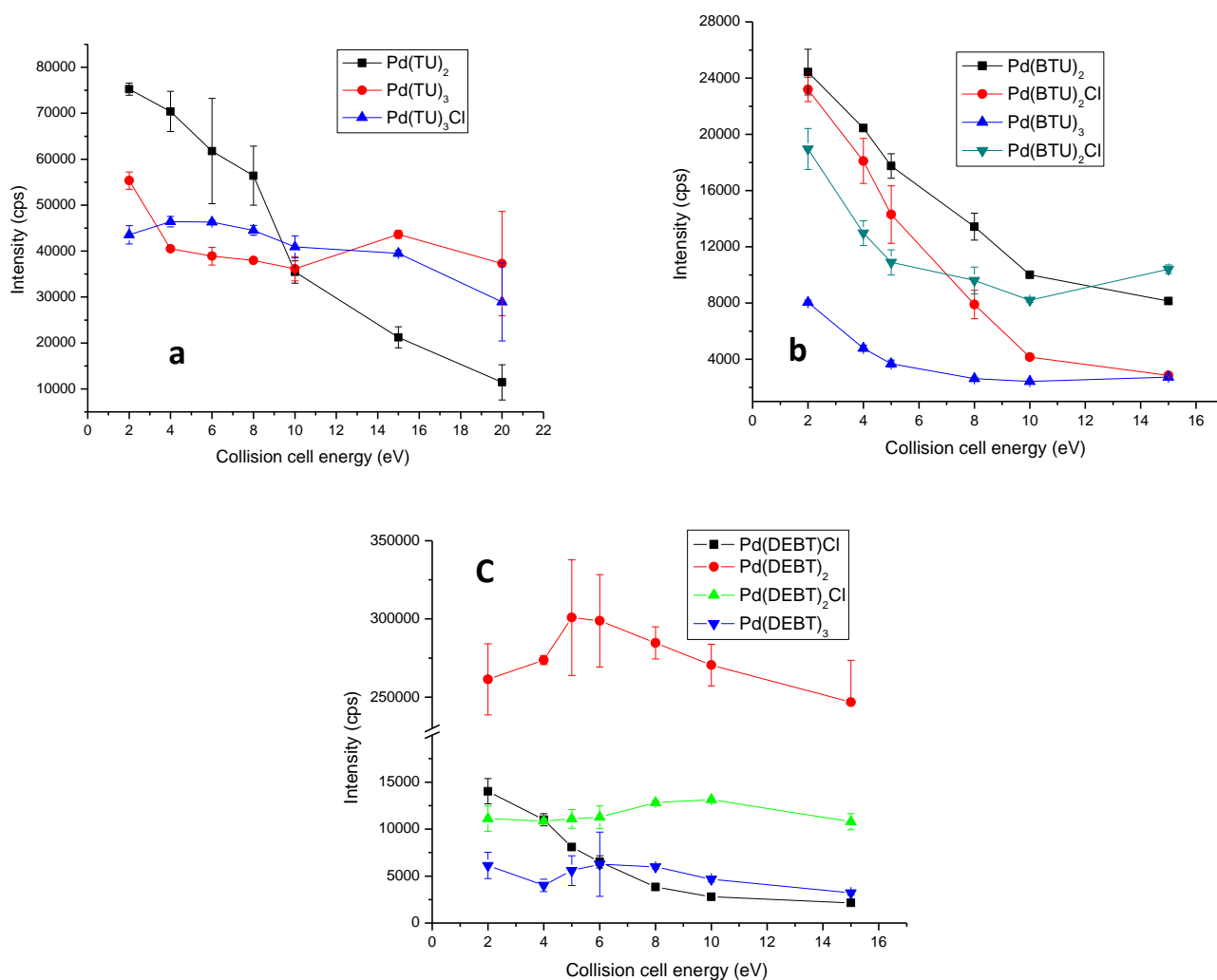


Fig. 4. 2 SI Effect of collision cell energy on intensities of Palladium complex species of (a) TU, b)BTU and (c) DEBT

trend with increase in the collision cell energy. However, both $[\text{Pd}(\text{BTU})_2]^+$ and $[\text{Pd}(\text{TU})_2]^+$ display sharply decreasing pattern whereas $[\text{Pd}(\text{DEBT})_2]^+$ shows a moderate trend. These trends confirms that $[\text{Pd}(\text{DEBT})_2]^+$ has a higher relative stability in comparison to $[\text{Pd}(\text{BTU})_2]^+$ and $[\text{Pd}(\text{TU})_2]^+$. In order to estimate the relative stability of these species, collision induced dissociation (CID) studies of these individual complexes were carried out using tandem mass spectrometry. In simple ms mode, a given daughter ion can be produced from different parent ions e.g. ML_1 can be produced by the fragmentation of ML_2 as well as ML_3 . Since in ms/ms mode, the parent ions were filtered by the primary quadrupole, there is no ambiguity exists about the formation of daughters while determining the intensity ratios.

4.4.2.3 Tandem mass spectrometric study

The major species of Pd were selected for collision induced dissociation (CID) study to investigate their relative binding strength. Species of the desired m/z were selected using quadrupole and allowed to collide with argon gas in the collision cell at energies from 0 to 22 eV. The resultant fragmented ionic species were then monitored by ToF. The ratio of sum of intensities of daughter ions to that of undissociated parent ions at different collision energies were compared as a way of establishing the relative stability of the complexes in the gas phase [115-117]. A lower value of daughter to parent ion intensity ratio at a given collision energy is indicative of the stability of the species. Fig 4.5a shows the ratio of intensities of daughters to parent for major Pd-TU species as a function of collision cell energy. Over the range of collision energies from 1 to 10 eV, $[\text{Pd}(\text{TU})_2]^+$ shows the highest stability followed by $[\text{Pd}(\text{TU})_3]^+$ and $[\text{Pd}(\text{TU})_3\text{Cl}]^+$. Monodentate binding of TU with Pd is reported in solid and solution phases. However, the stability of $[\text{Pd}(\text{TU})_2]^+$ compared to the other Pd-TU species observed in CID studies of this work could not be explained based on the monodentate nature of TU. Further studies are required to understand the stability of this species. The extent of fragmentation shown by all the PdTU species varied linearly with the collision energy

In case of BTU (Fig. 4.5b), the pattern of change in intensities of $[\text{Pd}(\text{BTU})_2\text{Cl}]^+$, $[\text{Pd}(\text{BTU})_3]$ and $[\text{Pd}(\text{BTU})_3\text{Cl}]^+$ were almost similar, However $[\text{Pd}(\text{BTU})_2]^+$ was showing more stability towards collisions compare to other major species. In $[\text{Pd}(\text{BTU})_2]^+$, both BTU ligands must be in cis form which facilitates the bidentate nature and helps to form a double six member chelating rings. The stability of $[\text{Pd}(\text{BTU})_2]^+$ against collision can be attributed to the formation of this chelating ring with Pd. In $[\text{Pd}(\text{BTU})_2\text{Cl}]^+$, $[\text{Pd}(\text{BTU})_3]^+$ and $[\text{Pd}(\text{BTU})_3\text{Cl}]^+$, at least one of the BTU ligands must be in monodentate mode of coordination. Therefore these species showed lesser stability compared to $[\text{Pd}(\text{BTU})_2]^+$. In Pd-DEBT system (Fig. 4.5c), the species $[\text{Pd}(\text{DEBT})_2]^+$ showed more stability compared to $[\text{Pd}(\text{DEBT})_3]^+$. The stability of $[\text{Pd}(\text{DEBT})_2]^+$ must be due to the formation of a double six membered ring similar to $[\text{Pd}(\text{BTU})_2]^+$. Substitution on N-moiety by diethyl group not only prevents the intra-molecular hydrogen bonding but also increases the charge density on sulphur.

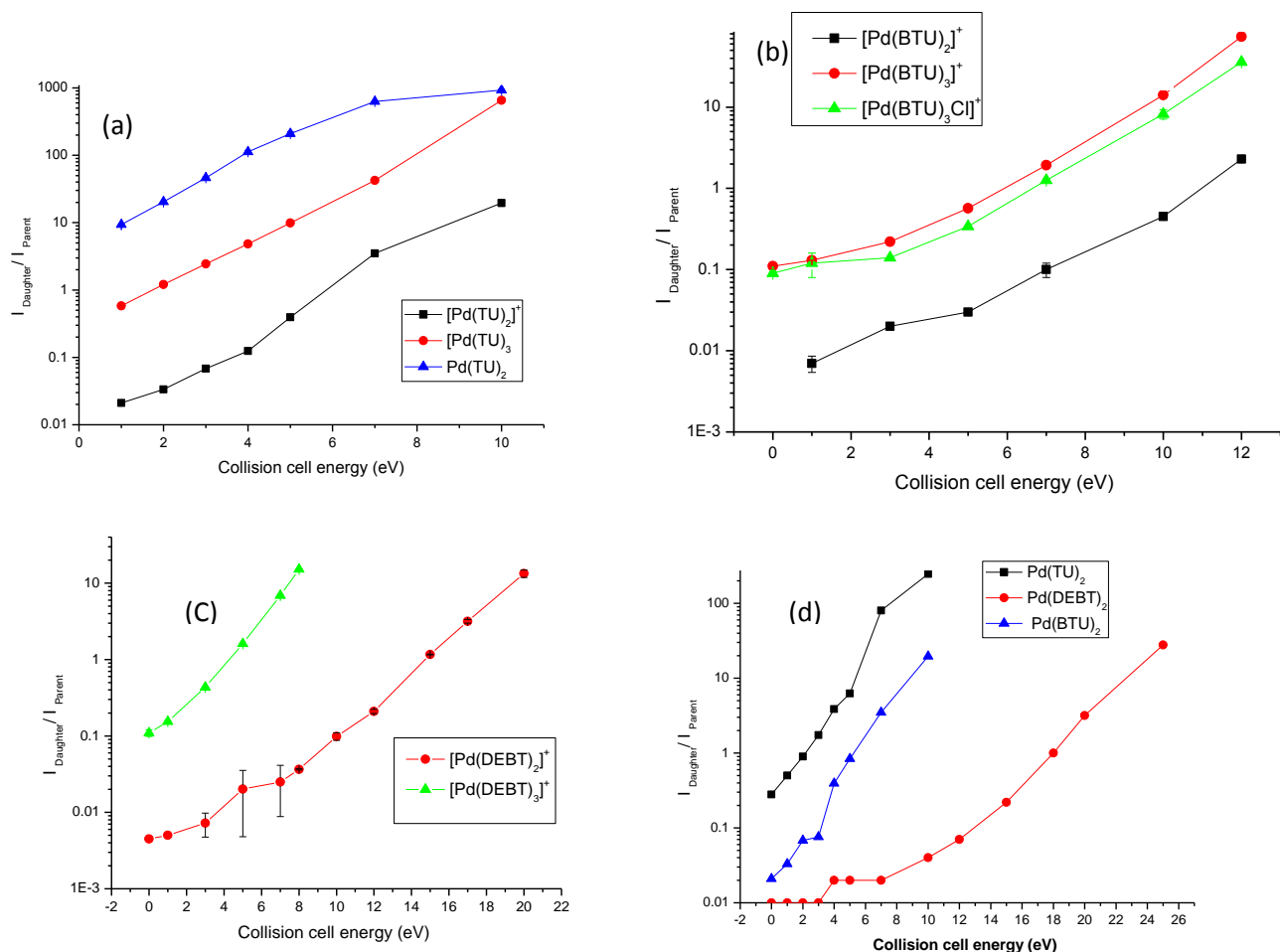


Fig. 4.5 Collision induced dissociation as function of collision energy for Pd complexes with (a) TU, (b) BTU (c) DEBT and (d) PdL₂ species

This increase in charge density must also be contributing to the stability of $[\text{Pd}(\text{DEBT})_2]^+$ complex. In $[\text{Pd}(\text{DEBT})_3]^+$, one DEBT is in bidentate form whereas other two must be in monodentate form and this explains the decrease in stability of the species. It is observed from the above studies of collision induced dissociation that the complexes in which ligands bind to metal through bidentate mode show greater stability compared to the complex in which ligands are monodentately coordinated. Thus PdL₂ type of species were found to be the most stable compared to PdL₃ and PdL₃Cl as a function of collision induced dissociation. In case of PdL₃ or PdL₃Cl species, at least two of the ligands must be in monodentate binding mode. The order of the stability observed during the CID experiment is PdL₂ > PdL₃ > PdL₃Cl. It would be

interesting to compare the stabilities of PdL₂ type species formed by the three ligands TU, BTU and DEBT. As shown in Fig. 4.5d, among PdL₂ species of these three ligands, [Pd(DEBT)₂]⁺ was found to be the most stable followed by [Pd(BTU)₂]⁺. Both DEBT and BTU form double six-member ring during coordination with Pd, resulting more stability to these complexes. The absence of intra-molecular hydrogen bonding as well as the higher electron density on sulphur lead to greater stability of [Pd(DEBT)₂]⁺ complex compared to [Pd(BTU)₂]⁺. This is in close resemblance with the reported studies [99]. In order to demonstrate the applicability of ligand for extraction studies, intensities of different ligands PdL₂ species were compared.

4.4.3 Intensities of PdL₂ species

ESI–MS intensities of PdL₂ species formed from three different complexing agents were compared in the ms mode. As shown in Fig. 4.6, better ESI responses of [Pd(DEBT)₂]⁺ and [Pd(BTU)₂]⁺ compared to [Pd(TU)₂]⁺ could be due to presence of an aromatic ring in the complex, which resulted in better charging of the analyte during ionization process [86]. It was found that the intensity of [Pd(DEBT)₂]⁺ was ~5 times higher than that of [Pd(BTU)₂]⁺, under similar conditions. The higher intensity of DEBT over BTU must be due to exclusive bidentate coordinate nature of DEBT. On the other hand, in addition to [Pd(BTU)₂]⁺, BTU forms a number of species such as [Pd(BTU)₃Cl]⁺, [Pd(BTU)₂Cl]⁺, [Pd₂(BTU)₃]⁺, [Pd₂(- BTU)₃Cl]⁺, [Pd₂(BTU)₃Cl₂]⁺ etc. This is attributed to the preferential formation of PdL₂ species by DEBT compare to BTU. The fact that DEBT forms more stable complex with Pd compared to other ligands should help in employing higher potentials in the ion transfer system of the mass spectrometer and this should lead to better ion transmission efficiency with minimal fragmentation. Better ion transfer efficiency as well as the inherent improved sensitivity make DEBT a preferred chelating agent for quantification of Pd using ESI–MS. Better ESI–MS sensitivity of Pd using DEBT ligand compared to TU and BTU paved the way for its application in separation studies.

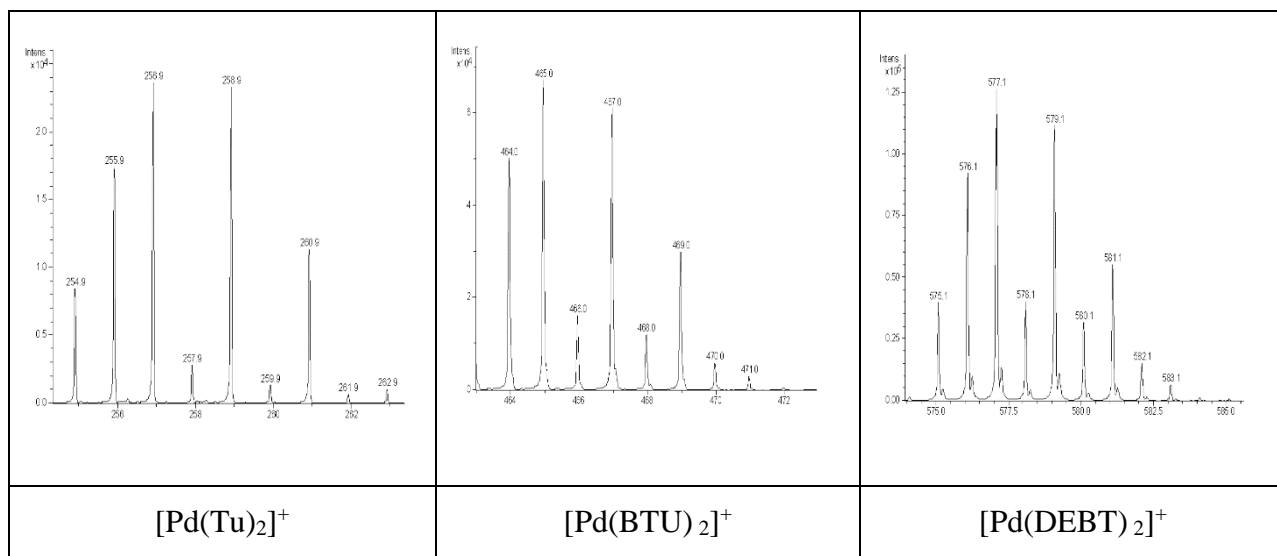
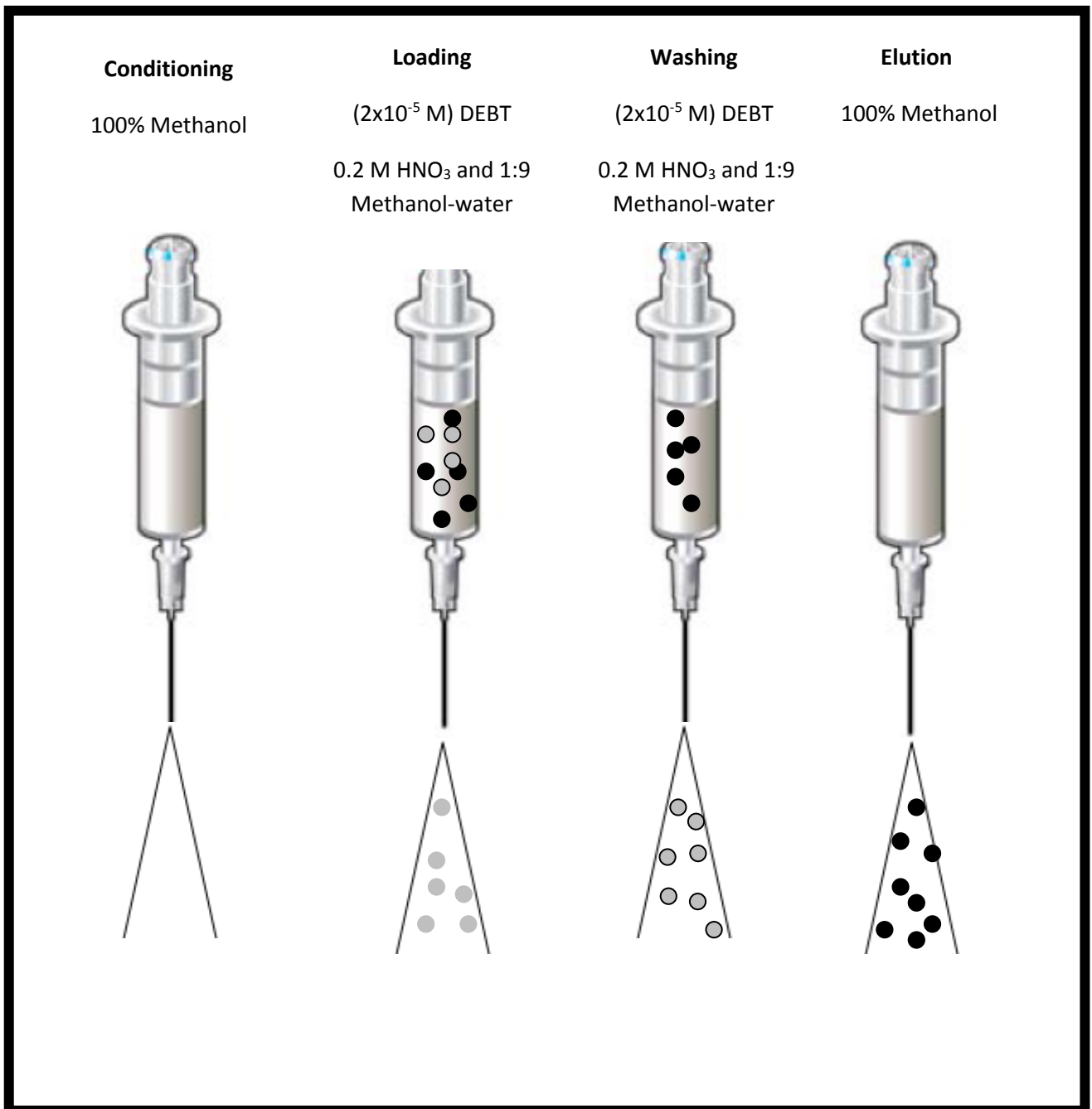


Fig. 4.6 Comparison of ESI-MS intensities of PdL₂ species using Pd (5x10⁻⁶ M) in methanol containing ligand (2x10⁻⁵ M) and NaClO₄ (1x10⁻⁵ M)

4.5 Development of auto-SPE method for palladium determination

Above findings were exploited to develop an auto-SPE method for separation of Pd employing DEBT as a chelating agent and subsequent determination by monitoring $[\text{Pd}(\text{DEBT})_2]^+$ species at m/z 577.08 using ESI-MS. Experimental parameters like concentration of DEBT, acidity, and proportion of water/methanol of the feed solution were optimized for the effective recovery of Pd using auto-SPE. Studies were carried out to optimize the loading volume for a fixed amount of Pd. The maximum volume of sample solution that can be loaded was found to be 4 mL. Further increase in loading volume led to bleeding of Pd from the C₁₈ cartridge. Studies on the effect of nitric acid showed an increase in Pd recovery till 0.2 M of HNO₃ and further increase in acidity led to decrease in Pd recovery. An increase in acidity enhances the ion pair formation (charge neutralization) of the $[\text{Pd}(\text{DEBT})_2]^+$ complex and the neutral complex is more preferred for the adsorption by hydrophobic stationary phase. This explains the initial

increase in the recovery of Pd with increased acidity. The decrease in recovery at higher acidity is attributed to dissociation of the complex $[\text{Pd}(\text{DEBT})_2]^+$. Studies showed that with the increase of methanol content in loading solution, recovery of Pd decreases. This is due to the hydrophobic nature of Pd complex. The presence of methanol increases the elution strength of the medium and thus reduces the retention of Pd-DEBT complex on to the C_{18} stationary phase during the loading stage. The intensities of metal–ligand species depends on the medium of solution to be infused into ESI–MS. Studies were also carried out with respect to methanol content for direct infusion of Pd complex in ESI–MS. It was found that the intensity of $[\text{Pd}(\text{DEBT})_2]^+$ increase with proportion of methanol. It was found that 50% of methanol is required for direct infusion of $[\text{Pd}(\text{DEBT})_2]^+$ complex. With increase in methanol content, surface tension of the solution decreases which helps in the enhancement of ionisation. Fig. 4.7 shows the schematic of the automated solid phase extraction process for Pd. The conditions optimised for sample loading consisted of (2×10^{-5} M) DEBT in 0.2 M HNO_3 and 1:9 methanol– water. Later on Pd was eluted using 2 mL of methanol. Eluted fraction was directly analyzed by ESI–MS after addition of 10 μL 10^{-3} M DEBT. To compare the performance of DEBT with BTU, similar studies were carried out with BTU as a complexing agent. ESI–MS response of $[\text{Pd}(\text{DEBT})_2]^+$ was found to be ~5 times more than that observed for $[\text{Pd}(\text{BTU})_2]^+$. Detection limits for $[\text{Pd}(\text{BTU})_2]$ and $[\text{Pd}(\text{DEBT})_2]^+$ were calculated from signal to noise ratio (S/N) > 3 and found to be 0.015 ppb and 0.007 ppb respectively



- ● Matrix Elements
- Palladium

Fig. 4.7 Schematic of the automated solid phase extraction process for Palladium

Under optimised conditions, a recovery of $> 87\% \pm 5\%$ was obtained for Pd using DEBT as a complexing agent. Interference study was carried out by preparing simulated high level waste solutions containing different concentrations of Pd (range 5–100 mg/L). These solutions were subjected to the pre-concentration followed by ESI– MS determination. The response of Pd obtained as shown in Fig. 4.8, demonstrates that the developed method offers quantitative recovery of Pd with Fe/Pd amount ratio in the range 1.5×10^5 to 7×10^3 . Under similar conditions the Na/Pd ratios were in the range 1.1×10^6 to 5.5×10^4 . Isobaric interference study was carried out to identify the possible interferences from Ru, Rh and Ag. There was no interference observed from these elements till a concentration of 100 ppb while monitoring the $[\text{Pd}(\text{DEBT})_2]^+$ peak. The optimized method was then applied for Pd determination in simulated HLLW solution. The developed method summarizes in Fig. 4.8, offered quantitative recovery of Pd in the concentration range of 1–100 ppb with precision from 1 to 2 %. This study showed that the uptake of Pd by DPX stationary phase as well as its ESI response are not affected by other ions present in the Simulated high level waste.

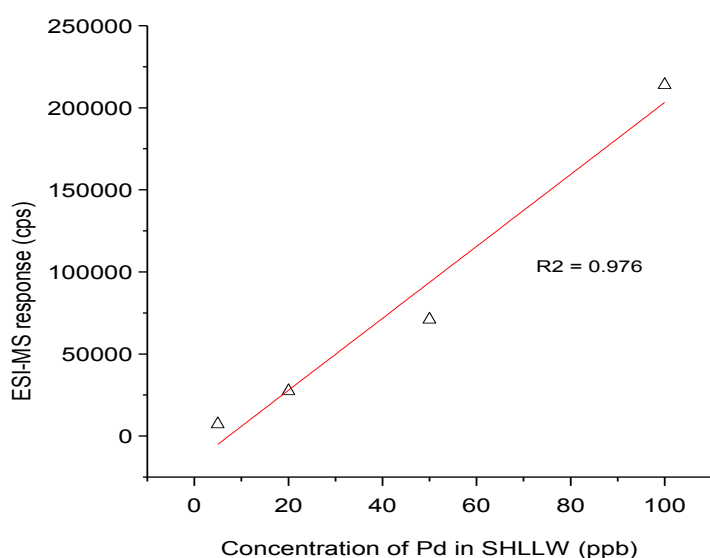


Fig. 4.8 ESI-MS response of $[\text{Pd}(\text{DEBT})_2]^+$ as a function of concentration of Pd in SHLLW solution

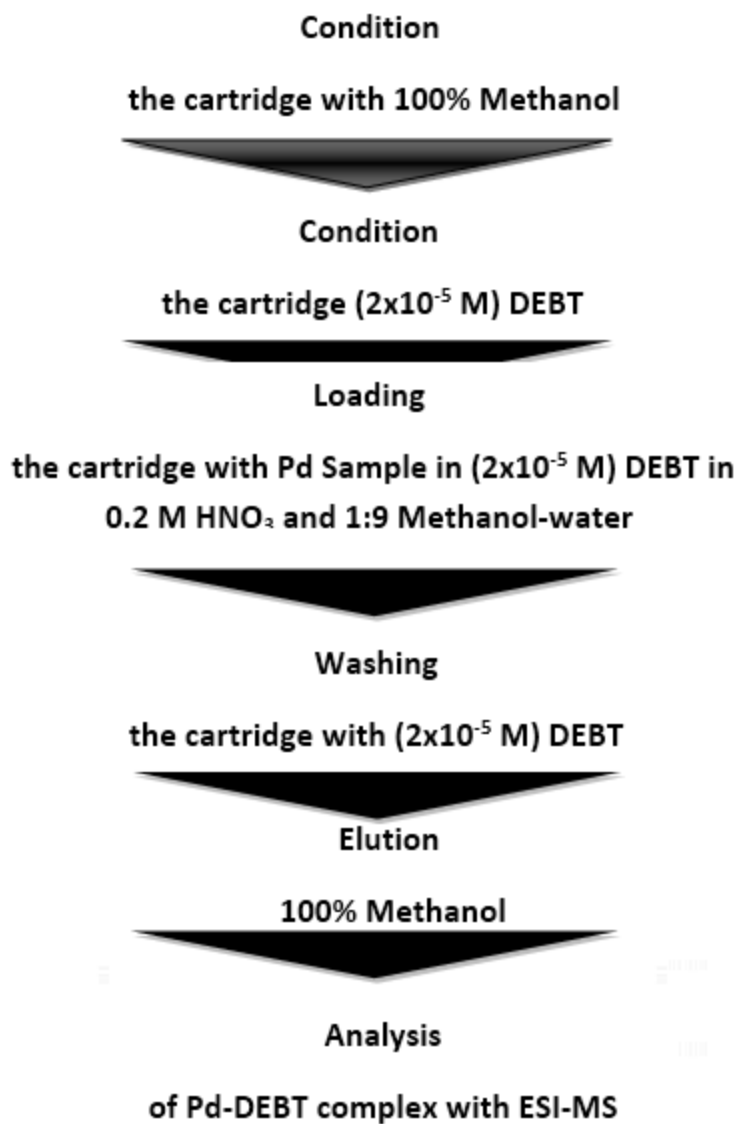


Fig. 4.09 Auto-SPE method for Pd determination in SHLW using ESI-MS

4.6 Comparison with other techniques

The developed auto-SPE method for determination of palladium was compared with the established methods available in the literature [118-119]. The method using DEBT offers a limit of detection of 7 ngL⁻¹ of Pd whereas the limits of detection for the commonly used methods like ICP-MS and GFAAS are 1 ngL⁻¹ and 2.4 ngL⁻¹, respectively. Developed method for Pd showed linearity in the concentration range of 5–100 ppb whereas the linearities exhibited by ICP-MS and GFAAS are in the range 0–100 ppb and 0.1–5 ppb, respectively. However, the present method offers the preconcentration in low pH condition which is suitable for the application to HLLW. Another advantage of ESI-MS is the tolerance to the organic extractant and this allows for the direct infusion of the eluted sample without any further treatment. Use of 100% methanol helps to recover the analyte in small volume of the eluent.

4.7 Conclusions

The present study shows the efficacy of ESI-MS as a tool for studying the complexation of Pd with TU, BTU and DEBT in gas phase. Major species formed in the gas phase by the three ligands with Pd were identified. For all the three ligands, PdL₂ type species were found to be stable. Collision induced dissociation experiments carried out in the ms/ms mode showed that in gas phase, PdL₂ complex formed with DEBT are relatively more stable as compared to those formed with BTU and TU. Greater stability, exclusive formation of a specific species and better ESI sensitivity makes DEBT as a preferred chelating agent for the quantitative determination of Pd using ESI-MS. The automated SPE method is useful for the sample preparation to minimize matrix effects. Trace amounts of Pd in simulated HLLW could be determined by ESI-MS with offline separation by auto-SPE. The developed SPE method would be suitable for analyzing SHLLW samples containing wide variety of metal ions.

Chapter 5

Separation and estimation of ^{229}Th and ^{233}U by alpha and gamma ray spectrometric technique

5.1 Introduction

In recent time, scientist are putting their effort to generate nuclear power based on the concept of fast reactor [120-124], advanced heavy water reactor (AHWR) [125-126] and accelerator driven sub-critical system (ADSs) [127-132]. In AHWR, ^{232}Th - ^{233}U is the primary fuel for power generation. The ^{232}Th - ^{233}U fuel in connection with ADSs [127-132] is one of the possibilities for power generation besides transmutation of long-lived fission products (e.g. ^{93}Zr , ^{99}Tc , ^{107}Pd , ^{129}I & ^{135}Cs) and incineration of long-lived minor actinides (e.g. ^{237}Np , ^{240}Pu , ^{241}Am , ^{243}Am & ^{244}Cm) to solve the problem of radioactive waste. The ADSs based on the ^{232}Th - ^{233}U fuel cycle is important because one can explore its potential to design a hybrid reactor system that can produce nuclear power with the use of thorium as a main fuel [133]. Thus, the concept of the energy amplifier (EA) [127-133] in the hybrid system is based on the thorium fuel cycle and a spallation neutron source (Pb, Bi) of ADSs. The ^{232}Th - ^{233}U fuel in AHWR and ADSs has an advantage from the point of production of thousand times less radiotoxic waste (long-lived minor actinides) than the present reactor based on uranium fuel. Besides these, thorium in the Earth's crust is three to four times more abundant than uranium. Thus, it is a fact that ^{232}Th is the only nucleus present in nature which can give rise to an excess of fissile material ^{233}U in presence of either thermal or fast neutrons, and thus making it an excellent choice for future nuclear reactors. In the thorium-uranium cycle, the fissile nucleus ^{233}U is generated by two successive β -decays after a neutron capture of the fertile nucleus ^{232}Th . A schematic diagram of ^{233}U production from ^{232}Th [134-136] is given below in Fig 5.0

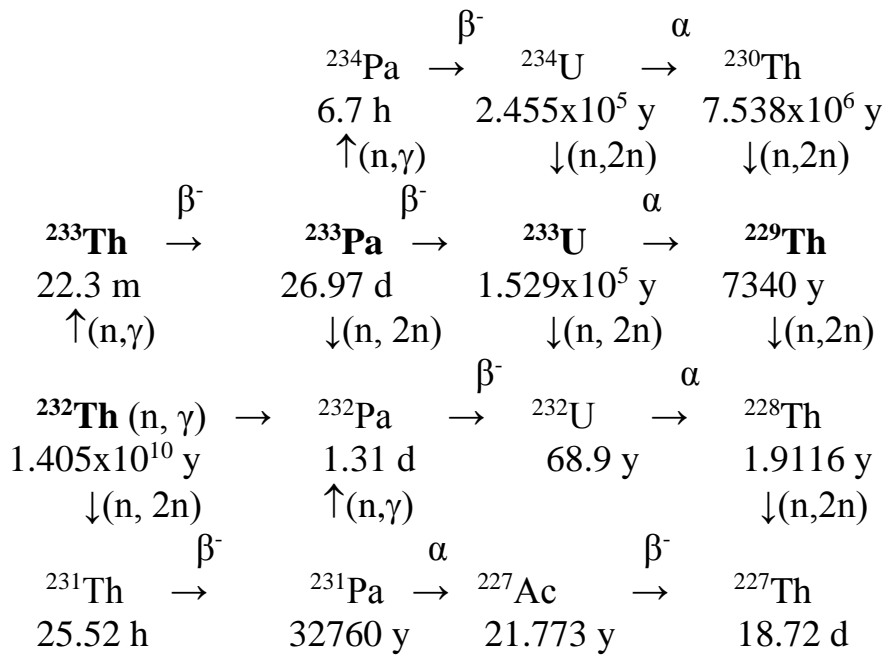


Fig. 5.0 Schematic diagram for the production of different isotopes of Th and U

The ^{233}U nuclide produced in the above fuel cycle has to be separated from ^{232}Th and other reaction/fission products after complete decay of ^{233}Pa for its use in AHWR. As can be seen from the above decay scheme that the separated ^{233}U is always associated with the $^{232,234}\text{U}$ and its daughter product ^{229}Th . So in each chemical purification stage, it is always necessary to estimate the amount of ^{233}U and ^{229}Th . Different methods such as mass spectrometry [137], Isotope Dilution Mass Spectrometry (IDMS) [138], Thermal ionization mass spectrometry (TIMS) [8], potentiometry [111], alpha and γ -ray scintillation counting technique [140], alpha [141] and γ -ray spectrometric [142] techniques are available to estimate the amount of ^{239}Pu - ^{238}U and ^{233}U - ^{232}Th . Among these methods, the IDMS can be employed for the quantification of actinide elements (U and Th) because the results are not affected by incomplete recovery after equilibration of sample and spike isotopes [138]. On the other hand, TIMS is a single element analysis technique and it is desired that the element is available in the pure form to achieve the best results. In IDMS or TIMS techniques, ^{229}Th is used as a spike for concentration determination of ^{232}Th . For this purpose, ^{229}Th was isolated from its parent nuclide ^{233}U and

daughter products by employing anion exchange separation. However, in the absence of an efficient separation procedure, there can be a possibility that ^{229}Th is associated with some amounts of ^{233}U . The decay of ^{233}U in the mixture would lead to uncertainty in the true concentration of ^{229}Th over a period of time and this would necessitate frequent calibrations with respect to its concentration. Hence it is of importance to estimate the ^{233}U content in ^{229}Th before the later is used as a spike. The estimate of ^{233}U content in ^{229}Th sample can be done by alpha spectrometric technique, which is a very good method for alpha active actinides with low gamma ray intensity such as $^{238,239,240}\text{Pu}$ and ^{233}U . However, this method fails when there is an overlapping or same alpha line for radionuclide pairs such as ^{233}U - ^{229}Th , ^{239}Pu - ^{240}Pu and ^{241}Am - ^{238}Pu . In all these types of estimation, except γ -ray spectrometry [142] rest all need a prior chemical separation, which is tedious process. In view of this, in the present work we have used both alpha and gamma ray spectrometric techniques [143] for simultaneous estimation of ^{229}Th and ^{233}U up to pico-gram level in unpurified liquid aliquot without their chemical separation.

5.2 Experimental method

From a long back purified stock of ^{233}U solution, 100 μl was pipetted out and diluted to 5 ml. 100 μl of the dilute solution was taken in another micro pipette and put on a stainless steel planchet. It was dried under IR lamp, fired to red hot and cooled for fifteen minutes. The plancheted source was taken for alpha and γ -ray spectrometric analysis.

First alpha counting of a plancheted standard source of known amount of ^{239}Pu and ^{241}Am was done by using silicon surface barrier detector connected to a Personal Computer (PC) based 4K channel analyzer. The alpha spectrum of the standard ^{239}Pu - ^{241}Am source was used for energy and efficiency calibration of the silicon surface barrier detector system. The resolution of the detector system was 30 keV at 5.485 MeV of ^{241}Am . Then alpha counting of the impure (^{233}U - ^{229}Th +daughter products) sample was done by using same set up at a fixed

geometry. A typical alpha ray spectrum of the impure (^{233}U - ^{229}Th +daughter products) sample is shown in Fig. 5.1.

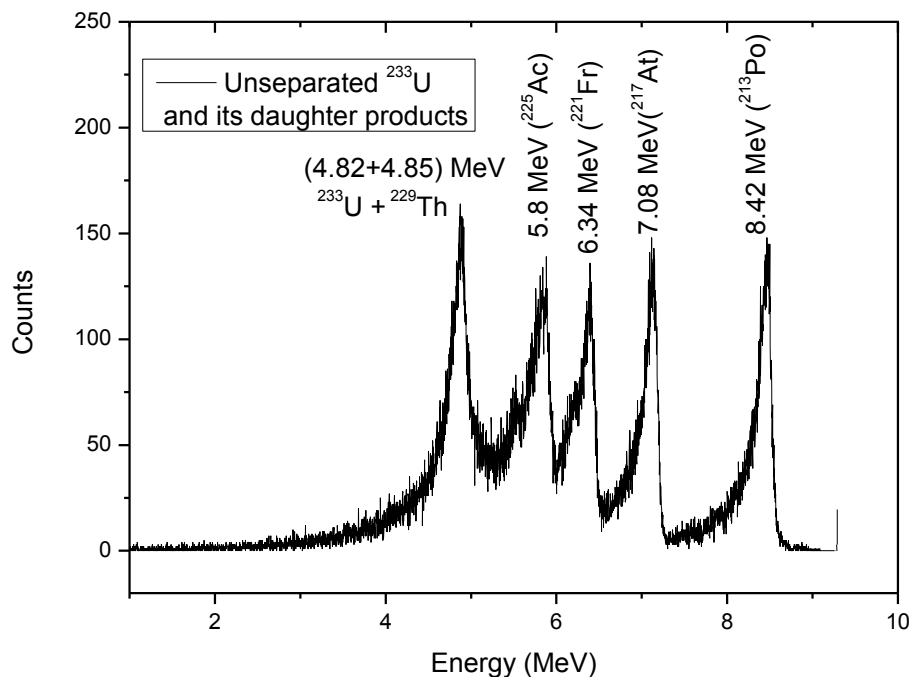


Fig. 5.1 Alpha spectrum of unpurified ^{233}U activity along with its daughter products activities

The same sample on stainless planchet was also counted for γ -ray using energy and efficiency calibrated high purity germanium (HPGe) detector coupled to a PC based 4K channel analyzer. The resolution of the detector system was 1.8 keV at 1332.0 keV γ -line of ^{60}Co . The energy calibration of the detector system was done by using ^{152}Eu source. However, efficiency calibration of the detector system was done by using standard sources of ^{133}Ba and ^{152}Eu . Gamma rays counting of the standard and unknown samples were done in the same geometry at 6 cm distance from the detector. A typical γ -ray spectrum of the impure (^{233}U - ^{229}Th +daughter products) sample is shown in Fig. 5.2.

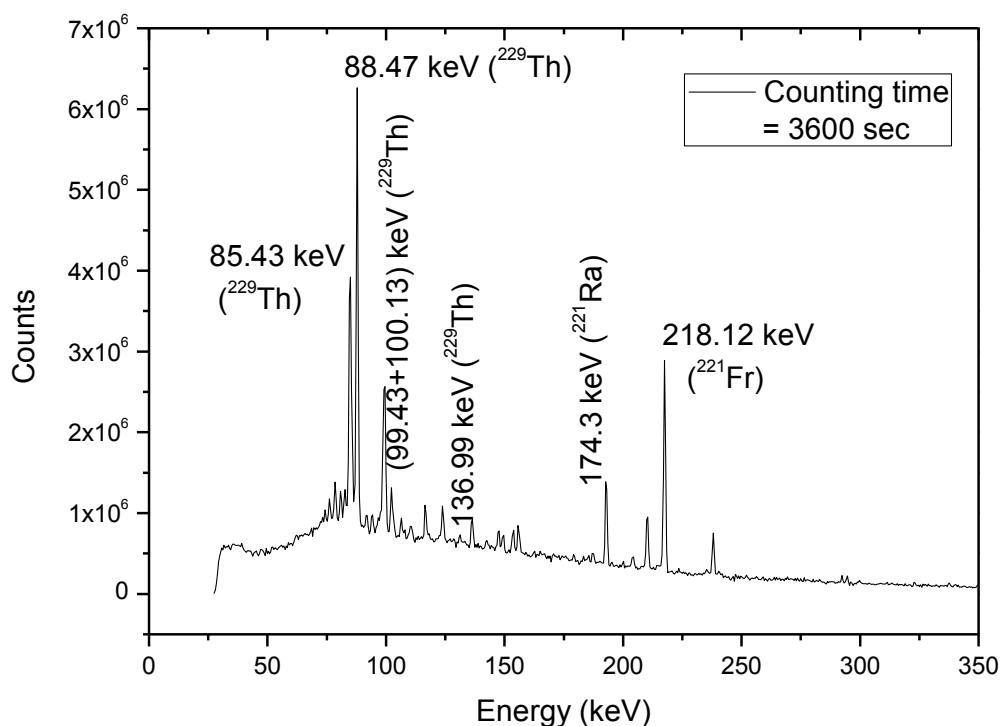


Fig. 5.2 Gamma-ray spectrum of unpurified ^{233}U activity along with its daughter products activities

The aliquot containing ^{233}U along with its daughter product in 1M nitric acid medium was subjected to separation by anion exchange using Dowex 1x8, 200-400 mesh resin [116-117]. When 9 M HCl was used as the mobile phase, uranium alone is retained on the stationary phase and ^{229}Th is wash down along with the decay products. After sufficient washing of the stationary phase, uranium was eluted using 0.1 M HNO_3 . ^{229}Th was separated from decay products using another column packed with Dowex 1x8 resin in 7 M HNO_3 . For this purpose, the washings from the first stage of separation were collected, dried and treated with concentrated HNO_3 for ensuring the complete removal of chlorine. Subsequently, the treated solutions were loaded onto the ion exchange column in 7M HNO_3 and washed with 7M HNO_3 .

Under these conditions, ^{229}Th alone is retained while the remaining decay products were removed during the loading and washings steps. Later, ^{229}Th was eluted with 0.1 M HNO_3 .

The purified fractions of ^{233}U and ^{229}Th were evaporated on a hot plate and redissolved in 1 M HNO_3 . The sources were prepared by spotting about 25 microlitre of the purified fractions on the polished surface of stainless steel planchets. After drying on a hot plate, these planchets were fired to red hot condition using bunsen burner. The plancheted sources of purified ^{233}U and ^{229}Th were used for alpha and gamma ray spectrometric techniques for both the sample as mentioned above for the unpurified ^{233}U sample. A typical alpha ray spectrum of the pure ^{233}U and ^{229}Th samples are shown in Fig. 5.3 and Fig. 5.4, respectively. On the other hand, a typical γ -ray spectrum of the pure ^{229}Th sample is shown in Fig. 5.5

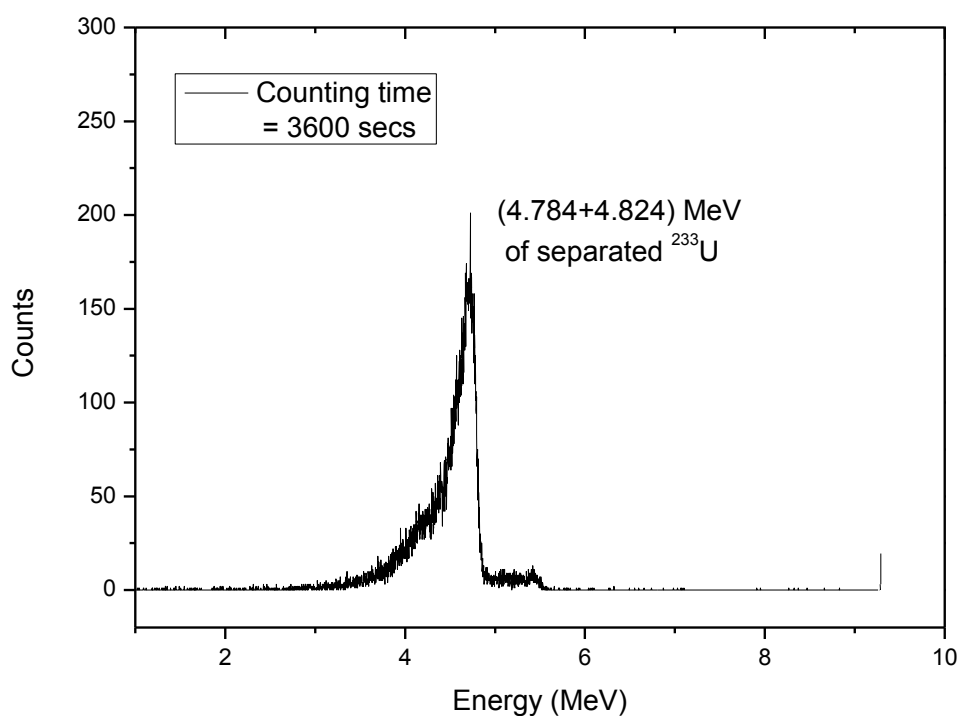


Fig. 5.3 Alpha spectrum of purified ^{233}U activity free from its daughter products activities

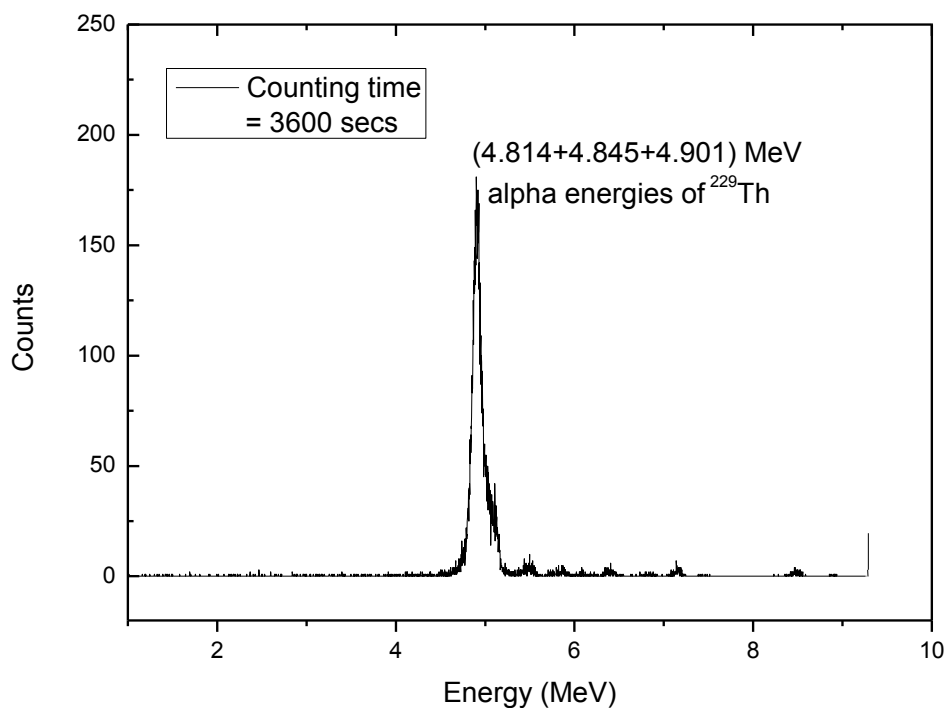


Fig. 5.4 Alpha spectrum of the purified ²²⁹Th activity

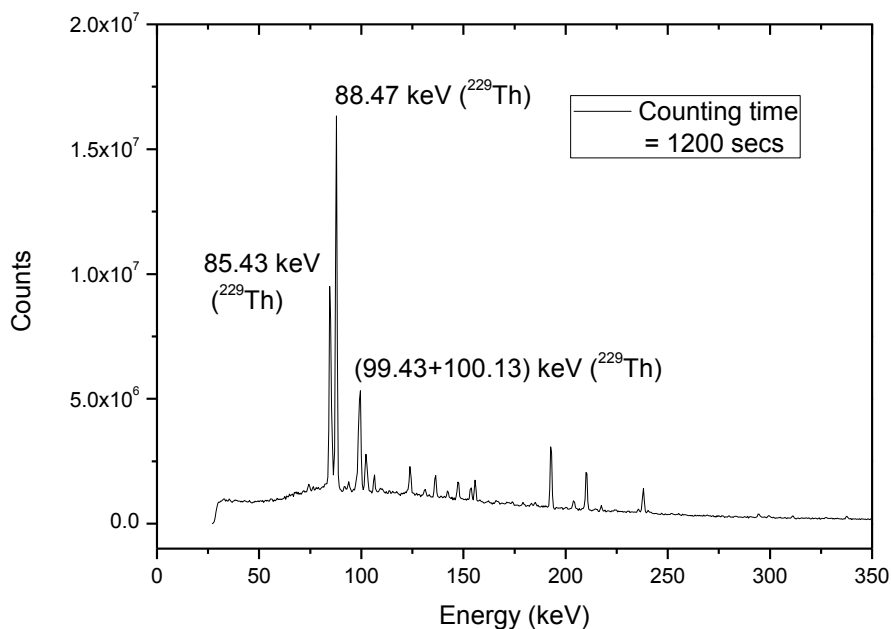


Fig. 5.5 Gamma-ray spectrum of the purified ²²⁹Th activity, which is free from its parent and daughter activities

5.3 Results

The present work is based on the alpha and gamma ray spectrometric techniques as described in our earlier work [143]. Thus it is necessary to obtain absolute efficiencies of the detector systems to determine the disintegration per second (DPS) from the observed counts per seconds (CPS). For the calculation of DPS, it also needs nuclear spectroscopic data such as half-life, alpha and γ -ray energies and their branching intensities, which was taken from reported literature. [134-136] and are given in Table 5.1. The observed CPS of alpha particles and γ -rays of the standard and sample were obtained from the alpha and γ -ray spectrum after subtracting the linear Compton background.

The α detection efficiency (ε_α) of the silicon surface barrier detector for a particular geometry was obtained from the $(\text{CPS})_\alpha$ values of the alpha energies of 5.124+5.168 MeV for ^{239}Pu and 5.443+5.485 MeV of ^{241}Am standard source by using Eq. (1). Similarly, from Eq. (2), the efficiency (ε_γ) of the HPGe detector for a particular geometry was obtained from the $(\text{CPS})_\gamma$ values of the various γ -ray energies (E_γ) such as 53.2 keV to 383.9 keV for ^{133}Ba and 121.8 keV to 1408.0 keV for ^{152}Eu standard sources.

$$\varepsilon_\alpha = (\text{CPS})_\alpha / [I_\alpha \times (\text{DPS})_\alpha], \quad (\text{CPS})_\alpha = [\text{Detected counts}]_\alpha / (\Delta t_\alpha) \quad (1)$$

$$\varepsilon_\gamma = (\text{CPS})_\gamma / [I_\gamma \times (\text{DPS})_\gamma], \quad (\text{CPS})_\gamma = [\text{Detected counts}]_\gamma / (\Delta t_\gamma) \quad (2)$$

where Δt_α and Δt_γ are the counting time of the alpha and γ -ray spectra. I_α is and I_γ are the branching intensity or the abundance of the chosen alpha and γ -ray energies, which were taken from literature [106-108]. $(\text{DPS})_\alpha$ and $(\text{DPS})_\gamma$ are the disintegration rate of the standard alpha and gamma ray sources, respectively.

Table 5.1 Nuclear spectroscopic data of ^{227,228,229,230}Th and ^{232,233,234}U. [134-136]

Nuclide	Half-life	Decay mode (%)	α -energy (MeV) (% abundance)	γ -ray energy (keV) (% abundance)
²²⁷ Th	18.68 d	α (100)	5.693 (1.5) 5.701 (3.63) 5.709 (8.3) 5.713 (4.89) 5.757 (20.4) 5.808 (1.27) 5.867 (2.42) 5.960 (3.0) 5.978 (23.5) 6.009 (2.9) 6.038 (24.2)	79.69 (1.95) 88.43 (1.34) 88.47 (2.18) 93.88 (1.51) 210.62 (1.25) 235.96 (12.9) 256.23 (7.0) 299.98 (2.21) 304.50 (1.15) 329.85 (2.9) 334.37 (1.14)
²²⁸ Th	1.9125 y	α (100) SF (1.0×10^{-11})	5.340 (26.0) 5.423 (73.4)	84.37 (1.19) 85.43 (0.0178) 88.47 (0.029)
²²⁹ Th	7340 y	α (100)	4.797 (1.5) 4.814 (9.3) 4.838 (5.0) 4.845 (56.2) 4.901 (10.2) 4.968 (5.97) 4.979 (3.17) 5.053 (6.6)	85.43 (14.7) 86.25 (1.33) 86.4 (2.57) 88.47 (23.9) 99.43(2.93) 100.13(5.61) 136.99 (1.18) 156.41 (1.19)
²³⁰ Th	7.538×10^6 y	α (100) SF (4.0×10^{-12})	4.480 (0.12) 4.621 (23.4) 4.687 (76.3)	67.67 (0.38) 85.43 (0.0042) 88.47 (0.006) 143.87 (0.04)
²³² Th	1.4×10^{10} y	α (100) SF (1.1×10^{-9})	3.811 (0.069) 3.947 (21.7) 4.012 (78.2)	63.81 (0.263) 85.43 (0.0017) 88.47 (0.0028)

^{232}U	68.9 y	α (100) SF (3.0×10^{-12})	5.263 (31.55) 5.320 (68.15)	89.96 (0.00521) 93.35 (0.00842) 104.82 (0.00104) 105.60 (0.00198) 129.08 (0.0682)
^{233}U	1.592×10^5 y	α (100) SF (6.0×10^{-11})	4.784 (13.2) 4.824 (84.3)	71.82 (0.00116) 71.83 (0.00181) 74.54 (0.00149)
^{234}U	2.455×10^5	α (100) SF (1.6×10^{-9})	4.722 (28.42) 4.775 (71.38)	53.2 (0.0123) 89.96 (0.0026) 93.35 (0.0041)
^{238}Pu	87.7 y	α (100) SF (1.85×10^{-7})	5.456 (28.98) 5.499 (70.91)	43.5 (0.0395) 99.85 (0.00729)
^{239}Pu	24100 y	α (100) SF (3.0×10^{-10})	5.106 (11.94) 5.144 (17.11) 5.157 (73.3)	51.62 (0.0271) 56.83 (0.00152) 98.43 (0.0056) 98.78 (0.00147) 129.3 (0.00631) 413.7 (0.001466)
^{240}Pu	6563 y	α (100) SF (5.75×10^{-6})	5.124 (27.1) 5.168 (72.8)	45.24 (0.045) 104.23 (0.00708) 160.31 (0.000402)
^{241}Am	432.2 y	α (100) SF (4.3×10^{-10})	5.338 (1.669) 5.443 (13.1) 5.485 (84.8)	59.54 (35.9)

In an unpurified ^{233}U sample, the $(\text{DPS})_{\text{Th}}$ value of ^{229}Th from its $(\text{CPS})_{\gamma}$ value was obtained by using Eq. (3) with appropriate efficiencies of the detector system and branching intensity (I_{γ}) from Refs. [106-108] (Table 5.1). The standard sources of ^{133}Ba and ^{152}Eu were used for efficiency calibration. The gamma ray energies of ^{133}Ba are 53.2, 81.0, 276.4, 302.85, 356.02

and 383.82 keV. Similarly the gamma ray energies of ^{152}Eu have a range from 121.8 to 1408.0 keV. The efficiency of the detector used goes down in both side for the gamma ray energy of 121.8 keV. In particular, at low energy side below 121.8 keV, the efficiency curve decreases very rapidly. So a fitted line was used for efficiencies calculations. Then with a well fitted calibrated efficiency curve efficiencies were applied for 85.43, 88.47, 99.43 and 100.13 keV gamma lines of ^{229}Th . Since the 99.43 and 100.13 keV γ -lines were not possible to resolve, the sum of the branching intensities for both are used. Similarly from the number of detected alpha particles $(\text{CPS})_{\alpha}$ of the combined alpha energy of 4.8 MeV, total disintegrations per second $(\text{DPS})_{\text{Total}}$ of ^{229}Th plus ^{233}U from the alpha spectrum in the unpurified ^{233}U sample was determined by using the equation (4).

$$(\text{DPS})_{\text{Th}} = (\text{CPS})_{\gamma} / [(\epsilon_{\gamma}) (I_{\gamma})] \quad (3)$$

$$(\text{DPS})_{\text{Total}} = (\text{CPS})_{\alpha} / [(\epsilon_{\alpha}) (I_{\alpha})] \quad (4)$$

From the total disintegration rate $(\text{DPS})_{\text{Total}}$ of ^{229}Th plus ^{233}U , disintegrations per second for ^{233}U $(\text{DPS})_{\text{U}}$ was obtained as

$$(\text{DPS})_{\text{U}} = (\text{DPS})_{\text{Total}} - (\text{DPS})_{\text{Th}} \quad (5)$$

Thus in the unpurified sample, the amount of ^{233}U in presence of its daughter product ^{229}Th can be determined within the uncertainty of 2-5%.

5.4 Discussion

The implementation of ^{232}Th - ^{233}U fuel cycle either in AHWR and/or ADSs requires development of methodologies for the determination of ^{232}Th and ^{233}U in various streams of reprocessing. In the ^{232}Th - ^{233}U fuel cycle, the amount of ^{232}Th in a processed fuel can be determined by using Isotope Dilution Mass Spectrometry (IDMS) [138] and/or Thermal ionization mass spectrometry (TIMS) [8]. In both the techniques, ^{229}Th is usually used as a

spike, which is obtained after radiochemical separation from its daughter products and parent nuclides ^{233}U . However, the spike ^{229}Th should be free from its parent ^{233}U . This is because traces of ^{233}U can hamper the mass spectrometric analysis of ^{232}Th due to their comparable masses. The amount of ^{233}U in a purified sample can be determined by using standard alpha spectrometric technique. However, in an unpurified processed fuel sample, it is not possible to estimate ^{233}U independently by alpha spectrometric technique. This is because ^{233}U has the same alpha line of 4.8 MeV with high branching intensity as of its daughter product ^{229}Th , which is shown in Table 5.1. Thus it is not possible to estimate amount of ^{233}U in the presence of its daughter ^{229}Th by alpha spectrometric technique alone unless it is freshly purified.

From the alpha spectrum of an unpurified ^{233}U sample as shown in Fig. 5.1, one can clearly say the alpha energies of the daughter products as well as ^{233}U and ^{229}Th at 4.8 MeV. Thus in an unpurified ^{233}U sample of low level liquid waste from nuclear reactor, it is not possible to estimate the amount of ^{233}U in presence of its daughter ^{229}Th by applying alpha spectrometric technique. From Table 5.1, it can be seen that branching intensities of the γ -rays of the ^{233}U is very low. Thus it is also not possible to estimate the amount of ^{233}U in any pure or unpurified sample of low level liquid waste from nuclear reactor by γ -ray spectrometric technique. Therefore the combined techniques of alpha and γ -ray spectrometry as discussed in the present work are necessary for the determination of ^{233}U in the presence of its daughter ^{229}Th . The amount of ^{229}Th in presence of ^{233}U in a purified or unpurified sample can be determined easily by γ -ray spectrometric technique. This is because ^{229}Th has 85.43, 88.47, 99.43 and 100.13 keV γ -lines with sufficient branching intensity (Table 5.1). It means the primary γ -lines seen in the γ -ray spectrum of the unpurified ^{233}U sample from Fig. 5.2 are of ^{229}Th besides some γ -lines of its daughter products. From the γ -ray spectrum of Fig. 5.2, the CPS of ^{229}Th can be obtained in presence of ^{233}U by using the γ -ray energies of 85.43, 88.47, 99.43 and 100.13 keV. From the CPS of ^{229}Th , its DPS can be estimated by using the Eq. (3) after applying the

efficiency of the detector system from Eq. (2) and the branching intensities from Refs. [136-138]. The DPS obtained based on the 99.43 and 100.13 keV photo-peaks are the sum of the branching intensities of both γ -lines. This is because the 99.43 and 100.13 keV γ -lines were not possible to resolve and thus the sum of the branching intensities for both are used together. On the other hand, the combined CPS of ^{233}U and ^{229}Th can be obtained from the alpha spectrum of Fig. 5.1. From the combine CPS of ^{233}U and ^{229}Th , total DPS can be estimated by using Eq. (4) after applying the efficiency of the silicon surface barrier detector from Eq. (1) and the branching intensity of the alpha lines from Refs. [134-136]. The total DPS of ^{233}U and ^{229}Th obtained from the alpha spectrum of the unpurified sample is certainly higher than the DPS of ^{229}Th obtained from the γ -ray spectrum. On the other hand, the DPS of ^{229}Th obtained from the alpha spectrum of purified sample of Fig. 5.4 is same as that of the value obtained from the γ -ray spectrum of Fig. 5.5. This indicates the perfect radiochemical separation of ^{229}Th from its parent ^{233}U and its daughter product. The alpha spectrum of the purified ^{233}U is shown in Fig. 5.3 for comparison. Once the DPS of ^{229}Th in an unpurified sample is estimated, the DPS of ^{233}U can be calculated from the total DPS of ^{229}Th and ^{233}U by using the Eq. (5). Therefore, the combined techniques of alpha and γ -ray spectrometry are important for the determination of ^{233}U in the presence of its daughter ^{229}Th .

The combined techniques of alpha and γ -ray spectrometry are suitable for ^{229}Th and ^{233}U estimation in low level nuclear waste generated at any stage of the ^{232}Th - ^{233}U fuel reprocessing cycle. In an alpha spectrometric technique, the decay product ^{229}Th from ^{233}U always interferes for the estimation of ^{233}U . In other technique such as potentiometry, the estimation of ^{229}Th and ^{233}U requires solutions of the separated elements. Alpha and γ -ray scintillation counting also requires purified samples to avoid the interference from fission products and other actinides. In each steps of chemical separation there is some loss of ^{233}U and potential contamination problem. Besides these problems, simultaneous estimation of ^{229}Th and ^{233}U in

low level nuclear waste is not possible in any of the above techniques. These difficulties can be avoided in the present work of alpha and γ -ray spectrometric techniques in compared to the above mentioned techniques. In the present technique, the amount of ^{229}Th and ^{233}U within the uncertainty of 2-5% can be estimated from a plancheted source of both separated and un-separated liquid waste. Besides this, the combined method of alpha and γ -ray spectrometry technique is useful to check the contamination of ^{229}Th and ^{233}U activity from one to other in the radio-chemically purified sample.

5.5 Conclusion

The combined method of alpha and γ -ray spectrometric techniques has been used for the simultaneous estimation of ^{229}Th and ^{233}U from a single plancheted source made out of unpurified ^{233}U liquid waste relevant to ^{232}Th - ^{233}U fuel cycle of AHWR and ADSs. The uncertainty of ^{229}Th and ^{233}U estimation in the present technique is within 2-5%.

The activity of ^{229}Th from its parent activity of ^{233}U was radiochemically separated by using an ion exchange resin and the purity was checked by using the present method of alpha and γ -ray spectrometric techniques.

Chapter 6

High performance liquid chromatographic separation of $^{228,229}\text{Th}$ and $^{232,233}\text{U}$ and their estimation by α - and γ -ray spectrometry

6.1 Introduction

In advanced heavy water reactor (AHWR) [97-98], the ^{232}Th - ^{233}U is the primary fuel for power generation. However, ^{232}Th - ^{233}U fuel in connection with accelerator driven sub-critical system (ADSs) [121-133] is also one of the possibilities for power generation besides transmutation of long-lived fission products and incineration of long-lived minor actinides. In the thorium-uranium fuel cycle, the fissile nucleus ^{233}U is generated by two successive β -decays after a neutron capture by the fertile nucleus ^{232}Th . A schematic diagram of ^{233}U production from ^{232}Th is given below in Fig. 5.0, whereas the nuclear spectroscopic data [134-136] such as half-life, alpha and gamma-ray energies and their branching intensities are given in Table 5.1.

From the above decay scheme it can be seen that the fissile nucleus ^{233}U decays to ^{229}Th , whereas ^{232}U decays to ^{228}Th . In a reactor, the energy of neutron spectrum varies within 0 to 20 MeV. The (n, γ) reactions has no threshold, whereas the threshold for the (n,2n) reactions of ^{229}Th , ^{232}Th , ^{233}Pa and ^{233}U are 5.28, 6.468, 6.557 and 5.787 MeV, respectively. The radionuclides ^{228}Th and ^{232}U are the (n,2n) reaction products of ^{229}Th and ^{233}U , respectively. The radionuclide ^{232}U is a also decay product of ^{232}Pa , which produced from (n,2n) reaction of ^{233}Pa and (n, γ) reaction of ^{231}Pa . The radionuclide ^{231}Pa is the decay product of ^{231}Th , which produced from (n,2n) reaction of ^{232}Th . Thus sufficiently cooled irradiated Th-U fuel will be always associated with the reaction products such as ^{227}Ac , ^{228}Th , ^{229}Th , ^{230}Th , ^{232}Th , ^{231}Pa , ^{232}U , ^{233}U and ^{234}U . Once the radiochemical separation of Th and U is done then the separated Th fraction will be primarily associated with ^{232}Th , ^{229}Th , ^{228}Th and extremely low quantity of ^{230}Th . On the other hand, a separated U fraction will be associated with ^{233}U , ^{232}U and very less quantity of ^{234}U . One of the daughter product of ^{232}U is ^{208}Tl , which is a high energy (2.6 MeV)

gamma ray emitter. This is a big hurdle for the use and processing of Th-U fuel. Thus it is always necessary to have knowledge about the amount of ^{232}U in irradiated Th-U fuel.

The amount of U-Th estimation can be done by using different methods such as mass spectrometry [137], Isotope Dilution Mass Spectrometry (IDMS) [138], Thermal ionization mass spectrometry (TIMS) [8], potentiometry [139], alpha and γ -ray scintillation counting technique [140], alpha [141,148] and γ -ray spectrometric [142] technique etc. In different mass spectrometry techniques [15,137-138], it is not possible to estimate ^{232}U accurately due to the probable contamination of ^{232}Th . Besides this, in mass spectrometry methods, it is necessary to add a spike. As an example, in a separated U-sample, ^{232}U is used as a spike for the concentration determination of $^{233,234}\text{U}$. Similarly, in a separated Th-sample, ^{229}Th is used as a spike for concentration determination of ^{232}Th . A separated U-sample from irradiated thoria itself contains ^{232}U besides ^{233}U and ^{234}U . Similarly, a separated Th sample from irradiated thoria itself contains ^{229}Th besides ^{228}Th , ^{230}Th and ^{232}Th . Thus adding a ^{232}U spike for the estimation of any U-isotopes and adding a ^{229}Th spike for the estimation of any Th-isotopes are not correct. In such cases, alpha spectrometric method is a very good technique for alpha emitting radionuclides such as ^{228}Th , ^{229}Th , ^{230}Th , ^{232}Th , ^{232}U , ^{233}U and ^{234}U . However, ^{232}Th is an alpha emitter with very long half-life ($t_{1/2} = 1.4 \times 10^{10}$ years) and thus is not possible to estimate even after long counting time. Similarly, ^{230}Th and ^{234}U are also not possible to estimate in irradiated thoria sample due to their low activity. On the other hand, in an unseparated irradiated thoria sample, ^{233}U has same alpha lines as of its daughter ^{229}Th . Similarly, ^{232}U has same alpha lines as of its daughter ^{228}Th . Besides this, the alpha emitting nuclides such as $^{232,233}\text{U}$ and ^{228}Th have gamma lines with very weak intensities, whereas ^{229}Th has low energy gamma lines with good intensities. In view of this, in the present work U and Th from irradiated thoria sample were radiochemically separated by using high pressure liquid chromatographic (HPLC) technique. The ^{232}U and ^{233}U isotopes from the separated U-fraction

as well as the ^{228}Th and ^{229}Th from the separated Th fraction were estimated by alpha spectrometric techniques. The radionuclide ^{229}Th was also estimated by gamma-ray spectrometric technique and compared with the results based on alpha spectrometric technique.

6.2 Experimental Details

Irradiated thoria containing thorium, uranium and fission products was dissolved in conc. HNO_3 and 0.005 NaF solution. It was evaporated to dryness and treated many times with conc. HNO_3 to make it free from fluoride. Then stock solution was prepared by adding 1 M HNO_3 . About 20 μl from the stock solution was taken in a micro pipette and put on a stainless steel planchet. It was dried under IR lamp, fired to red hot and cooled for 15 min [15]. The plancheted source was taken for alpha spectrometric analysis. The alpha counting of the plancheted source was done by using pre-calibrated silicon surface barrier detector connected to a PC based 4096 channel analyzer. The energy and efficiency calibration of the silicon surface barrier detector was done by using a standard source of $^{239}\text{Pu} + ^{241}\text{Am}$. The resolution of the detector system was 30 keV at 5.485 MeV of ^{241}Am . A typical alpha-spectrum of a long cooled and short time irradiated dissolved thoria sample is shown in Fig. 6.1

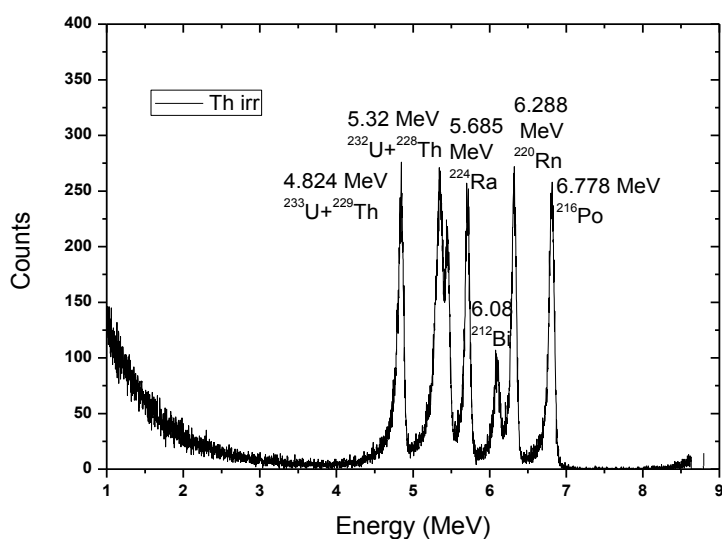


Fig. 6.1 Alpha spectrum of mixed sample of $^{228,229}\text{Th}$ and $^{232,233}\text{U}$ along with its daughter products activities from a long cooled and short time irradiated thoria sample.

The individual separation of the uranium and thorium from the dissolved irradiated thoria sample can be done by using conventional ion-exchange methods [15,146-147]. However, in the present work, individual separation of the uranium and thorium fractions from the long cooled and short time irradiated dissolved thoria sample were done by using High Performance Liquid Chromatography (HPLC) separation. For this purpose, one ml of the dissolver solution from the stock containing uranium, thorium and fission products was evaporated to near dryness and redissolved in 1M HNO₃. Separation and purification of U and Th were carried out on a HPLC containing C₁₈ Reversed Phase (RP) column [18,150-152]. The HPLC system consist of an L-2130 (Elite La Chrom, Hitachi) low-pressure quaternary gradient pump and an L-2420 (Elite La Chrom) variable wavelength UV-Vis detector. Solutions were injected into the column using a Rheodyne injector (Model 9725i) with a 100 µL loop. C₁₈ monolith RP column (Chromolith, Merck) of the dimension, 100 mm×4.6 mm was used as the stationary phase. The final dilutions of the sample was made in the mobile phase containing 0.15 M HIBA of pH 4 for carrying out the separation. The eluted species were monitored using the UV-Vis detector at 650 nm after post-column reaction (PCR) with a metallochromic reagent, which was added using a reciprocating pump (Eldex Laboratories Inc) into a low dead volume-mixing tee (Valco). The signal from the detector was processed by EZChrom software package. Resolution was optimised appropriately so that high amount of Th should not interfere with small amount of uranium as seen in Fig 6.2

Under the chromatographic conditions, Th and U exist in IV and VI oxidation states, respectively. Uranium forms [UO₂(IBA)]⁺, [UO₂(IBA)₂] and [UO₂(IBA)₃], whereas thorium forms [Th(IBA)]³⁺, [Th(IBA)₂]²⁺, [Th(IBA)₃]⁺, [Th(IBA)₄], [Th(IBA)₄(OH)]⁻ and [Th(IBA)₄(OH)₂]²⁻ complexes with α-HIBA. The pH and concentration of α- HIBA play very important role in deciding the dominance of one species over the other for the relative difference in the retention times of Th and U [153-154]. The pH and concentration of mobile

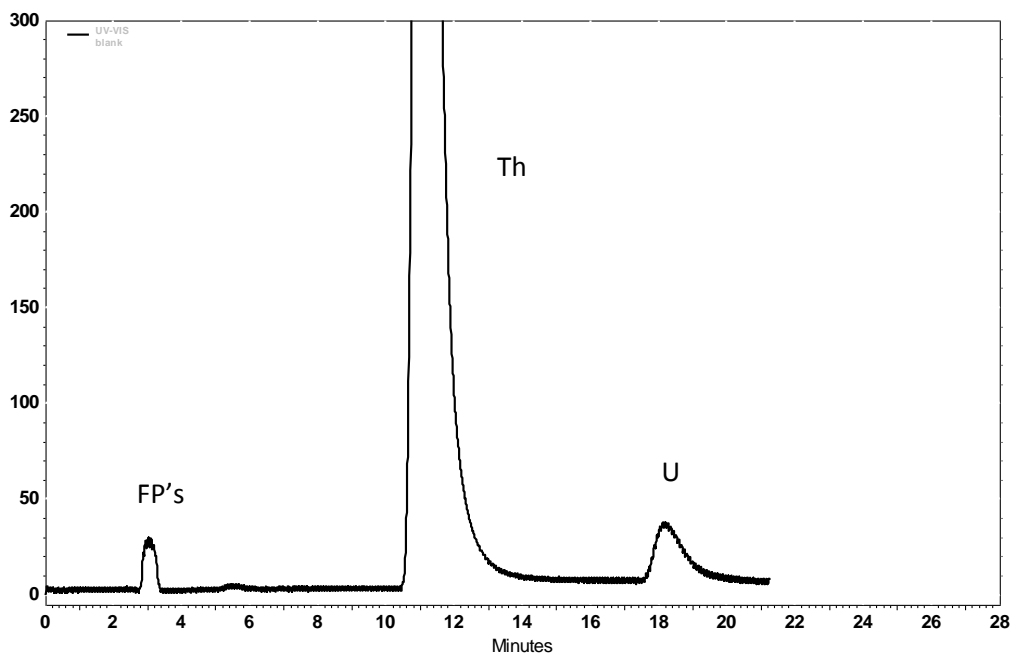


Fig.6.2 Chromatogram of separation of Th and U from dissolver solution of irradiated thoria. Conditions: 0.15 M HIBA, pH 4.0, methanol v/v% changed from 1 to 7 in 0 - 15 min; stationary phase: C₁₈RP (150 mm × 4.6 mm); flow rate: 1mL min⁻¹; post-column reagent [0.15mM Arsenazo (III) and 0.01M urea in 0.1M HNO₃] flow rate: 0.3mL min⁻¹; Monitoring wavelength: 650 nm

phase as well as percentage of methanol were optimised for achieving good separation between Th and U.[18] On a reversed phase stationary phase, complex species of Th and U are retained by hydrophobic interaction. Hence the optimisation of chromatographic conditions such as pH of the mobile phase, concentration of HIBA on the retention of Th and U was very important. The separation was completed within 20 min. Resolution was optimised appropriately so that high amount of Th should not interfere with small amount of uranium. After the optimisation of chromatographic method UV detector was removed from the flow stream and a fractional collector (Model SF 2120) was employed for collecting the desired fractions from the column effluent. Separated fractions containing Th and U were accumulated from a number of chromatographic runs. The fractions collected from multiple chromatographic runs were accumulated, treated with conc HNO₃ and H₂O₂ followed by evaporation near dryness. Then

plancheted sources of Th and U were made from the above treated solution and taken for alpha spectrometric measurements of their isotopic composition.

About 20 μl from each of the purified U and Th solutions were taken in two different micro pipettes and put on two stainless steel planchets. They were dried under IR lamp, fired to red hot and cooled for 15 min [15]. The plancheted sources were taken for alpha and γ -ray spectrometric analysis. The alpha spectrometric analysis of individual planchets containing U and Th were done as described before for the unseparated thoria sample. Alpha spectra of the separated U and Th samples from stainless steel plancheted sources are shown in Fig. 6.3 and Fig. 6.4, respectively.

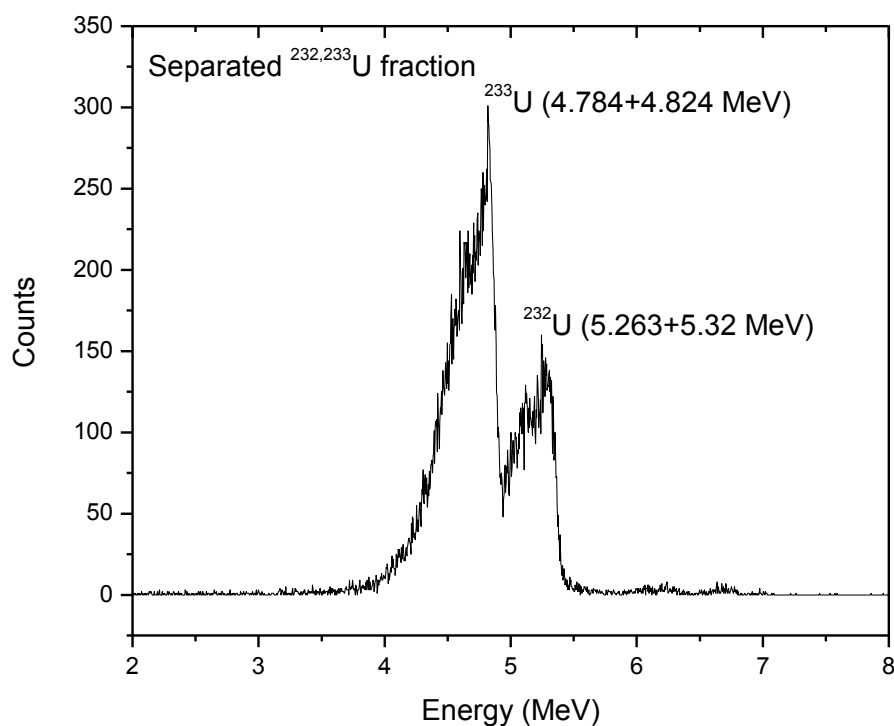


Fig. 6.3 Alpha spectrum of purified U fraction, which is free from its daughter products activities

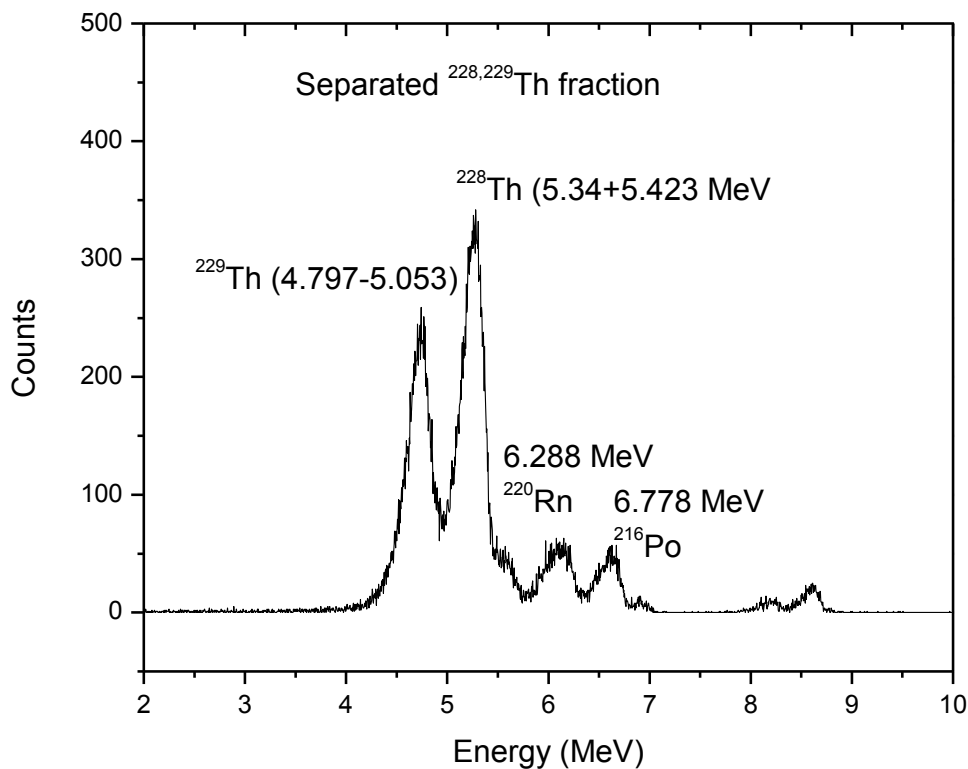


Fig.6.4 Alpha spectrum of the purified Th fraction, which is free from its parent products activities but shows decay products of ^{228}Th

On the other hand, the γ -ray spectrum of the separated Th sample from the same plunched source was done by using energy and efficiency calibrated high purity germanium (HPGe) detector coupled to a PC based 4K channel analyzer. The resolution of the detector system was 1.8 keV FWHM at 1332.0 keV γ -line of ^{60}Co . The energy calibration of the detector system was done by using ^{152}Eu standard source. However, efficiency calibration of the detector system was done by using standard sources of ^{133}Ba and ^{152}Eu . Gamma rays counting of the standard and unknown samples were done in the same geometry of the detector system. A γ -ray spectrum of the irradiated thoria sample is shown in Fig. 6.5.

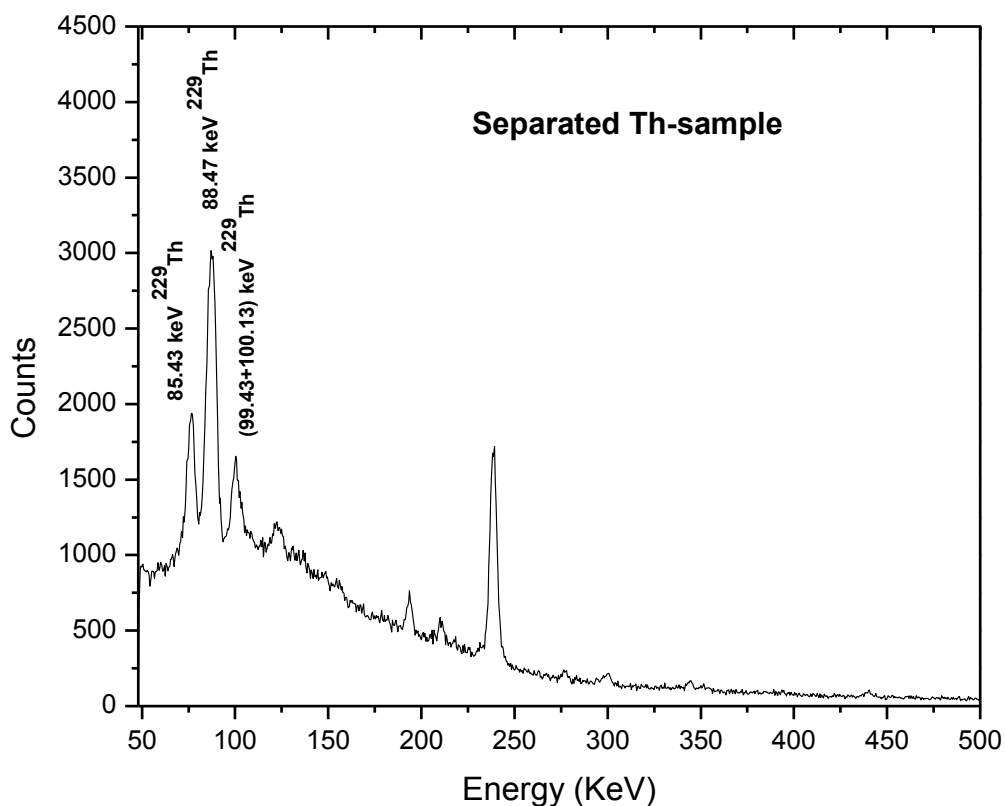


Fig. 6.5 Gamma-ray spectrum of the purified Th activity showing the gamma lines of ^{229}Th

6.3 Results and Discussion

In Fig. 6.1, the alpha energies of daughter products and the unresolved alpha energies of ^{233}U and ^{229}Th pair as well as that of ^{232}U and ^{228}Th pair is very well seen. On the other hand, in the alpha spectrum of the separated U-sample (Fig.6.3), the alpha energies peaks of 4.784+4.824 MeV for ^{233}U and 5.263+5.32 MeV for ^{232}U are clearly seen. The radionuclide, ^{234}U has the alpha energy of 4.722+4.775 MeV, which can interfere with the alpha energy of ^{233}U . However, in short time irradiated sample the formation of ^{234}U from $^{233}\text{U}(n,\gamma)$ reaction

will be extremely low or negligible. If the activity of ^{234}U is measurable then its amount can be determined by using the fitting procedure with WinALPHA software [155-156] for deconvolution.

The amounts i.e. the disintegration per second of ^{232}U ($\text{DPS}_{232\text{U}}$) and ^{233}U ($\text{DPS}_{233\text{U}}$) were estimated from the detected counts per second (CPS_{U}) of the 5.263+5.32 and 4.784+4.824 MeV alpha energies peaks in Fig. 6.3 by using following equations.

$$\text{DPS}_{232\text{U}} = \text{CPS}_{232\text{U}} / (\text{I}_{\alpha 232\text{U}} \times \varepsilon_{\alpha 232\text{U}}) \quad (1)$$

$$\text{DPS}_{233\text{U}} = \text{CPS}_{233\text{U}} / (\text{I}_{\alpha 233\text{U}} \times \varepsilon_{\alpha 233\text{U}}) \quad (2)$$

where ε_{α} and I_{α} are the efficiency for the detector system and the branching intensity of the alpha energy used. The nuclear spectroscopic data such as half-life, alpha and γ -ray energies and their branching intensities were taken from Table 5.1 based on Refs. [134-136]. The alpha energy detection efficiency (ε_{α}) of the silicon surface barrier detector for a particular geometry was obtained from the (CPS) values of the alpha energies of 5.124+5.168 MeV for ^{239}Pu and 5.443+5.485 MeV for ^{241}Am standard source.

In the alpha spectrum of the separated Th-sample (Fig. 6.4), the alpha energies peaks of 4.784+4.824 MeV for ^{229}Th and 5.263+5.32 MeV for ^{228}Th are clearly seen. However, the alpha energy peak of 4.621+4.687 MeV for ^{230}Th is not visible. The radionuclide ^{230}Th , which produced from $^{229}\text{Th}(\text{n},\gamma)$ reaction is expected to be extremely low or negligible in short time irradiated Th-sample. Besides this some of the alpha energies peaks of 6.288 MeV for ^{220}Rn and 6.778 MeV for ^{216}Po are also seen in Fig. 6.4. These are the decay daughter products of ^{228}Th due to its half-life of 1.9125 y. The amounts i.e. the disintegration per second of ^{228}Th ($\text{DPS}_{228\text{Th}}$) and ^{229}Th ($\text{DPS}_{229\text{Th}}$) were estimated from the detected counts per second (CPS_{Th})

of the 5.34+5.423 and 4.797-5.053 MeV alpha energies peaks in Fig. 6.4 by using following equations

$$\text{DPS}_{228\text{Th}} = \text{CPS}_{228\text{Th}} / (\text{I}_{\alpha 228\text{Th}} \times \epsilon_{\alpha 228\text{Th}}) \quad (3)$$

$$\text{DPS}_{229\text{Th}} = \text{CPS}_{229\text{Th}} / (\text{I}_{\alpha 229\text{Th}} \times \epsilon_{\alpha 229\text{Th}}) \quad (4)$$

All the terms in equations (3) and (4) have same meaning as in the equations (1) and (2).

The radionuclide, ^{230}Th has the alpha energy of 4.621+4.687 MeV, which can interfere with the alpha energy of ^{229}Th . If the amount of ^{230}Th would have been significant then an alpha energy peak of 4.621+4.687 MeV should have seen in Fig. 6.4. However, in short time irradiated sample formation of ^{230}Th from $^{229}\text{Th}(n,\gamma)$ reaction will be extremely low or negligible. This is because ^{229}Th itself is a daughter product of ^{233}U . If the activity of ^{230}Th is measurable then the amount of ^{230}Th and ^{229}Th from the close by alpha energy peak can be deconvoluted by using the fitting procedure with WinALPHA software [155-156]. In other way, γ -ray spectrometric technique can be used for the estimation of ^{229}Th , which has been done in the present work. Thus the photo-peak activities of the 85.43, 88.47, 99.43 and 100.13 γ -lines can be very well seen in Fig. 6.5 from the long-counted γ -ray spectrum of same planchated source of the Th-separated sample. From the photo-peak activities of 85.43 and 99.43+100.13 γ -lines, the detected amounts per second of ^{229}Th ($\text{DPS}_{229\text{Th}}$) was estimated from the detected counts per second (CPS_{Th}) by using following equation.

$$\text{DPS}_{29\text{Th}} = \text{CPS}_{29\text{Th}} / (\text{I}_{\alpha 29\text{Th}} \times \epsilon_{\gamma 29\text{Th}}) \quad (5)$$

where ϵ_{γ} and I_{γ} are the efficiency for the detector system and the branching intensity of the γ -rays used. The nuclear spectroscopic data such as half-life, alpha and γ -ray energies and their branching intensities were taken from Table 5.1 based on Refs. [134-136]. The standard sources used for the efficiency calibration were ^{133}Ba and ^{152}Eu . The γ -ray energies of ^{133}Ba

and ^{152}Eu have a range within 53.2-383.82 keV and 121.8-1408.0 keV, respectively. A fitted line was used for efficiencies calculations. Then the efficiencies the 85.43, 88.47, 99.43 and 100.13 keV γ -lines of ^{229}Th were applied for its estimation. Since the 99.43 and 100.13 keV peaks were not possible to resolve, the sum of the branching intensities for both are used. The amount of ^{229}Th i.e. the $\text{DPS}_{229\text{Th}}$ obtained from the gamma spectrometric and alpha spectrometric techniques is nearly same within uncertainty. This indicates that the formation of ^{230}Th is insignificant in a long cooled short time irradiated thoria sample.

6.4 Conclusions

The uranium and thorium fractions of the irradiated thoria sample were separated within 20 minutes by using high performance liquid chromatography (HPLC). From the separated uranium fraction, the amount of ^{232}U and ^{233}U were estimated by using an alpha spectrometric technique. Similarly, in the separated thorium fraction, the amount of ^{228}Th and ^{229}Th were also estimated by alpha spectrometric technique. The amount of ^{229}Th was also estimated by γ -ray spectrometric technique and found to be nearly same. The estimation of amount and uranium and thorium isotopes in an irradiated thoria sample is important from the point of the design of AHWR and ADSs.

Chapter 7

Summary and Future Outlook

Summary and Future Outlook

1. Separation and determination of individual Lns in Zr matrix are reported first time using HPLC. Pre-concentration and quantification of Lns from 2 ppb to 100 ppb can be possible by this method. Identification of Zr species $[\text{Zr}(\text{NO}_3)_5]^-$ using ESI-MS responsible for elution is identified. Elements like Hf, Cd, B also have very high neutron absorption cross-section. Therefore, HPLC methods are require for determination of these nuclides from zirconium matrix. This method involves pre-concentration of Lns in low pH condition on cation exchange column. Same methodology can be applied for other matrix like thorium and Plutonium also.
2. Development of an auto SPE-ESI method for Pd the determination in SHLLW offers good selectivity and sensitivity using a DEBT as complexing agent. Feature of auto-SPE allows you to carry out remote handling of radioactive elements. This method takes care of the potential interfering elements like Pt, Ru, Ag and Rh etc. Very good linearity is obtained for 5 to 100 ppb of Pd in simulated high level liquid waste. This method can be applied for determination of Pallidum in other matrices like geological samples. Pd-DEBT system can be used in advance separation techniques like cloud point extraction or dispersive solvent micro-extractions. In future, determination of other Platinum group of elements like platinum, Ruthenium and Rhodium from SHLLW can be explored.
3. Determination of ^{229}Th and ^{233}U is in presence of each other from a single planchated source is developed. It is a simple method can be employed for routine analysis. ^{233}U and ^{229}Th are separated using anion exchange column. Separated fraction of ^{233}U and ^{229}Th were determined by radiometric method and compared with unpurified fraction. In future, determination of ^{234}U and ^{233}U in presence of each other can be explored by this methodology using alpha and gamma ray spectrometry.

4. Development of method for the separation of U & Th from Irradiated thoria by using HPLC. $^{232}, ^{233}\text{U}$ and $^{228}, ^{229}\text{Th}$ were determined by radiometric method from separated fraction. HPLC method for the determination of lanthanides like La and Nd from irradiated thoria can be explored in future.
-

References



References

1. The evolution of the Indian nuclear power programme S. Banerjee, H.P. Gupta , *Progress in Nuclear Energy* **2017**,101, 4-18
2. Spectroscopic Investigations of Radiation Damage in Glasses used for Immobilization of Radioactive M. Mohapatra and B.S.Tomar, *Waste Defect and Diffusion Forum* **2013**, 341, 107-128
3. Nuclear Fuels Functional Materials Preparation, Processing and Applications S.Banerjee, T.R.Govindan Kutty **2012**, 387-466
4. Standard practice for determining equivalent boron contents of nuclear materials ASTM C1233-15
5. Comparison of alpha-spectrometry and alpha/gamma ratio method for the determination of americium in plutonium bearing fuel materials N. N. Mirashi, P. M. Shah, S.K. Aggarwal, *j. Radioanal Nucl Chem* **2008**,275,479-482
6. S.V. Godbole Trace metal assay of nuclear materials *INCAS bulletin* **2008** 169-179
7. Y.S. Sayi, K.L. Ramakumar and V. Venugopal Determination of non-metallic impurities in nuclear fuels *INCAS bulletin* **2008**, 180-189
8. Burn-up Determination of Irradiated Thoria Samples by Isotope Dilution-Thermal Ionisation Mass Spectrometry S.K. Aggarwal, P.G. Jaison, V.M. Telmore, R.V. Shah, V.L. Sant, K. Sasibhushan, A.R. Parab and D.Alamelu *BARC Report*, **2010**,BARC/2010/E/003.
9. Determination of Burn-Up of Irradiated PHWR Fuel Samples from KAPS-1 by Mass Spectrometry S. K. Aggarwal, P.G. Jaison, V. M. Telmore, P. S. Khodade,R.V.Shah, R.Govindan,V. L. Sant, P. M. Shah *BARC Report*, **2007**,BARC/2007/E/020.
10. Study on complexation of palladium with thiourea-based ligands and its determination in simulated high-level liquid waste using solid phase extraction-electrospray mass spectrometry, Vijay M. Telmore, Pranaw Kumar, P. G. Jaison, *j. Radioanal Nucl Chem* **2018**,318,1249–1259
11. Radioactive waste engineering and management. Springer S. Nagasaki, S. Nakayama, Tokyo **2015**,146
12. Promethium and Plutonium as Fuels for Pacemaker Power Sources Engineering in Medicine, E. J. Wheelwright P. A. Fuqua *Advances in Pacemaker Technology* **1975**,1 383-400

13. Symposium on Opportunities and Approaches for Supplying Molybdenum-99 and Associated Medical Isotopes to Global Markets **2017**,9-12
14. High performance liquid chromatographic separation of $^{228,229}\text{Th}$ and $^{232,233}\text{U}$ and their estimation by α - and γ - ray spectrometry Vijay M. Telmore, Pranaw Kumar, P. G. Jaison, A. Mhatre, H. Naik *j. Radioanal Nucl Chem* **2017**,313,319-326
15. Separation and estimation of ^{229}Th and ^{233}U by alpha and gamma ray spectrometric technique Pranaw Kumar, Vijay M. Telmore, P. G. Jaison, A. Mhatre, H. Naik *j. Radioanal Nucl Chem* **2016**,308,1113–1119
16. Application of mass spectrometer for determination of trace elemental analysis of nuclear materials S.B. Deb and M.K. Saxsena *IANCAS bulletin* **2016**,18-25
17. Inorganic mass spectrometer for determination of isotopic composition in nuclear materials Radhika M. Rao *IANCAS bulletin* **2016**, 26-33
18. Determination of Lanthanides, Thorium, Uranium and Plutonium in Irradiated (Th, Pu) O_2 by Liquid Chromatography Using α -Hydroxyisobutyric Acid (α -HIBA) Pranaw Kumar, P. G. Jaison, Vijay M. Telmore, Sumana Paul, Suresh K. Aggarwal *International Journal of Analytical Mass Spectrometry and Chromatography*, **2013**,1,72-80
19. Simultaneous determination of fluorine, chlorine and bromine in cement with ion chromatography after pyrolysis. Noguchi Y, Zhang L, Maruta T, Yamane T, Nobutoshi Kiba *analytica Chimica Acta*, 640,**2009**,106-109
20. A review of recent trends in electrospray ionisation–mass spectrometry for the analysis of metal–organic ligand complexes. Keith-Roach M. *J. Anal. Chim. Acta.* **2010**, 678 ,140–148.
21. Gas phase reactions of uranyl with α -hydroxyisobutyric acid using electrospray ionization mass spectrometry and density functional theory Pranaw Kumar,P. G. Jaison1,V. M. Telmore,D. Alamelu, S. K. Aggarwal, Biswajit Sadhu Mahesh Sundararajan *J Radioanal Nucl Chem* **2016**,308,303–310
22. Fundamental of Analytical chemistry 8th Edition, DA Skoog, DM West, J. Holler, S.R. Crouch **2004**,906-907.
23. IUPAC. Compendium of Chemical Terminology, 2nd ed. (the "Gold Book"). D. McNaught and A. Wilkinson. Blackwell Scientific Publications, Oxford **1997**. <https://doi.org/10.1351/goldbook.C01075>
24. Practical High-Performance Liquid Chromatography 4th Edition, V. R. Meyer **2004**,7-8

25. Monolithic Materials: Promises, Challenges, Achievements, F. Svec and C. G. Huber, *Anal. Chem.* **2006**, *78*, 2100-2107
26. "Trace analysis of lanthanides and actinides using Liquid chromatography" Ph.D. Thesis P.G. Jaison **2013**, 54-55
27. Determination of lanthanides and actinides in uranium materials by high-performance liquid chromatography with inductively coupled plasma mass spectrometric detection. Rollin S, et al. *J Chromatogr A* 1996, *739*, 139–149.
28. Rapid, high-purity, lanthanide separations using HPLC. Schwantes JM, et al. *J Alloys Compd* 2006, *418*, 189–194.
29. Group Separation of heavy metals followed by subsequent and individual separation of lanthanides by chelation chromatography. Borai E, Eklom P, Harjula R. *J Liq Chromatogr Related Technol* 2014, *37*, 1614–1631.
30. Separation and purification of magnesium, lead and neodymium from dissolver solution of irradiated fuel. Ramakumar KL, Aggarwal SK, Kavimandan VD, Raman VA, Khodade PS, Jain HC *Sep Sci Tech*, 1980, *15*(7), 1471–1481
31. Addition of complexing agents in ion chromatography for separation of polyvalent metal ions. Sevenich GJ, Fritz JS. *Anal Chem* 1983, *55*, 12–16.
32. Complementary analytical methods for cyanide, sulphide, certain transition metals and lanthanides in ion chromatography. Wang WN, Chen YJ, Wu MT. *Analyst* 1984, *109*, 281–286.
33. Comparison of performance of INAA, RNAA and ion chromatography for the determination of individual lanthanides. Dybczynski RS, et al. *Appl Radiat Isot* 2010, *68*, 23–27.
34. Separation of lanthanides by SA-2 ion-exchange paper chromatography. III. Separation of yttrium rare earths. Dubuquoy C, Gusmini S, Poupard D. *J Chromatogr* 1972, *70*, 216–219.
35. Reversed-phase paper chromatography for the separation of rare earth elements by primary amine N 1923 as a stationary phase. Chen L, Yuan B. *Nat Sci J Xiangtan Univ* 1986, *32*, 81–85.
36. Separation of rare-earth elements Lederer M.. *Nature* 1955, *176*, 462–463.
37. Thin-layer chromatographic behaviour and separation of rare earths on silica gel in aqueous ammonium nitrate solution Ishida K, et al.. *J Chromatogr A* 1986, *351*, 489–494.
38. Separation of U(VI) and Th(IV) from some rare earths by thin layer chromatography with di-(2-ethylhexyl)-dithiophosphoric acid on silica gel. Soran ML, Curtui M, Marutoiu C. *J Liq Chromatogr Related Technol* 2005, *28*, 2515–2524.

39. TLC separation of rare earths using di(2-ethylhexyl)dithiophosphoric acid as complexing reagent. J. Planar Chromatogr. Soran M-L, et al. -Mod. TLC 2005, 18, 160–163.
40. Determination of trace rare earth impurities in high-purity cerium oxide by using electrothermal vaporization ICP-AES after HPLC separation with 2-ethylhexylhydrogen 2-ethylhexylphosphonate resin as the stationary phase. Qin S, et al. J Anal At Spectrom 2000, 15, 1413–1416.
41. An evaluation of a single-step extraction chromatography separation method for Sm-Nd isotope analysis of micro-samples of silicate rocks by high-sensitivity thermal ionization mass spectrometry. Li CF, et al. Anal Chim Acta 2011, 706, 297–304.
42. Capillary zone electrophoresis of rare-earth-metals with indirect UV absorbency detection Foret F, et al.. Electrophoresis 1990, 11, 780–783.
43. Electrophoretic capillary ion analysis: origins, principle, and applications Jandick P, et al.. LC-GC 1991, 9, 634–645.
44. Bonded-phase capillaries and the separation of inorganic-ions by high-voltage capillary electrophoresis. Chen M, Cassidy RM. J Chromatogr. 1992, 602, 227–234.
45. Highly sensitive detection of neodymium ion in small amount of spent nuclear fuel samples using novel fluorescent macrocyclic hexadentate polyaminocarboxylate probe in capillary electrophoresis-laser-induced fluorescence detection. Saito S, et al. J Chromatogr A 2012, 1232, 152–157.
46. A brief study of the supercritical fluid chromatographic behavior of lanthanide β -diketonates Laintz KE, et al.. J High Res Chromatogr 1994, 17, 603–606.
47. Dynamic ion exchange chromatography for determination of number of fissions in thorium–uranium dioxide fuels. Knight, C.H.; Cassidy, R.M.; Recoskie, B.M.; Green, L.W. Anal. Chem. 1984, 56 (3), 474–478.
48. Dynamic ion exchange chromatography for the determination of number of fissions in uranium dioxide fuels. Cassidy, R.M.; Elchuk, S.; Elliot, N.L.; Green, L.W.; Knight, C.H.; Recoskie, B.M. Anal. Chem. 1986, 58 (6), 1181–1186.
49. Burn-up measurements on nuclear reactor fuels using high performance liquid chromatography Sivaraman, N.; Subramaniam, S.; Srinivasan, T.G.; Vasudeva Rao, P.R.. J. Radioanal. Nucl. Chem. 2002, 253 (1), 35–40.
50. High-resolution determination of ^{147}Pm in urine using dynamic ion-exchange chromatography. Elchuk, S.; Lucy, C.A.; Burns, K.I. Anal. Chem. 1992, 64 (20), 2339–2343.

51. Dynamic chromatographic systems for the determination of rare earths and thorium in samples from uranium ore refining processes. Barkley, D.J.; Blanchette, M.; Cassidy, R.M.; Elchuk, S. *Anal. Chem.* 1986, 58 (11), 2222–2226.
52. Advances in the Analytical Chromatography of the Lanthanides ANALYST, DECEMBER 1988, VOL. 113 1757-1779 Kevin Robards and Sally Clarke
53. Analytical-scale separations of the lanthanides: A review of techniques and fundamentals. Nash, K.L.; Jensen, M.P. *Sep. Sci. Technol.* 2001, 36, 1257–1282.
54. Evaluation of dynamic ion exchange for the isolation of metal ions for characterization by mass and a spectrometry. Cassidy, R.M.; Miller, F.C.; Knight, C.H.; Roddick, J.C.; Sullivan, R.W. *Anal. Chem.* 1986, 58 (7), 1389–1394.
55. Introduction to mass spectrometry, SK Aggarwal and HC Jain **1997** ISMAS publication
56. Mass Spectrometry for the Novice J.Greaves and J.Roboz, **2014**, Taylor & Francis Group, LLC
57. Mass Spectrometry Principles and Applications Third Edition V Stroobant E. Hoffmann **2007**, John Wiley & Sons Ltd, England
58. Electrospray Ionization Mass Spectrometry: A Technique to Access the Information beyond the Molecular Weight of the Analyte, S.Banerjee and S.Mazumdar *International Journal of Analytical Chemistry*, vol. 2012, Article ID 282574, **2012**, 40. <https://doi.org/10.1155/2012/282574>.
59. Radiation detection and measurement, G.F. Knoll, 3 rd edition, Jhon-Wiley Sons Ney York
60. Proceedings of DAE-BRNS discussion meet on current trends and future prospective of neutron activation analysis **2006 (CFNAA)**
61. Determination of pu isotopic composition and 241am by High resolution gamma spectrometry on solid SAMPLES, A. Sarkar, S. Paul and S.K. Aggarwal B.S. Tomar **2018**, BARC/2011/E/018
62. Nuclear Analytical Techniques P.K. Mohapatra and A.K. Pandey *INCAS bulletin* **2003**, **143**
63. Non-Destructive assay techniques in nuclear fuel cycle S. Gangotra, PM Ousheph, KC Sahoo *INCAS Bulletin*. **2013**, 215
64. Suresh Kumar Aggarwal alpha particle spectrometry for the determination of alpha emitting isotopes in nuclear, environmental and biological samples: past, present and future. *Anal. Methods*, **2016**, 8, 5353
65. Fundamental of nuclear and radiochemistry D.D. Sood, A.V.R. Reddy and N. Ramamoorthy IANCAS publication

66. Chemically selective polymer substrate based direct isotope dilution alpha spectrometry of Pu; Sumana Paul, Ashok K. Pandey, R.V. Shah and S.K. Aggarwal; *Analytica Chimica Acta*, **2015**, 878, 54–62.
67. N.N. Mirashi Thesis “studies in radiometric studies for the determination of actinides”. Submitted to Mumbai university **2010**
68. Characterization of Zr-based hard coatings for medical implant applications, M. Balaceanu, T. Petreus, V. Braic, C.N. Zoita, A. Vladescu, C.E. Cotrutz, M. Braic, *Surface and Coatings Technology* **2010**, 204(12), 2046-2050.
69. Use of zirconium heat exchangers in the viscose rayon process industrial applications of titanium and zirconium, L.B. Bowen, ASTM International, West Conshohocken, PA, **1981**.
70. Zirconium for sodium peroxide fusions, G. Petretic, *Analytical Chemistry* **1951**, 23(8) 1183-1184.
71. Material development for india's nuclear power programme, A.K. Suri, *Sadhana* **2013** 38(5).
72. Standard specification for nuclear grade zirconium oxide powder, ASTM C1065 – 08 - 2015.
73. Determination of rare earth impurities in high purity zirconium dioxide by electrothermal vaporization inductively coupled plasma atomic emission spectrometry using 1-phenyl-3-methyl-4-benzoyl-5-pyrazone as extractant and chemical modifier, S. Chen, T. Peng, Z. Jiang, *Analytical Letters* **1999**, 32(2), 411-421.
74. Determination of traces of certain rare earths in zirconium ion exchange separation and spectrographic determination of fractional part-per-million amounts, H.J. Hettel, V.A. Fassel, *Analytical Chemistry* **1955**, 27(8) 1311-1314.
75. Microwave-assisted quantitative determination of trace rare earth elements in zirconia and zirconium alloys by inductively coupled plasma mass spectrometry and validation of separation procedure by standard addition and tracer techniques, B.K.N. S.B. Deb, M.K. Saxena, K.L. Ramkumar, *Atomic Spectroscopy* 31) **2010**, 122-133.
76. The determination of traces of rare earths in zirconium and its alloys, D.F. Wood, M. Turner, *Analyst* **1959**, 84(1005), 725-731.
77. Separation of zirconium, thorium, and rare earth elements as their 2-(2-Arsenophenylazo)-1,8-dihydroxyl-7-(4-chloro-2,6-dibromo-phenylazo)-naphthalene-3,6-disulfonic acid complexes by reversed-phase ion-pair HPLC X.-x. Zhang, M.-s. Wang, J.-k. Cheng, *Journal of Chromatographic Science* 26(10) **1988**, 517-520.

78. P.G. Jaison, Raut, N.M., Aggarwal, S.K, Direct determination of lanthanides in simulated irradiated thoria fuels using reversed-phase high-performance liquid chromatography, *J. Chromatogr. A* **2006**,47.
79. Comparative study of ion interaction reagents for the separation of lanthanides by reversed-phase high performance liquid chromatography (rp-hplc), P.G. Jaison, P. Kumar, V.M. Telmore, S.K. Aggarwal, *Journal of Liquid Chromatography & Related Technologies* **2009**,32(15),2146-2163.
80. Determination of lanthanides and yttrium in high purity dysprosium by rp-hplc using α -hydroxyisobutyric acid as an eluent, P. Kumar, P.G. Jaison, D.R.M. Rao, V.M. Telmore, A. Sarkar, S.K. Aggarwal, *Journal of Liquid Chromatography & Related Technologies* **2013**,36(11),1513-1527.
81. Some aspects of the solution chemistry of zirconium, B.A.J. Lister, L.A. McDonald, *Journal of the Chemical Society (Resumed) (0)***1952**, 4315-4330.
82. Purification of zirconium by ion exchange columns, J.A. Ayres, *Journal of the American Chemical Society***1947** 69(11) 2879-2881.
83. The use of ion exchangers for the determination of physicochemical properties of substances, particularly radiotracers, in solution. III. The radiocolloids of zirconium and niobium, J. Schubert, J.W. Richter, *Journal of Colloid Science* **1950**, 5(4),376-385.
84. The chemistry of aqueous solutions of zirconium salts (does the zirconyl ion exist?), A.S. Solovkin, Z.N. Tsvetkova, *Russian Chemical Reviews* **1962**. 31(11) 655-669.
85. Detection of polynuclear zirconium hydroxide species in aqueous solution by desktop ESI-MS, T. Sasaki, O. Nakaoka, R. Arakawa, T. Kobayashi, I. Takagi, H. Moriyama, *Journal of Nuclear Science and Technology* **2010**,47(12) 1211-1218.
86. Recovery of platinum group metals from high level radioactive waste. Bush RP *Platin Met Rev*, **1991**,35,202–208
87. Separation of palladium from high level liquid waste—a review. Ruhela R, Singh AK, Tomar BS, Hublia RC, *RSC Adv* **2014**,4,24344–24350
88. Separation of palladium from high level liquid waste, generated from reprocessing of PHWR spent fuel. Dakshinamoorthy A, Dhami PS, Munshi SK, Dey PK, *BARC News Lett* **2008**,292,7–16
89. Ion exchange characteristics of rhodium and ruthenium from a simulated radioactive liquid waste. Korean Lee SH, Yoo JH, Kim JH, *J Chem Eng*,**2004**,21,1038–1043

90. On the correlation between mechanical and TEM studies of the aging of palladium during tritium storage. Fabre A, Decamps B, Finot E, Penisson JM, Demoment J, Thiebaut S, Contreras S, Percheron-Guegan A, *J Nucl Mater*, **2005**, *342*, 101–107
91. Improvement in oxidation resistance of Zircaloy-4 by surface alloying with a thin layer of palladium. Eloff GA, Greyling CJ, Viljoen P, *J Nucl Mater* **1993**, *202*, 239–244
92. Asymmetric surface recombination of hydrogen on palladium exposed to plasma. Takagi I, Moritani K, Moriyama H, *J Nucl Mater* **2003**, *313*, 102–106
93. Hard and soft acids and bases. Pearson RG, *J Am Chem Soc* **1963**, *85*, 3533–3539
94. Ion exchange separation of platinum and palladium by nucleophilic displacement with thiocyanate or thiourea. Warshawsky A *Sep Purif Methods* **1983**, *12*, 37–48
95. Electrospray ionisation mass spectrometric studies for the determination of palladium after pre-concentration by disposable pipette extraction. Jaison PG, Kumar P, Telmore VM, Aggarwal SK, *Rapid Commun Mass Spectrom*, **2012**, *26*, 1971–1979
96. Determination of palladium in human urine by high-performance liquid chromatography and ultraviolet detection after ultraviolet photolysis and selective solid-phase extraction. Philippeit G, Angerer J, *J Chromatogr B* **2001**, *760*, 237–245
97. Determination of platinum and palladium in soil as their chelates with N,N-diethyl-N0-benzoylthiourea by RP-HPLC. Alshana U, Aygu'n RS *J Liq Chromatogr Rel Technol* **2011**, *34*, 1326–1339
98. Liquid–liquid extraction of palladium(II) and gold(III) with N-benzoyl-N0, N0-diethylthiourea and the synthesis of a palladium benzoylthiourea complex. Domínguez M, Antico' E, Beyer L, Aguirre A, Garcí'a-Granda S, Salvado' V *Polyhedron* **2002**, *21*, 1429–1437
99. New chemistry with old ligands: N-alkyl- and N, N-dialkyl-N0-acyl(aro)ylthioureas in co-ordination, analytical and process chemistry of the platinum group metals. Koch KR (2001) *Coord Chem Rev* **2001**, *216*, 473–488
100. A review of recent trends in electrospray ionisation–mass spectrometry for the analysis of metal–organic ligand complexes. Keith-Roach MJ *Anal Chim Acta*, **2010**, *678*, 140–148
101. Analysis of metal complex azo dyes by high-performance liquid chromatography/electrospray ionization mass spectrometry and multistage mass spectrometry. Holcbrevék LK, Jandera P, Lycbrevéka A, *Rapid Commun Mass Spectrom*, **2000**, *14*, 1881–1888

102. Capillary electrophoresis–electrospray ionization–mass spectrometry interfaces: fundamental concepts and technical developments. Bonvin G, Schappler J, Rudaz S, *J Chromatogr A* **2012**,126717–31
103. Determination of divalent trace metals in a soil sample using electrospray ionization mass spectrometry Hotta H, Kogure Y, Tsunoda K, *Anal. Methods* **2012**,4,1160–1162
104. Evaluation of electrospray mass spectrometry as a technique for quantitative analysis of kinetically labile solution species. Wang H, Agnes GR, *Anal Chem*,**1999**,71,3785–3792
105. Quantification of trace elements in natural samples by electrospray ionization mass spectrometry with a size-exclusion column based on the formation of metalaminopolycarboxylate complexes. Hotta H, Takayuki M, Takahashi A, Yuta Kogure Y, Johno K, Umemura T, Tsunoda K, *Anal Chem*,**2009**,81,6357–6363
106. New determination methods of halides and cyanide ions by electrospray ionization mass spectrometry based on ternary complex formation. Hotta H, Kurihara S, Johno K, Kitazume M, Sato K, Tsunoda K *Anal Sci*,**2011**,27,953–956
107. Trace-level analysis of hexavalent chromium in lake sediment samples using ion chromatography tandem mass spectrometry. Mañdler S, Sun F, Tat C, Sudakova N, Drouin P, Tooley RJ, Reiner EJ, Switzer TA, Dyer R, Kingston S, Pamuku M, Furdui VI *J Environ Prot*,**2016**,7,422–434
108. Determination of chromium (III), chromium(VI) and total chromium in chromate and trivalent chromium conversion coatings by electrospray ionization mass spectrometry. Hottaa H, Yatab K, Kamarudinb KFB, Kuriharab S, Tsunodab K, Fukumotoc N, Kojimac I, Kinugasac S,*Talanta*,**2012**,88,533–536
109. Quantification of intact covalently metal labeled proteins using ESI–MS/ MS. Benda D, Schwarz G, Beck S, Linscheid MW,*J Mass Spectrom*,**2014**,49,13–18
110. Some derivatives of benzoyl and furoyl isothiocyanates and their use in synthesizing heterocyclic compounds. Douglass IB, Dains FB, *J Am Chem Soc*,**1934**,56,719–721
111. Laser induced breakdown spectroscopic quantification of platinum group metals in simulated high level nuclear waste. Sarkar A, Telmore VM, Alamelu D, Aggarwal SK, *J Anal At Spectrom*, **2009**,24,1545–1550
112. Clustering of palladium(II) chloride in acetonitrile solution investigated by electrospray mass spectrometry. Sa’deka V, Schro’dera D, Tsierk NG, *Int J Mass Spectrom*, **2011**,304,9–14
113. Speciation of platinum-benzoylthiourea in the gas phase using electrospray ionization mass spectrometry and density functional theory. Kumar P, Jaison PG, Sundararajan M,

- Telmore VM, Ghosh SK, Aggarwal SK, *Rapid Commun Mass Spectrom*,**2013**,27,947–954
114. Practical implications of some recent studies in electrospray ionization fundamentals. Cech N, Enke CG, *Mass Spec Rev.*,**2001**, 20,362–387
115. Relative binding energies of gas-phase pyridyl ligand/metal complexes by energy-variable collisionally activated dissociation in a quadrupole ion trap. Satterfield M, Brodbelt JS, *Inorg Chem*,**2001**,40:5393–5400
116. Noncovalent metal-ligand bond energies as studied by threshold collision-induced dissociation. Rodgers MT, Armentrout PB *Mass Spec Rev.*,**2000** 19, 215–247
117. Electrospray ionization mass spectrometric studies on uranyl complex with α -hydroxyisobutyric acid in water–methanol medium. Jaison PG, Kumar P, Telmore VM, Aggarwal SK *Rapid Commun Mass Spectrom*,**2013**,27,1105–1118
118. On-line preconcentration of palladium on alumina microcolumns and determination in urban waters by inductively coupled plasma mass spectrometry. Moldovan M, Gómez MM, Palacios MA *Anal Chim Acta*, **2003**, 478, 209–217
119. Dispersive liquid–liquid microextraction preconcentration of palladium in water samples and determination by graphite furnace atomic absorption spectrometry. Liang P, Zhao E, Li F *Talanta*,**2009**, 77:1854–1857
120. Science and Technology of nuclear installations, Allen TR, Craford DC (2007) Article ID 97486
121. Nuttin A, Heuer D, Billebaud A, Brissot R, Le Brun C, Liatard E, Loiseaux JM, Mathieu L, Meplan O, Merle-Lucotte E, Nifenecker H, Perdu F, David S, *Proc Nucl Energy* **2005**,46(1),77–99
122. Annual Project Status Report 2000, MIT-ANP-PR-071, MacDonald PE, Todreas N 2009 INEFL/EXT-2009-00994
123. Fast Reactors and Accelerator Driven Systems Knowledge Base, IAEA-TECDOC-1319: Thorium fuel utilization: options and trends **2002**
124. Proposal for a simplified thorium molten salt reactor, Mathieu L, Heuer D, Brissot R, Garzenne C, Le Brun C, Lecarpentier D, Liatard E, Loiseaux JM, Meplan O, Merle-Lucotte E, Nuttin A Proceedings of the global international conference, **2005**, Paper No 428, Tsukuba, Japan
125. Design and development of AHWR: the Indian thorium fuel innovative reactor. Sinha RK, Kakodkar A, *Nucl Eng Des* **2006**,236(7–8),683–700

126. Creation of Indian experimental benchmarks for thorium fuel cycle, IAEA Coordinated research project on “Evaluated data for thorium–uranium fuel cycle,” Third research coordination meeting, Ganesan S, Vienna, INDC (NDS)-0494 **2006**
127. An energy amplifier for cleaner and inexhaustible nuclear energy production driven by particle beam accelerator, Carminati F, Klapisch R, Revol JP, Roche Ch., Rubio JA, Rubbia C CERN Report No. CERN/AT/93-47 (ET) **1993**
128. Conceptual design of a fast neutron operated high powerenergy amplifier, Rubio JA, Buono S, Carminati F, Fietier N, Galvez J, Geles C, Kadi Y, Klapisch R, Mandrillon P, Revol JP, Roche Ch. (1995) CERN/AT/95-44(ET)**1995**
129. The international conference on accelerator-driven transmutation technologies and applications, Las Vegas, AIP conference proceedings, Arthur ED, Schriber SA, Rodriguez A (Eds) ,**1994**,346
130. Accelerator Driven Systems: Energy Generation and Transmutation of Nuclear Waste, Status report **1997** IAEA,Vienna,IAEA-TECDO-985
131. Accelerator-Driven systems for nuclear waste transmutation. Bowman CD Ann Rev Nucl Part Sci,1998,48,505–556
132. Nuclear data requirements for accelerator driven sub-critical systems—A roadmap in the Indian context Ganesan S Pramana (J Phys),2007,68(2),257–268
133. Accelerator-Driven sub critical reactor systems (ADS) for nuclear energy generation Kapoor SS Pramana (J Phys),2002,59(6),941–950
134. NuDat 2.6, National Nuclear Data Center, Brookhaven National Laboratory, updated **2011**. Available on <http://www.nndc.bnl.gov/JRadioanalNuclChem123>
135. Table of radioactive isotopes, Lawrence Berkeley National Laboratory, Berkeley Version 2.1[<http://ie.lbl.gov/toi/index.asp>]Firestone RB, Ekstrom LP **2004**
136. Table of radioactive isotopes and their main decay characteristics Blachot J, Fiche Ch . *Ann Phys*, **1981**6,3–218
137. DAE international symposium on radiochemistry and radiation chemistry (Plutonium-50 years), Chitamber SA, Khodade PS, Parab AR, Jain HC (1991) BARC, Bombay, 4–7 Feb 1991, Paper no. AC-16
138. Simultaneous isotopic analysis of uranium and plutonium by thermal ionisation mass spectrometry coupled to a variable multicollection detection system. Ramakumar KL, Rao RM, Gnanayyan L, Jain HC, *Int J Mass Spectrom Ion Process* **1994**,134(2–3),183–190

139. Vogel AI (1961) A text book of quantitative inorganic analysis, 3rd edn. Longmans Green & Co., Ltd., London
140. Comparison of alpha-spectrometry and alpha/gamma ratio method for the determination of americium in plutonium bearing fuel materials Mirashi NN, Shah PM, Aggrawal SK, *J Radioanal Nucl Chem*, **2008**, 275, 479–479
141. Isotope Dilution Alpha Spectrometry for the Determination of Plutonium Concentration in Irradiated Fuel Dissolver Solution: IDAS and R-IDAS Ramaniah MV, Jain HC, Aggrawal SK, Chitamber SA, Kavimandn VD, Almaula AI, Shah PM, Parab AR, Sant VL, *Nucl Technol* **1980**, 49, 121–128
142. Gamma spectrometry for quantification of trace amounts of actinides in concentrated ammonium nitrate solution Mirashi NN, Aggrawal SK *J Radioanal Nucl Chem*, **2009**, 281, 457–459
143. Low level Pu and Am estimation in liquid waste from nuclear reactor Naik H, Renuka M, Chaudhury S *J Radioanal Nucl Chem*, **2011**, 287, 697–700
144. Anion-exchange studies of Th(IV) and U(IV) in hydrochloric acid. Kraus KA, Moore GE, Nelson F, *J Am Chem Soc* **1956**, 78(12), 2692–2695
145. Separation and purification of magnesium, lead and neodymium from dissolver solution of irradiated fuel. Ramakumar KL, Aggarwal SK, Kavimandan VD, Raman VA, Khodade PS, Jain HC *Sep Sci Tech*, **1980**, 15(7), 1471–1481
146. Determination of isotopic composition of uranium samples using alpha spectrometry. Alamelu D, Jagadish Kumar S, *J. Radioanal. Nucl. Chem.* **2016**, 310, 541–546
147. Gamma spectrometry for quantification of trace amounts of actinides in concentrated ammonium nitrate solution. Mirashi NN, Aggrawal SK *.Radioanal. Nucl. Chem.* **2009**, 281, 457–459
148. Dynamic ion exchange chromatography for determination of number of fissions in thorium-uranium dioxide fuels. Knight CH, Cassidy RM, Recoskie BM, Green LW *Anal Chem* **1984**, 56, 474–478
149. Dynamic ion exchange chromatography for the determination of number of fissions in uranium dioxide fuels. Cassidy RM, Elchuk S, Elliot NL, Green LW, Knight CH, Recoskie BM *Anal Chem* **1986**, 58, 1181–1186
150. Burn-up measurements on dissolver solution of mixed oxide fuel using HPLC-mass spectrometric method. Bera S, Balasubramanian R, Datta A, Sajimol R, Nalini S, Narasimhan TSLakshmi, Antony MP, Sivaraman N, Nagarajan K, Rao PRV (2013) *Int J Anal Mass Spectrom Chromatogr* **2013**, 1, 55–60

151. Retention studies on uranium, thorium and lanthanides with amide modified reverse phase support and its applications. Raju Siva Kesava, Subramanian MS, Sivaraman N, Srinivasan TG, Rao PRV *J Chromatogr A* **2007**, *1156*, 340–347
 152. Correlation of retention of lanthanide and actinide complexes with stability constants and their speciation. Datta A, Sivaraman N, Viswanathan KS, Ghosh S, Srinivasan TG, Rao PRV *Radiochim Acta* **2013**, *101*(2): 81–92
 153. A model shape for the analysis of alpha particle spectra. Garcia-Torano E *Nucl Instr Meth Phys Res A* **2003**, *498*, 289–291
 154. The Win ALPHA code for the analysis of alpha-particle spectra. Noy RC, Garcia-Torano E, Mainegra E, Lopez E *Nucl Instr Meth Phys Res A* **2004**, *525*, 522–528
 155. Alamelu D, Aggarwal SK (2012) Determination of uranium isotopes in irradiated thorium dioxide by alpha spectrometry using WinALPHA for deconvolution of complex spectra. *J Radioanal Nucl Chem* *294*: 405–408
-